AD-A099 418 LOCKHEED MISSILES AND SPACE CO INC SUNNYVALE CA MISSI--ETC F/G 11/1
CURE MONITORING TECHNIQUES FOR ADHESIVE BONDING TECHNIQUES.(U)
NOV 80 C A MAY, A WERETA, J S FRITZEN F33615-79-C-5046
UNCLASSIFIED LMSC-D058816 AFWAL-TR-80-4171 NL

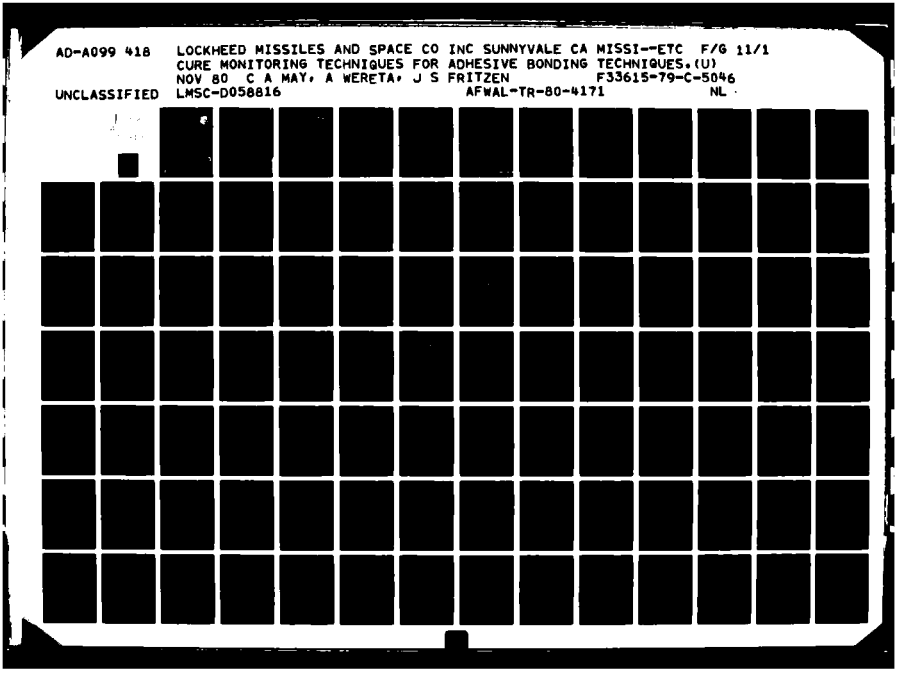

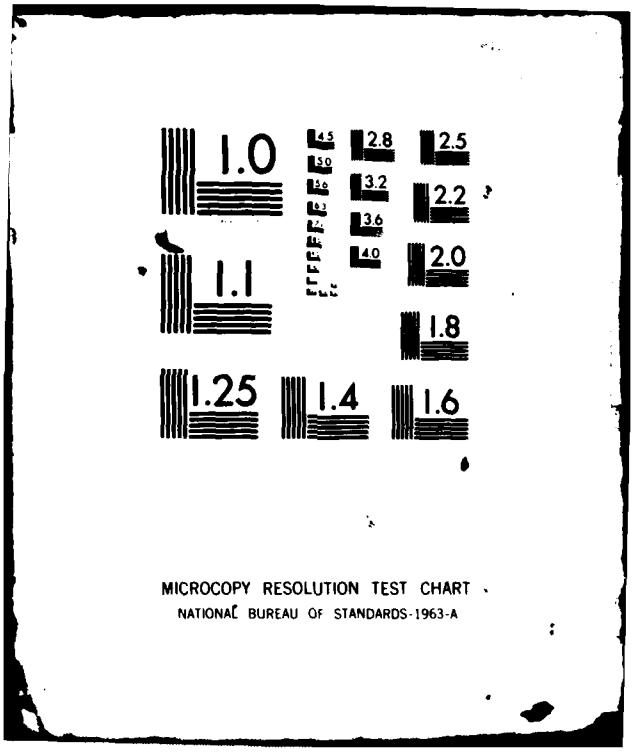
1.0
1.1
1.25
1.4
1.6
1.8
2.0
2.2
2.5
2.8
3.2
3.6
4.0
4.5
5.0
5.6
MICROCOPY RESOLUTION TEST CHART
NATIONAL BUREAU OF STANDARDS-1963-A

AFWAL-TR-80-4171

CURE MONITORING OF STRUCTURAL ADHESIVE BONDED JOINTS

C. A. MAY
A. WERETA, JR.
J. S. FRITZEN
F. L. KECK

LOCKHEED MISSILES & SPACE COMPANY, INC.
MISSILES SYSTEMS DIVISION
P. O. BOX 504
SUNNYVALE, CALIFORNIA 94086

NOVEMBER, 1980

TECHNICAL REPORT AFWAL-TR-80-4171

FINAL REPORT May 1979 - September 1980

APPROVED FOR PUBLIC RELEASE; DISTRIBUTION UNLIMITED

MATERIALS LABORATORY
AIR FORCE WRIGHT AERONAUTICAL LABORATORIES
AIR FORCE SYSTEMS COMMAND
WRIGHT-PATTERSON AIR FORCE BASE, OHIO 45433

NOTICE

When Government drawings, specifications, or other data are used for any purpo other than in connection with a definitely related Government procurement operati the United States Government thereby incurs no responsibility nor any obligation whatsoever; and the fact that the government may have formulated, furnished, or i any way supplied the said drawings, specifications, or other data, is not to be r garded by implication or otherwise as in any manner licensing the holder or any other person or corporation, or conveying any rights or permission to manufacture, use, or sell any patented invention that may in any way be related thereto.

This report has been reviewed by the Office of Public Affairs (ASD/PA) and is releasable to the National Technical Information Service (NTIS). At NTIS, it will be available to the general public, including foreign nations.

This technical report has been reviewed and is approved for publication.

Herbert S. Schwartz

HERBERT S. SCHWARTZ
Project Monitor
FOR THE COMMANDER

T. J. Reinhart for

T. J. REINHART, JR., Chief
Composites, Adhesives & Fibrous
Materials Branch
Nonmetallic Materials Division

F. D. Cherry

FRANKLIN D. CHERRY, Chief
Nonmetallic Materials Division

"If your address has changed, if you wish to be removed from our mailing list, or if the addressee is no longer employed by your organization please notify AFWAL/MLBC W-PAFB, OH 45433 to help us maintain a current mailing list".

Copies of this report should not be returned unless return is required by security considerations, contractual obligations, or notice on a specific document.

AIR FORCE/86780/26 March 1981 — 400

SECURITY CLASSIFICATION OF THIS PAGE (When Data Entered)

REPORT DOCUMENTATION PAGE

READ INSTRUCTIONS BEFORE COMPLETING FORM

1. REPORT NUMBER: AFWAL-TR-80-4171 — AD-A099 418

4. TITLE (and Subtitle): CURE MONITORING TECHNIQUES FOR ADHESIVE BONDING TECHNIQUES

5. TYPE OF REPORT & PERIOD COVERED: FINAL REPORT, 1 May 79 - Sep 80

6. PERFORMING ORG. REPORT NUMBER: LMSC-D858816

7. AUTHOR(s): C. A. May, A. Wereta, Jr., J. S. Fritzen, F. L. Keck

8. CONTRACT OR GRANT NUMBER(s): F33615-79-C-5046

9. PERFORMING ORGANIZATION NAME AND ADDRESS: Lockheed Missiles & Space Company, A Group Division of Lockheed Corporation, Sunnyvale, Calif.

10. PROGRAM ELEMENT, PROJECT, TASK AREA & WORK UNIT NUMBERS: PE 62102F; 24190210; 17 03

11. CONTROLLING OFFICE NAME AND ADDRESS: MATERIALS LABORATORY (AFWAL/MLBC), AIR FORCE WRIGHT AERONAUTICAL LABORATORIES, AIR FORCE SYSTEMS COMMAND, WRIGHT-PATTERSON AIR FORCE BASE, OHIO 45433

12. REPORT DATE: Nov 80

13. NUMBER OF PAGES: 176

14. MONITORING AGENCY NAME & ADDRESS (if different from Controlling Office)

15. SECURITY CLASS. (of this report): Unclassified

15a. DECLASSIFICATION/DOWNGRADING SCHEDULE

16. DISTRIBUTION STATEMENT (of this Report)

Approved for public release; distribution unlimited.

17. DISTRIBUTION STATEMENT (of the abstract entered in Block 20, if different from Report)

18. SUPPLEMENTARY NOTES

19. KEY WORDS (Continue on reverse side if necessary and identify by block number)

Dielectric Monitoring, Phasemeter, Phaseangle, Vector Voltage, Dissipation Factor, Capacitance, Dielectric Probe, Chemorheology, Thermoset Resins, Adhesives, Cure Cycles, Environmental Testing.

20. ABSTRACT (Continue on reverse side if necessary and identify by block number)

As a result of the work reported herein a foundation has been developed for automated bonding cycle control. The monitoring system was improved through the development of a mathematical model which affords a theoretical understanding of the dielectric signals and permits their chemorheological interpretation. The mechanical reliability of the probe was improved to minimize in-process failures. It was demonstrated that the shape of the dielectric curve was dependent on the chemical composition of the adhesive

DD FORM 1 JAN 73 1473 EDITION OF 1 NOV 65 IS OBSOLETE

404832

SECURITY CLASSIFICATION OF THIS PAGE (When Data Entered)

6 pgs

and was a useful tool for the optimization of cure cycles. Environmental testing of joints containing probes indicated that combinations of moist environments and elevated temperatures caused a degradation of bond performance. However, surface treatments can be applied to the probe without destroying the dielectric monitoring capability and should be evaluated as a solution to this problem. Evidence was also developed that it may be feasible to use the probe to detect the ingress of moisture into a bonded joint.

FOREWORD

This technical report summarizes the work conducted by the Advanced Manufacturing Technology Department of Lockheed Missiles & Space Company, Inc., Sunnyvale, California, 94086, under USAF Contract No. F33615-78-C-5046, Cure Monitoring Techniques for Adhesive Bonding Techniques, 24190210. The work is being administered under the direction of the Nonmetallics Materials Division, Air Force Wright Aeronautical Laboratories, with Mr. E. A. Arvay (AFWAL/MLBC) as Project Engineer.

The program manager is Mr. C. A. May. The principal investigator is Dr. A. Wereta, Jr., assisted by Mssrs. W. G. Caple, J. S. Fritzen, F. A. Karsten, F. L. Keck, and R. J. Boeddiker. This final report covers work conducted during the period 1 May 1979 to 30 September 1980 and was submitted by the authors in September 1980. During this period, LMSC underwent a reorganization which included a relocation of the personnel involved. This caused a delay in the program and the work was not completed according to the original schedule.

TABLE OF CONTENTS

LIST OF ILLUSTRATIONS

SECTION I

INTRODUCTION

1. Program Overview

At the onset of this study on the dielectric monitoring of the adhesive bonding process, earlier studies at LMSC [1-3] and work by other investigators[4-10] showed that the chemorheological changes which occur during the cure of a thermoset resin matrix would be related to changes in the dielectric properties. Thus if the dielectric signal represented the real time changes in the resin chemistry and physical properties, a means was at hand to control the adhesive bonding process using these real life parameters. Subsequently, in brief investigations Arvay and Centers[11] and Crabtree and Bischoff[12] demonstrated that the dielectric properties of a curing thermoset adhesive could be monitored. During subsequent work under contract to the Air Force[13] various methods (equipment) for monitoring the adhesive bonding were studied and feasible probe technology was evolved. This work was summarized and expanded at recent SAMPE Meetings[14] [15] and the utility of the monitoring procedure in production environment was demonstrated on a PABST Program sub-contract[16]. May and Wereta[17] enlarged on the polymer dielectric property, mechanical property parallelism at a recent meeting of the Adhesion Society.

The program described herein was designed with the objective of providing a firm basis for developing an automated, microprocessor controlled curing process based on dielectric signals originating in the adhesive bondline being produced. Based on the aforementioned background, two additional studies were required to establish an adequate starting point for a closed-loop, real life bonding control system. Since any such control system must be based on a mathematical/statistical analysis of the dielectric signals, a mathematical model of the monitoring system had to be developed which would relate dielectric signals to true material parameters. Further, the dielectric signals required chemorheological interpretation. The second requirement was to develop a probing system which would be highly reliable in a production environment. Since the PABST Program demonstrated the probes used at that stage of the development had about the same failure rate as the bondline thermocouples, the goals for this phase of the investigation were indeed high.

2. Summary

The investigation, as planned, has proceeded to this point where a closed-loop control system based on the chemical and physical changes that occur during bondline formation can now be started. Throughout the investigation FM-73 was used as the demonstration adhesive except for the studies on the effect of chemical composition on the dielectric signals. This was the primary adhesive used in the PABST Program.

The key elements of the bond monitoring systems (Audrey and phasemeter) were understood and the mathematical model permitted calculation of true material parameters ($\tan \delta$) from phase angle measurements. This means that phasemeter measurements, with their greater voltage and frequency range and more stable production environment signals can be used for a real life, closed-loop control system. A chemorheological interpretation of the dielectric signal was also developed.

The mechanical performance of the probes were greatly improved. Very few failures were observed during the many bonding operations conducted during the course of the investigation. Dielectric monitoring was also demonstrated to be a useful tool for cure cycle optimization. If proper care is exercised near the edges of the faying surfaces, the probe can be curved either axially or across its width. Indications are that probes left in hardware bondlines may be useful in detecting the presence of moisture. However, based on Raab and wedge crack opening specimens the probe did appear to adversely affect bondline performance, particularly at elevated temperatures. Special probe treatments such as anodizing and priming can be used without affecting monitoring efficiency and may well improve upon this condition. Because of the large amount of statistical analysis required this would involve a separate program.

SECTION I

MONITORING SYSTEM IMPROVEMENTS

1. Development of a Mathematical Model

A relationship between the measured phase angle ϕ_m and the sample phase angle ϕ_s was developed with two goals in mind. The first goal was to aid in the selection of phasemeter parameters such as input voltage V_{in}, reference resistor R_{ref}, and frequency f. The second was to compare the phasemeter data to Audrey data, the latter being more widely used and better understood. The Audrey dissipation factor D is equal to tan ϕ_s, so an equation was developed in this form for the phasemeter as well.

The basic elements of the phasemeter circuit consist of a signal generator, reference resistor, and adhesive sample. A phasemeter is connected in parallel with the reference resistor. Impedance of the phasemeter, multiplexer and connecting cables have been neglected for simplicity. The sample is modeled as a resistor and capacitor in parallel as shown in Fig. 1.

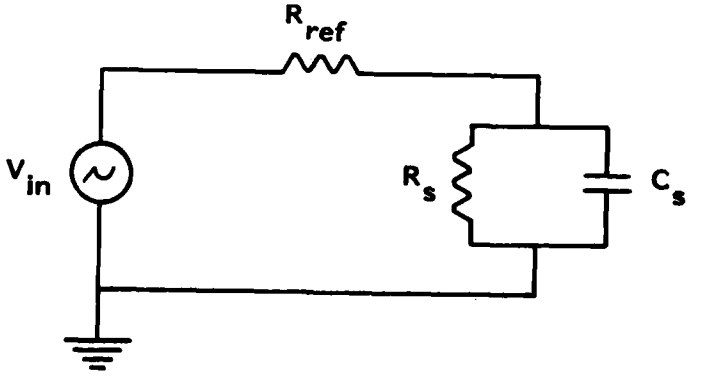

Fig. 1 Circuit Diagram for Phasemeter Monitoring

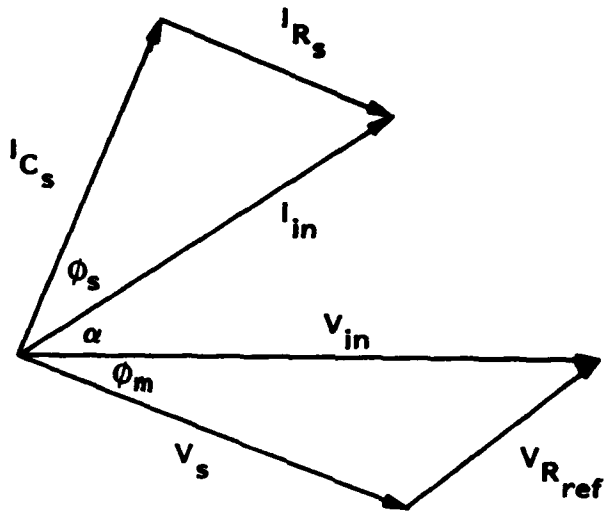

Fig. 2 Phasor Diagram for Phasemeter Monitoring Circuit

Note that the sample voltage V_s lags behind the input voltage V_{in} by the phase angle ϕ_m which is measured by the phasemeter. The vector sum of the sample voltage and the reference resistor voltage $V_{R_{ref}}$ is equal to the input voltage. The current I_{C_s} through the capacitive element of the sample leads the sample voltage V_s by 90 deg while the current through the resistive element I_{R_s} is in phase with the sample voltage. The vector sum of current components is equal to the current I_{in} which flows through both the voltage source and the reference resistor.

In order to relate the measure phase angle ϕ_m to the dissipation factor given by Audrey, the phasor diagram shown above is used.

Angles ϕ_s and ϕ_m are related through the angle α as follows:

$$\phi_s + \alpha + \phi_m = 90^\circ \tag{1}$$

Angle α can be expressed in terms of V_s, $V_{R_{ref}}$ and ϕ_m by using the Law of Sines, i.e.

$$\frac{V_s}{\sin \alpha} = \frac{V_{R_{ref}}}{\sin \phi_m} \tag{2}$$

The unknown $V_{R_{ref}}$ can be expressed in terms of V_s, V_{in}, and ϕ_m by using the Law of Cosines, i.e.

$$V_{R_{ref}}^2 = V_{in}^2 + V_s^2 - 2\, V_{in}\, V_s \cos \phi_m \tag{3}$$

Substituting Eqs. (2) and (3) into (1) and rearranging yields

$$\phi_s = 90^\circ - \phi_m - \sin^{-1} \left\{ \frac{\left(V_s/V_{in}\right) \sin \phi_m}{\left[1 + \left(V_s/V_{in}\right)^2 - 2 \left(V_s/V_{in}\right) \cos \phi_m\right]^{1/2}} \right\} \tag{4}$$

Taking the tangent of both sides

$$\tan \phi_s = \tan \left[90^\circ - \phi_m - \sin^{-1} \{\,\}\right] \tag{5}$$

Using the following trigonometric identities,

$$\tan (90^\circ - A) = \cot A = \frac{1}{\tan A} \tag{6}$$

$$\tan (A + B) = \frac{\tan A + \tan B}{1 - \tan A \tan B} \tag{7}$$

Eq. (4) can be rewritten as

$$\tan \phi_s = \frac{1 - \tan \left\{ \sin^{-1} \left(\frac{\left(V_s/V_{in}\right) \sin \phi_m}{\left[1 + \left(V_s/V_{in}\right)^2 - 2\left(V_s/V_{in}\right) \cos \phi_m\right]^{1/2}} \right) \right\} \tan \phi_m}{\tan \left\{ \sin^{-1} \left(\frac{\left(V_s/V_{in}\right) \sin \phi_m}{\left[1 + \left(V_s/V_{in}\right)^2 - 2\left(V_s/V_{in}\right) \cos \phi_m\right]^{1/2}} \right) \right\} + \tan \phi_m} \tag{8}$$

This equation for tan ϕ_s in terms of input voltage V_{in} and the measured quantities ϕ_m and V_s is comparable to the dissipation factor D determined by the Audrey. The impedance of the phasemeter, connecting cables, and the multiplexer were neglected. The adhesive model used for both Audrey and phasemeter analysis is identical. Parallel capacitor plates of equal area and no edge effects are assumed. The equation is significant in that neither bondline thickness nor probe area affect the dissipation factor as indicated by Eq. (17).

The equation was tested by comparing calculated values of tan ϕ_s from phasemeter data vs. D from Audrey data for runs in which the reference resistor, input voltage, probe area, and bondline thickness were varied. The results are shown and discussed in following subsections.

A second equation relating tan ϕ_s to tan ϕ_m was derived as follows. The ratio of the sample voltage to input voltage can be expressed in phasor notation as

$$\frac{\vec{V}_s}{\vec{V}_{in}} = \frac{V_s}{V_{in}} \angle \phi m \qquad (9)$$

where

$$V_s = I Z_s \qquad (10)$$

$$V_{in} = I \left(R_{ref} + Z_s \right) \qquad (11)$$

I is the common current flowing through both the reference resistor R_{ref} and the adhesive sample modeled as a parallel combination of a resistor R_s and a capacitor C_s. The sample impedance Z_s is shown to be

$$\frac{1}{Z_s} = \frac{1}{R_s} + \frac{1}{j C_s} \qquad (12)$$

and upon rearranging

$$Z_s = \frac{R_s}{1 + j C_s R_s} \qquad (13)$$

Inserting equations (10) and (11) into (12) and then substituting for Z_s using equation (13) yields

$$\frac{V_s}{V_{in}} = \frac{Z_s}{R_{ref} + Z_s} = \frac{\dfrac{R_s}{1 + j C_s R_s}}{R_{ref} + \dfrac{R_s}{1 + j C_s R_s}} \qquad (14)$$

$$= \frac{R_s}{R_{ref} (1 + j C_s R_s) + R_s}$$

$$= \frac{R_s}{R_s + R_{ref} + j\omega C_s R_s R_{ref}}$$

$$= \frac{R_s\left(R_s + R_{ref} - j\omega C_s R_s R_{ref}\right)}{\left(R_s + R_{ref}\right)^2 - \omega^2 C_s^2 R_s^2 R_{ref}^2} \qquad (15)$$

The associated phase angle is given by

$$\tan \phi_m = - \frac{\omega C_s R_s R_{ref}}{R_s + R_{ref}} \qquad (16)$$

Referring to Fig. 3, $\tan \phi_s$ is expressed as

$$\tan \phi_s = - \frac{I_{R_s}}{I_{C_s}} = - \frac{V_s/R_s}{V_s\left/\frac{1}{\omega C_s}\right.} = - \frac{1}{\omega R_s C_s} \qquad (17)$$

Substituting Eq. (17) into Eq. (16) gives the following relationship between $\tan \phi_s$ and $\tan \phi_m$

$$\tan \phi_m = \frac{R_{ref}}{R_{ref} + R_s} \frac{1}{\tan \phi_s} \qquad (18)$$

Thus the tangent of the measured phase angle is inversely proportional to the sample phase angle and the reference resistor influences the scale factor relating these two functions. As discussed in the following section, the scale factor increases as R_s decreases with adhesive softening.

2. Application of the Mathematical Model

a. Selecting a Reference Resistor

The scale factor $R_{ref}/(R_{ref} \quad R_s)$ in Eq. (18) varies from a minimum when R_{ref} is small compared to R_s and approaches unity when R_{ref} is very large compared to R_s. The actual values of R_s have not been accurately measured, but reasonable values range between 25 MΩ at either end of the cure cycle to 50 kΩ during minimum viscosity. Thus the magnitude of the scale factor varies from 0.004 to $0.66\bar{7}$ for a 100 kΩ reference resistor and from 0.286 to 0.995 for a 10 MΩ reference resistor. Hence it is clear that a large reference resistor is desirable in terms of resolving dissipation factor or tan ϕ_s. However, a compromise may be required since the input impedance of the phasemeter and multiplexer is also in the megaohm range and therefore may influence the very value of the phase angle which is to be measured. This represents a case where the observation of a phenomenon may seriously influence it. One further comment concerns resolution of dissipation factors when the viscosity is low. Although the magnification factor is highest at this point in cure, the phase angle approaches 90 deg and its tangent approaches infinity. Thus, very small differences in phase angle, well within experimental error, can lead to very large differences in dissipation factor.

Reference resistor values of 1 and 10 MΩ were selected and compared to the original value of 100 kΩ as shown in Figs. 3 and 4 where phase angle and vector voltage are plotted vs. time. The shaded portion of the 10 MΩ curve indicates an unstable signal. Measurements were made on three different samples of FM-73 adhesive cured individually according to a common temperature program. Bondline thicknesses were controlled by using 0.00055-in. diam copper wire, and probe sizes were fixed at 1/4 in. width and 1 in. penetration into the bondline. For phase angle, an increase in reference resistance enhances definition of the curve but also increases the breadth of the valley. Note too that the position of the initial peak changes with choice of reference

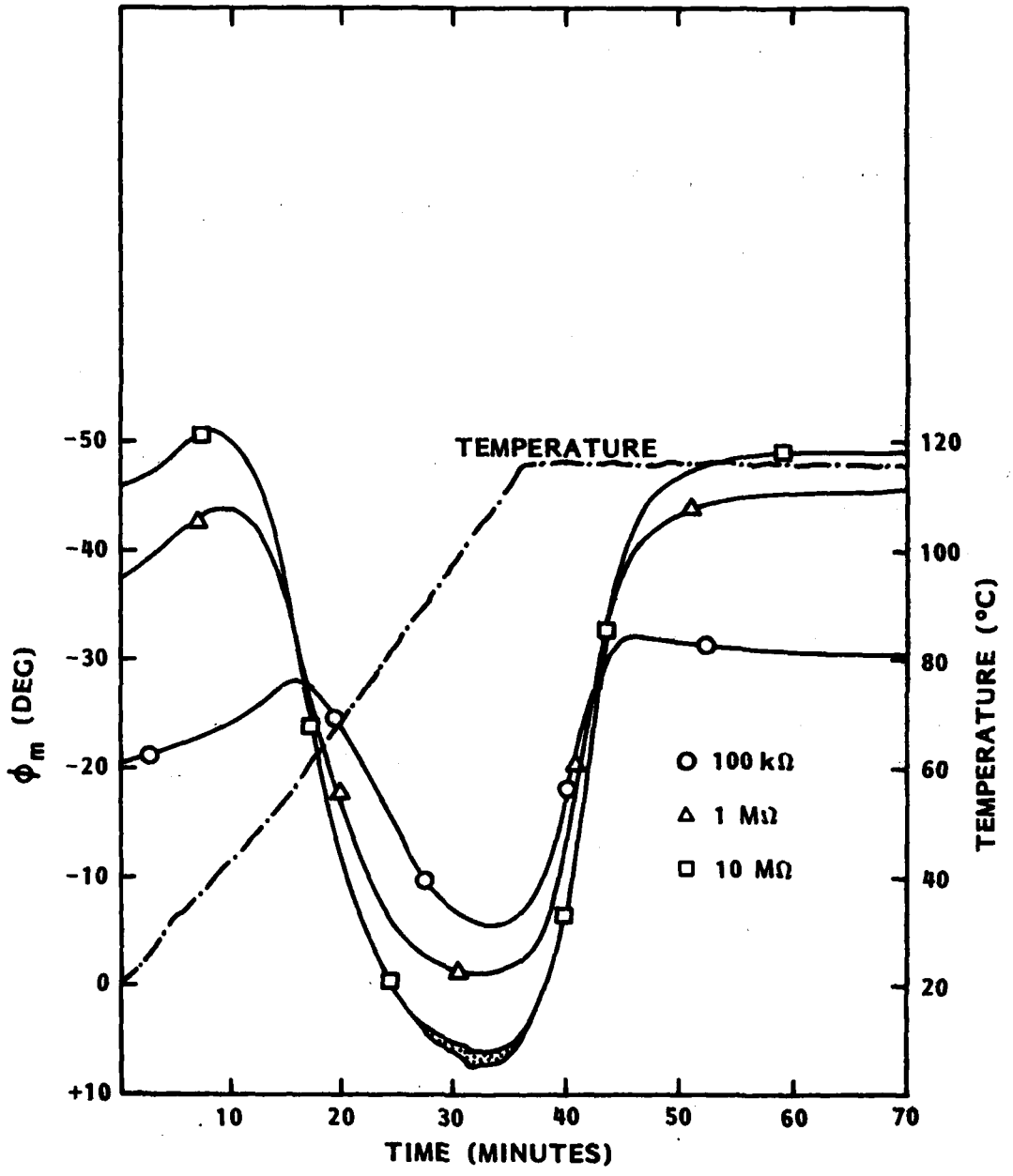

Fig. 3 Effect of Reference Resistor on Measured Phase Angle for FM-73 Adhesive.

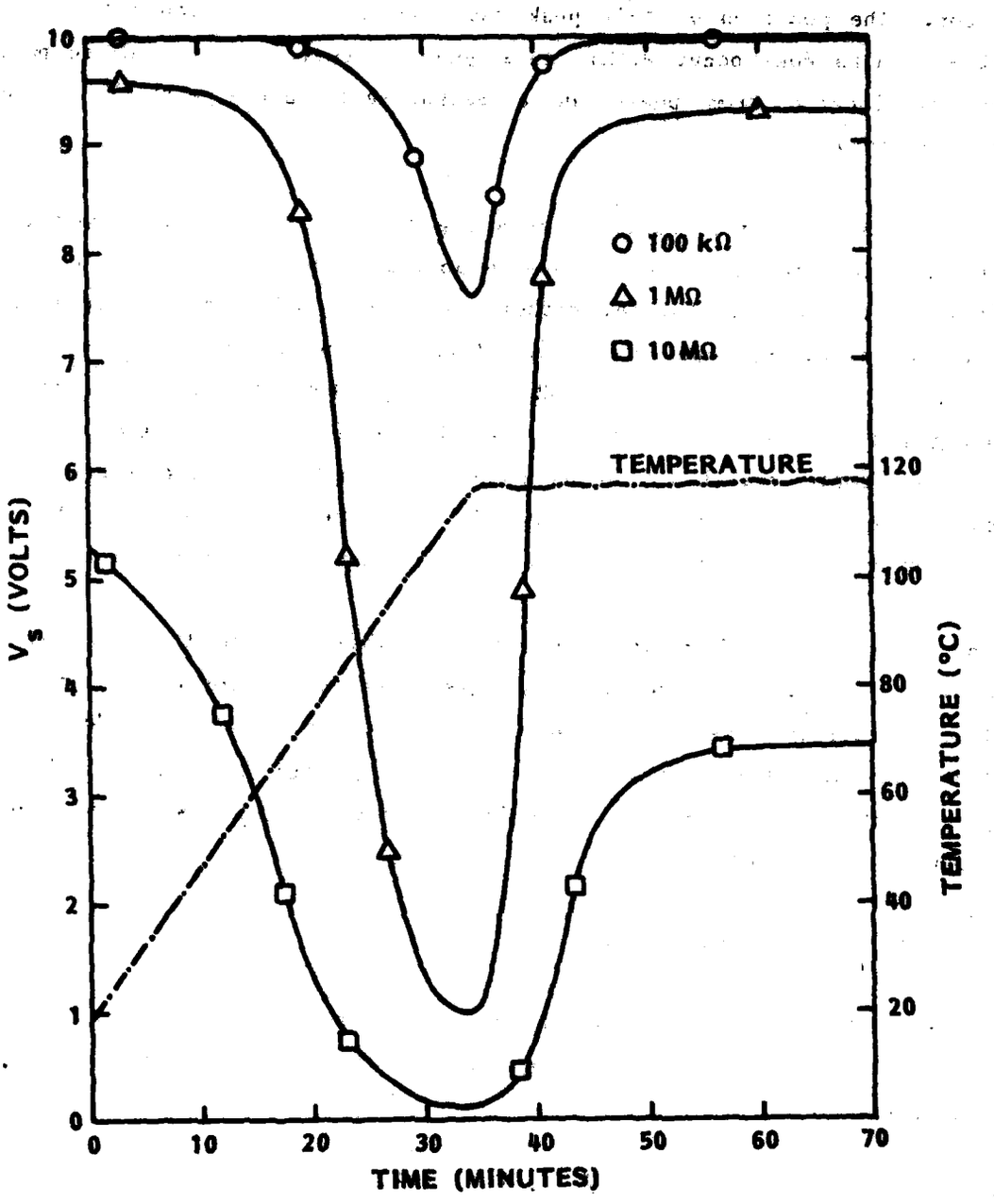

Fig. 4 Effect of Reference Resistor on Sample Voltage for FM-73 Adhesive.

resistor. The position of this peak has been associated with softening. No doubt softening does occur within this general area, but its precise position cannot be located from phase angle measurements alone without supporting analytical data.

Note also that the phase angle crosses the zero line and becomes positive for a 10 MΩ reference resistor. Since a positive phase angle for the sample defies physical interpretation, either the sample model or the assumption of negligible instrument impedance breaks down. The plots of sample voltage as a function of reference resistance show a similar but more dramatic trend. By choosing a low reference resistance, no change in sample voltage is apparent until the sample resistance drops sharply during cure. The sensitivity is enhanced significantly by increasing the reference resistor to 1 MΩ, with further enhancement at 10 MΩ, particularly in the initial portion of cure.

On the basis of signal definition and compatibility with the multiplexer in particular, a 1 MΩ reference resistor was selected for future cure monitoring studies. Recorded phase angles were found to vary by about 1 deg with and without the multiplexer in line for R_{ref} = 1 MΩ but by tens of degrees for R_{ref} = 10 MΩ. The effect of the multiplexer will be addressed at length in a following subsection.

b. Selection of Input Voltage

Inspection of the circuit diagram, Fig. 1, shows that the input voltage equals the sum of the voltage drops across the reference resistor and the sample, i.e.,

$$\vec{V}_{in} = \vec{V}_{R_{ref}} + \vec{V}_s \tag{19}$$

Increasing $\vec{V}_{in}$ by a scalar factor increases $\vec{V}_{R_{ref}}$ and $\vec{V}_s$ by the same factor.

Hence, the angles ϕ_m and α shown in Fig. 2 remained unchanged. Consequently, the angle ϕ_s also remains the same as shown by Eq. (1). The magnitude V_{in} has significance only as far as the signal-to-noise ratio is concerned. This is shown in Figure 5 where phasemeter readings are compared for V_{in} values of both 1 and 10 volts using a 1-MΩ reference resistor. An input of 1 volt is comparable to that used for the Audrey dielectrometer. A sizeable difference in sample voltage but little difference in phase angle is evident. When ϕ_s values were calculated for these runs and compared in Figure 6 it became clear that the input voltage was indeed a scaling factor which did not affect the dissipation factor, at least in the vicinity of the peak. This supported the analytical findings discussed earlier. The value of choosing a higher input voltage is to strengthen the signal-to-noise ratio. A significantly higher noise level is evident for the lower input voltage when the original data are compared. Thus, an input voltage of 10 volts appears satisfactory and will continue to be used for phasemeter monitoring.

3. Audrey/Phasemeter Comparison

Audrey and phasemeter data were compared for bondlines cured side by side in a single press run. Embedded foil probes were used in each bondline. The experimental setup was as follows: Two mil thick Kapton film separated the aluminum adherends from each of the press platens in order to satisfy the Audrey's requirement for isolation from ground. One Audrey lead was connected to a bondline probe and the other was connected to each of the corresponding adherends. The second bondline was monitored with the phasemeter by connecting the hot lead to a probe and by shorting each of the corresponding adherends to ground. Thus, the requirements for each method were satisfied while maintaining a single heating rate. The results are shown in Figure 7 where FM-73 bondlines at a controlled thickness of 0.0072 in. were monitored at a frequency of 1,000 Hz.

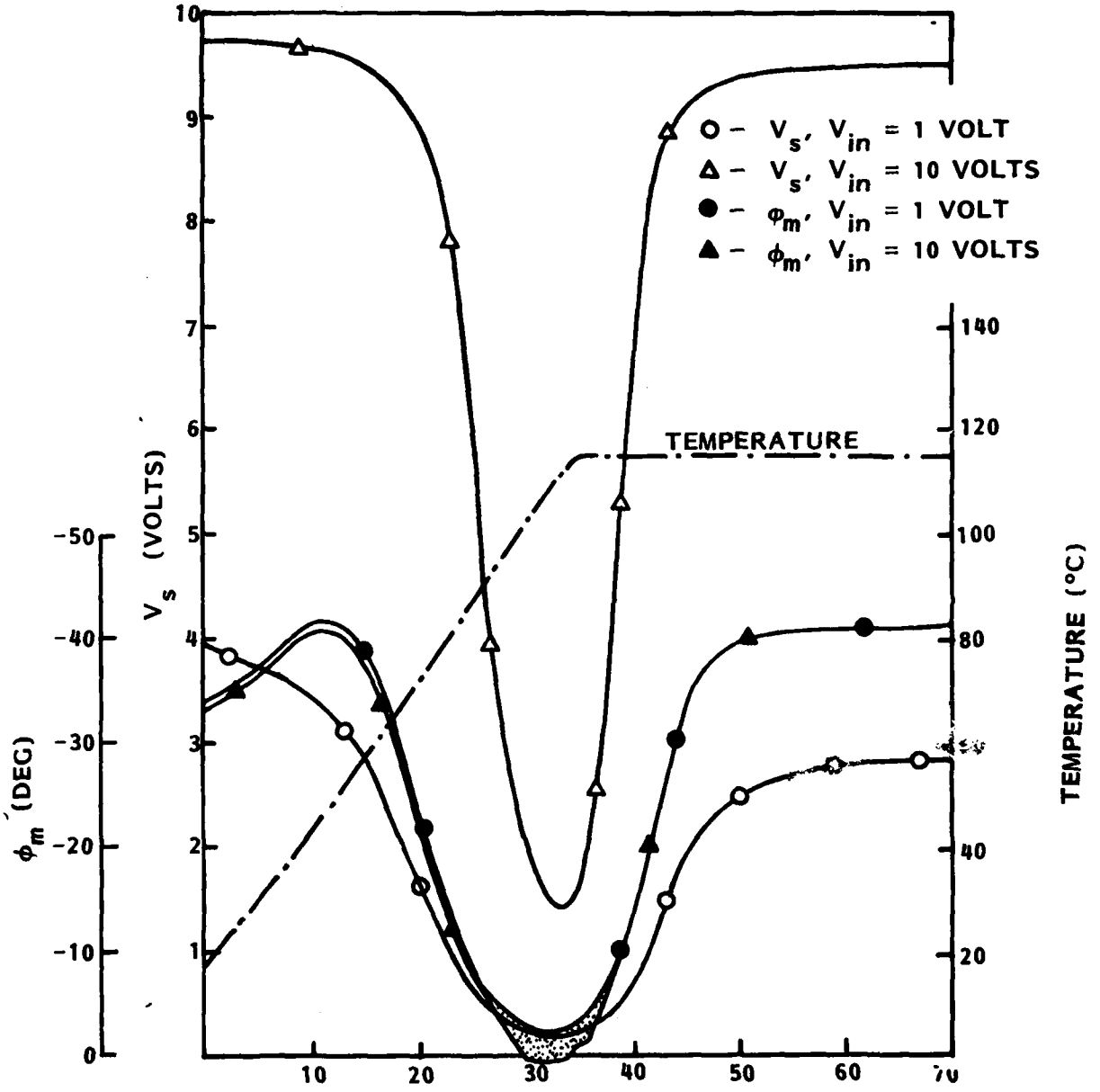

Fig. 5 Effect of Input Voltage on Phasemeter Monitoring Signals for FM-73 Adhesive

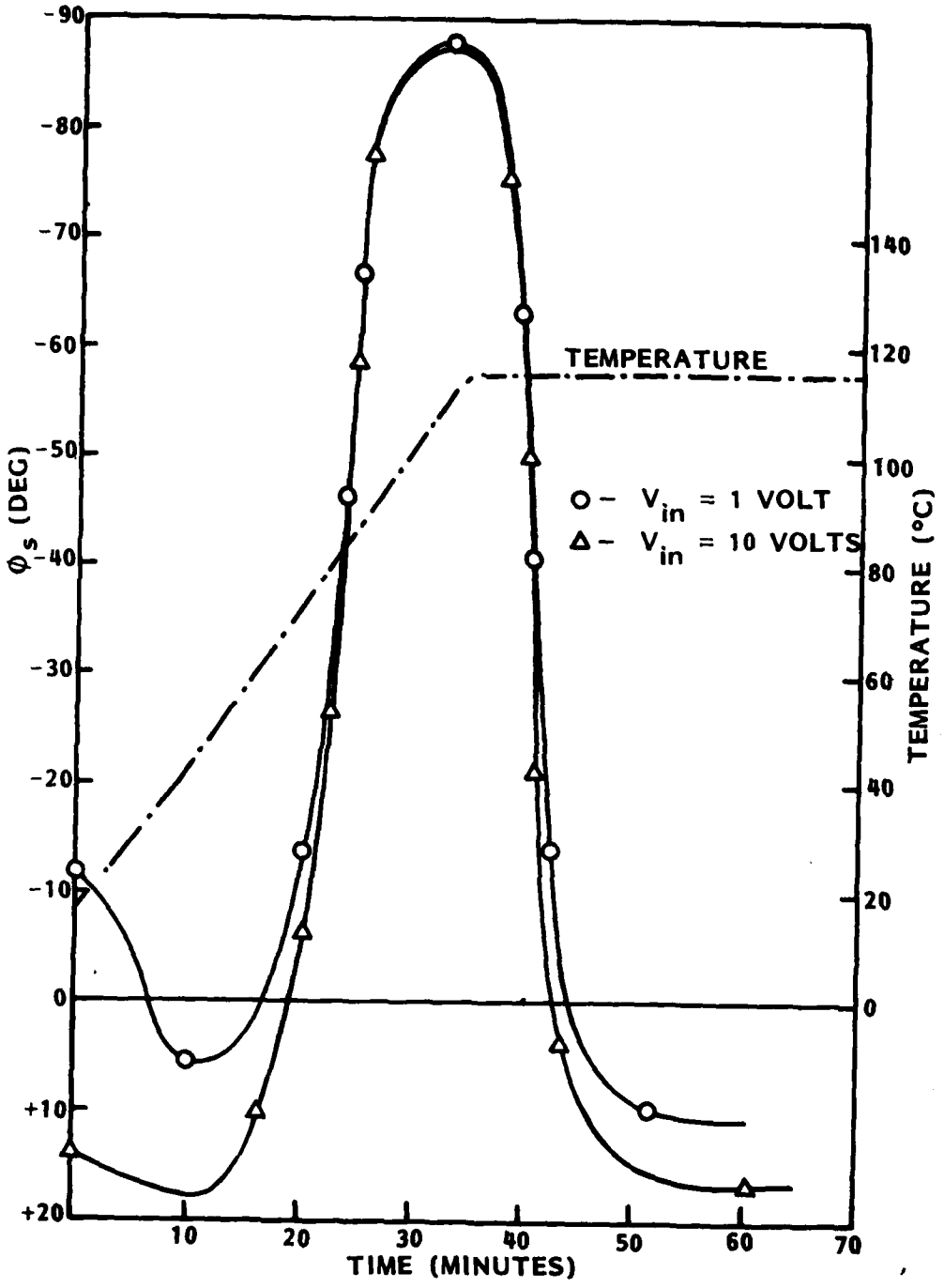

Fig. 6 Comparison of Derived Sample Angles for Phasemeter Input Voltages of 1 and 10 Volts. FM-73 Adhesive

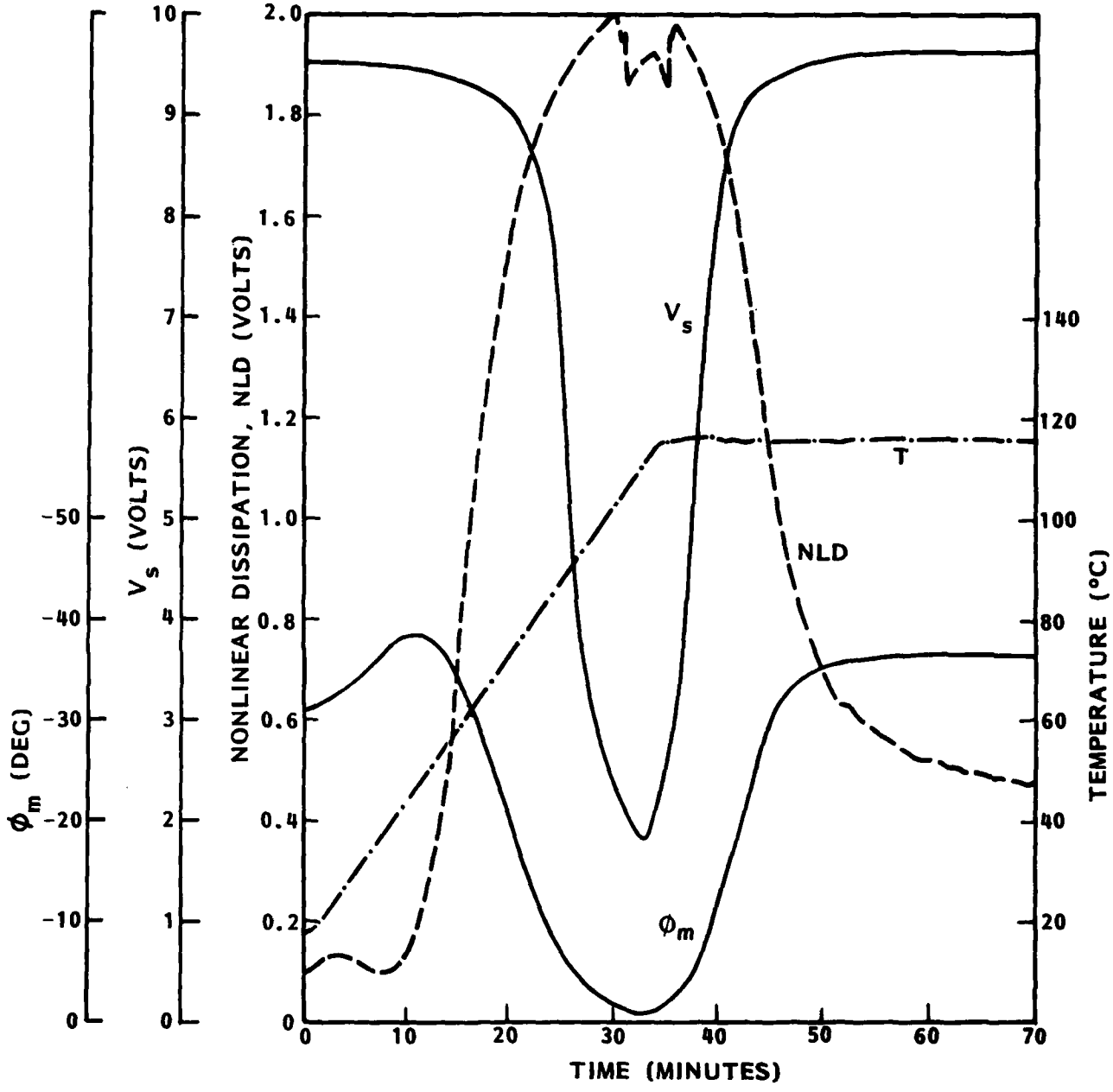

Fig. 7 Comparison of Audrey and Phasemeter Monitoring Signals for FM-73 Adhesive

The position of the initial peaks in ϕ_m and nonlinear dissipation (NLD) voltage vary considerably, but the maxima in LND voltage occurs over a comparable time frame to the minima for V_s and ϕ_m. Each technique provides useful data for bondline monitoring during cure. The data can be used to calculate the dissipation factor D = tan ϕ_s for each set of data. Audrey data are converted to a dissipation factor by using the vendor supplied calibration curve shown in Fig. 8 and phasemeter data are converted by using Eq. (8). Note that the Audrey data show a discontinuity near the 2-volt maximum which corresponds to an infinite dissipation factor.

A comparison of tan ϕ_s derived from both Audrey and phasemeter data is shown in Fig. 9 where the absolute value of tan ϕ_s is plotted vs. time. Notice how the abrupt dip in the original Audrey data between 30 and 35.5 minutes is greatly magnified. No rheological significance is attached to this disturbance because of its erractic nature. A smooth peak as shown by the phasemeter data is more realistic. Indeed, there is fair agreement between both experimental methods when the dissipation factors are compared. The major difference is the magnitude of the peak associated with minimum viscosity. Any differences in the initial features of the curves cannot be resolved on this scale.

Although the difference in tan ϕ_s peak heights appear quite large in Fig. 9, corresponding values of ϕ_s shown in Fig. 10 are actually quite similar. Comparing data in this fashion minimizes peak difference but accentuate differences in ϕ_s on either side of the peak. Plotting the data on a semi-log scale is more desirable, but because both algebraic signs of ϕ_s are obtained a semi-log scale presents another problem. This problem may be circumvented by plotting absolute values and noting positive and negative regions.

Another Audrey/phasemeter comparison was made using similar data treated in the same way for which phasemeter reference resistors of 1 and 10 MΩ were used. The results are shown (Fig. 11) on a semi-log scale where the absolute value of tan ϕ_s is plotted vs. time. For this Audrey curve a smooth

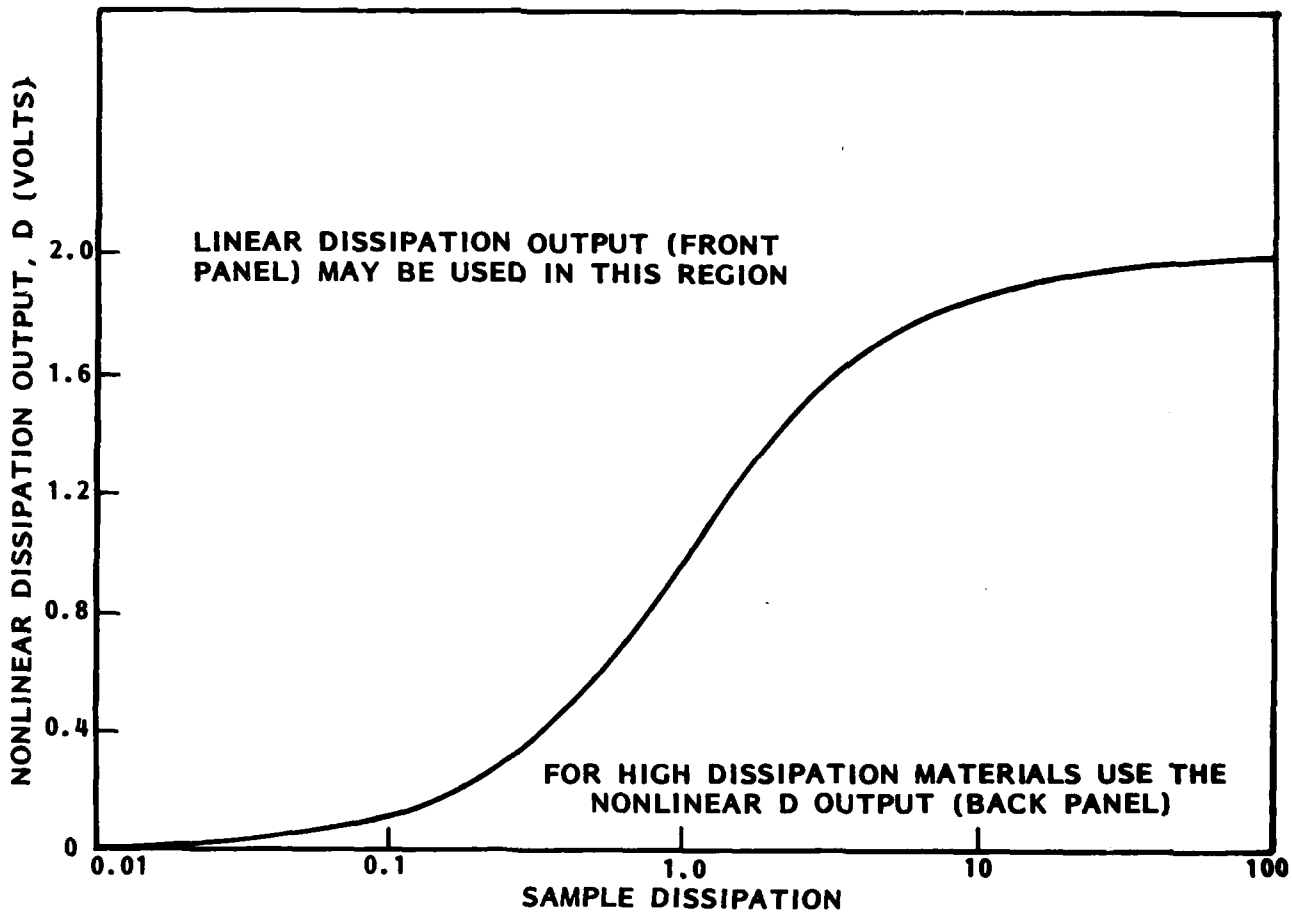

Fig. 8 Audrey Calibration Curve Relating NLD Voltage to Sample Dissipation.

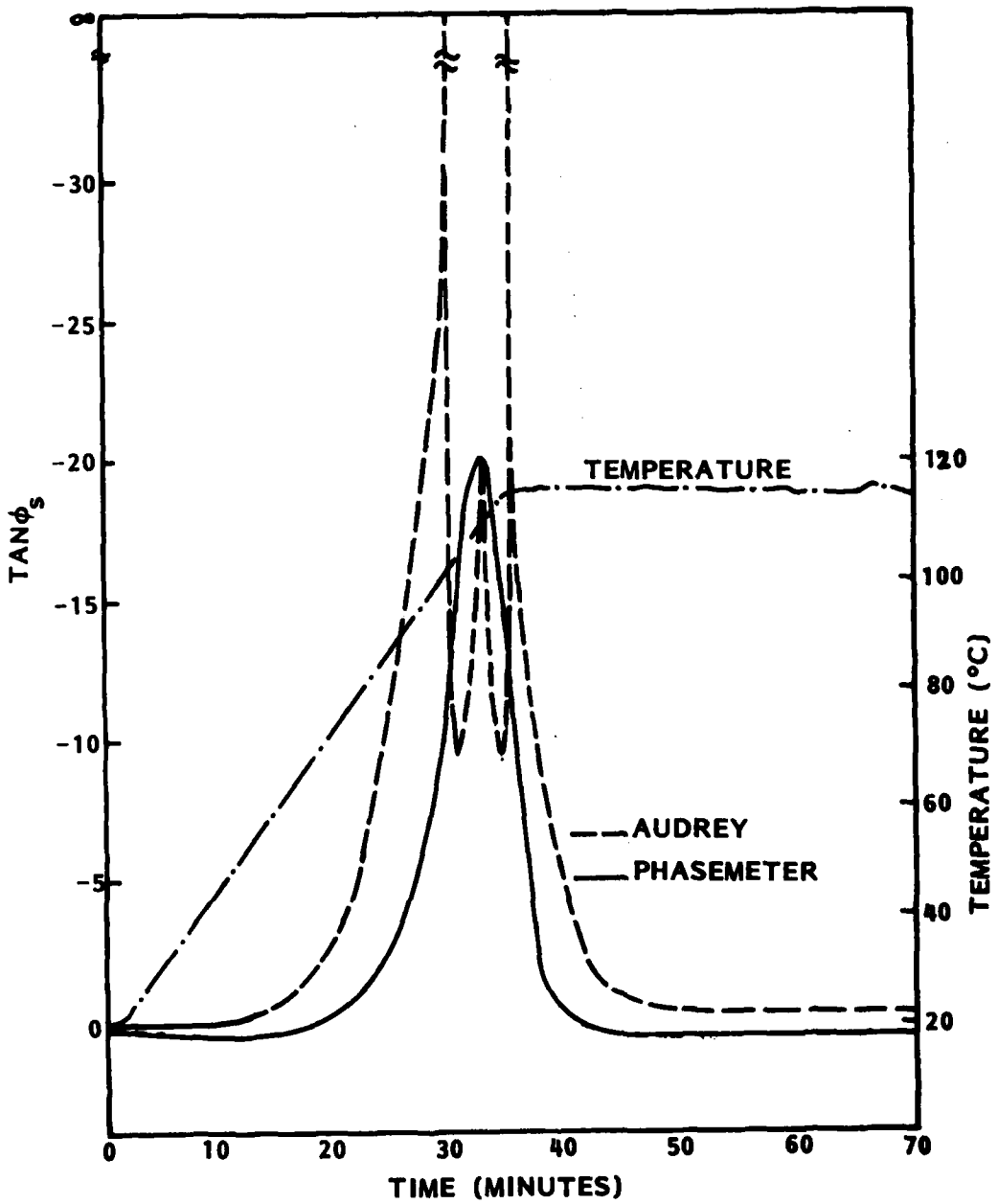

Fig. 9 Comparison of Dissipation Factors Derived From Audrey And Phasemeter Data For FM-73 Adhesive.

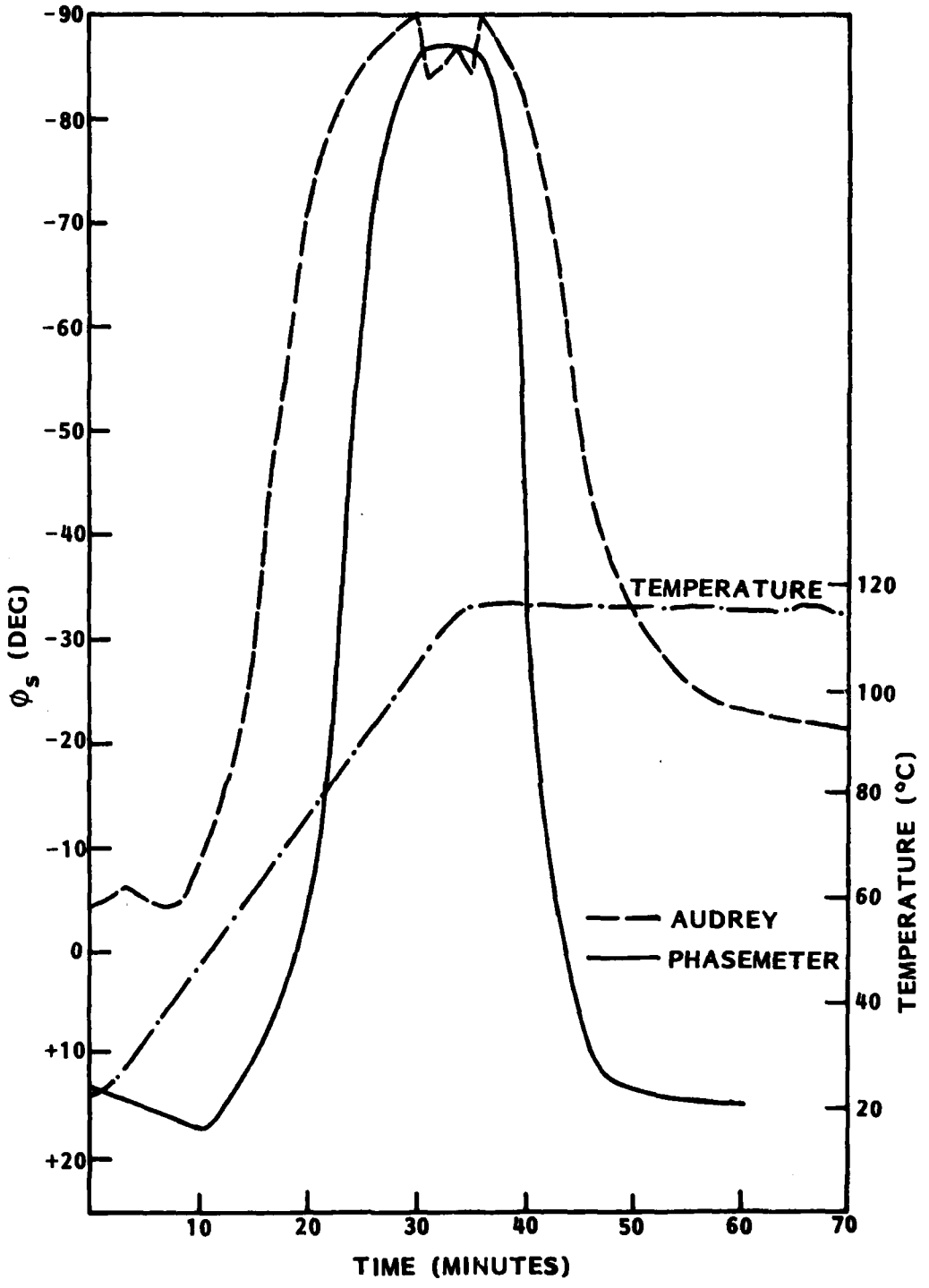

Fig. 10 Comparison of Sample Phase Angle Derived From Audrey And Phasemeter Data For FM-73 Adhesive.

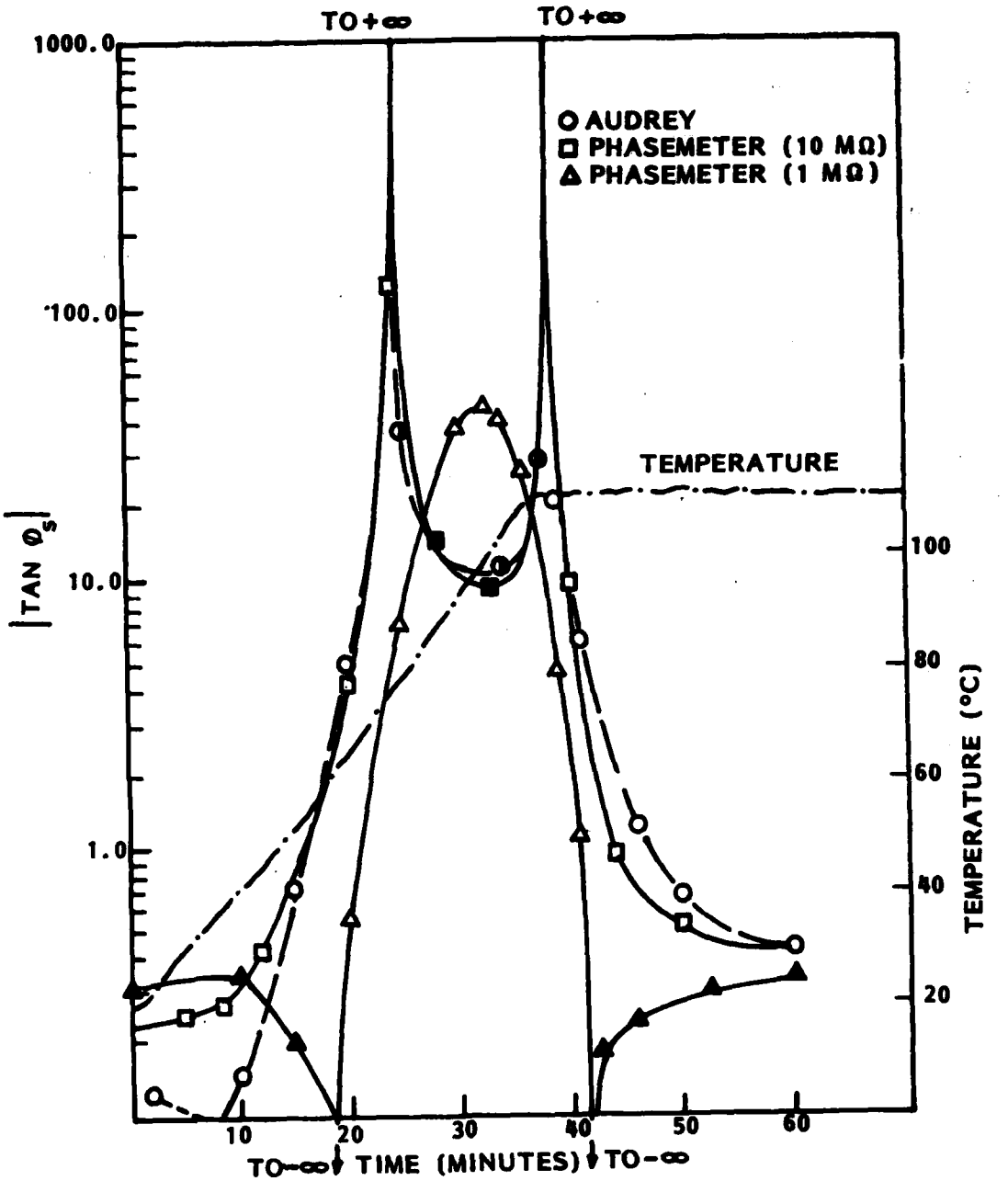

Fig. 11 Comparison of Absolute Values of Dissipation Factor Derived from Audrey and Phasemeter Data for FM-73 Adhesive. Filled symbols represent positive values of tan ϕ_s; hollow symbols, negative ones; and half-filled symbols, assumed positive ones.

dip appeared in the region of maximum dissipation. Note that the mirror image of this dip around the maximum voltage level seems to continue the truncated peak. In the case of the 10 MΩ phasemeter data, the calculations show that the dip in the curve between these times corresponds to positive ϕ_m values. Since tan ϕ_m and tan ϕ_s are inversely proportional as shown by equation (18), a sign change from negative to positive for ϕ_m corresponds to a discontinuity from $-\infty$ to $+\infty$ for tan ϕ_s. Because of the excellent agreement between the Audrey and phasemeter results in this region, the origin of the Audrey dip is similiarly explained. Positive phase angles lack a physical interpretation and are thought to arise from failure of the simplistic model used for both the Audrey and phasemeter the circuit analysis.

Note that by diminishing the magnitude of the reference resistor from 10 to 1 MΩ lower dissipation factors are obtained and the maximum ϕ_s no longer exceeds 90 deg. While the previous discontinuities are avoided, two new discontinuities arise at 19 and 41.5 minutes. Values of tan ϕ_s between these times are negative while remaining values are positive. These discontinuities arise when the product tan ϕ_m tan ϕ_s exceeds unity in equation (8), however, no physical significance can be attached to them. In fact, equation (18) which also relates tan ϕ_s and tan ϕ_m has no provision for one phase angle being negative and the other positive. This appears to be an artifact but we have no explanation for it.

4. Variation of Probe Area

Two variations in probe size were investigated with Audrey and phasemeter instrumentation. The first variation was a rectangular strip measuring 1/4 in. wide x 3 in. long and the second was a flag-shaped section measuring 1 in. x 1 in. in the square area and 1/4 in. x 2 in. in the adjoining tail. One inch of each probe was embedded in a bondline during monitoring so that there is a fourfold difference in area between variations. As the adhesive (FM-73)

flowed during heating there was a small expulsion of the probe from the bondline, typically 1/16 in. or less. Only the nominal probe area was considered. All probes were cut from 2 mil thick aluminum foil and carefully burnished to remove sharp edges.

The effect of probe area on dielectric monitoring signals is shown in Figs. 12 and 13 for Audrey and phasemeter measurements, respectively. There is very little difference in the Audrey curves initially but a significant difference appears in both the peak region and in the level of the final plateau. It appears that the larger probe area causes a higher NLD voltage. These differences would be highly magnified if the data were replotted to show the dimensionless dissipation factor corresponding to these voltages. The phasemeter data (Fig. 13), gathered under comparable conditions, show a very distinct difference in V_s with the larger voltage drop corresponding to the larger probe area. Phase angle readings are higher for the smaller area probe on both sides of the curve's minimum, but the curves cross one another in between. The crossover points may be related to the discontinuities discussed in Section 3 since they occur at similar times. When the data for ϕ_m and V_s are used to calculate tan ϕ_s, it becomes apparent that the larger probe area leads to a higher peak dissipation factor as shown in Fig. 14. This finding is consistent with that observed qualtitatively for the Audrey.

A significant effect due to probe area appears surprising since the dissipation factor is a material and frequency parameter. The explanation may be traced to edge effects introduced by a probe since the mathematical analysis treated the case with capacitor plates of equal area.

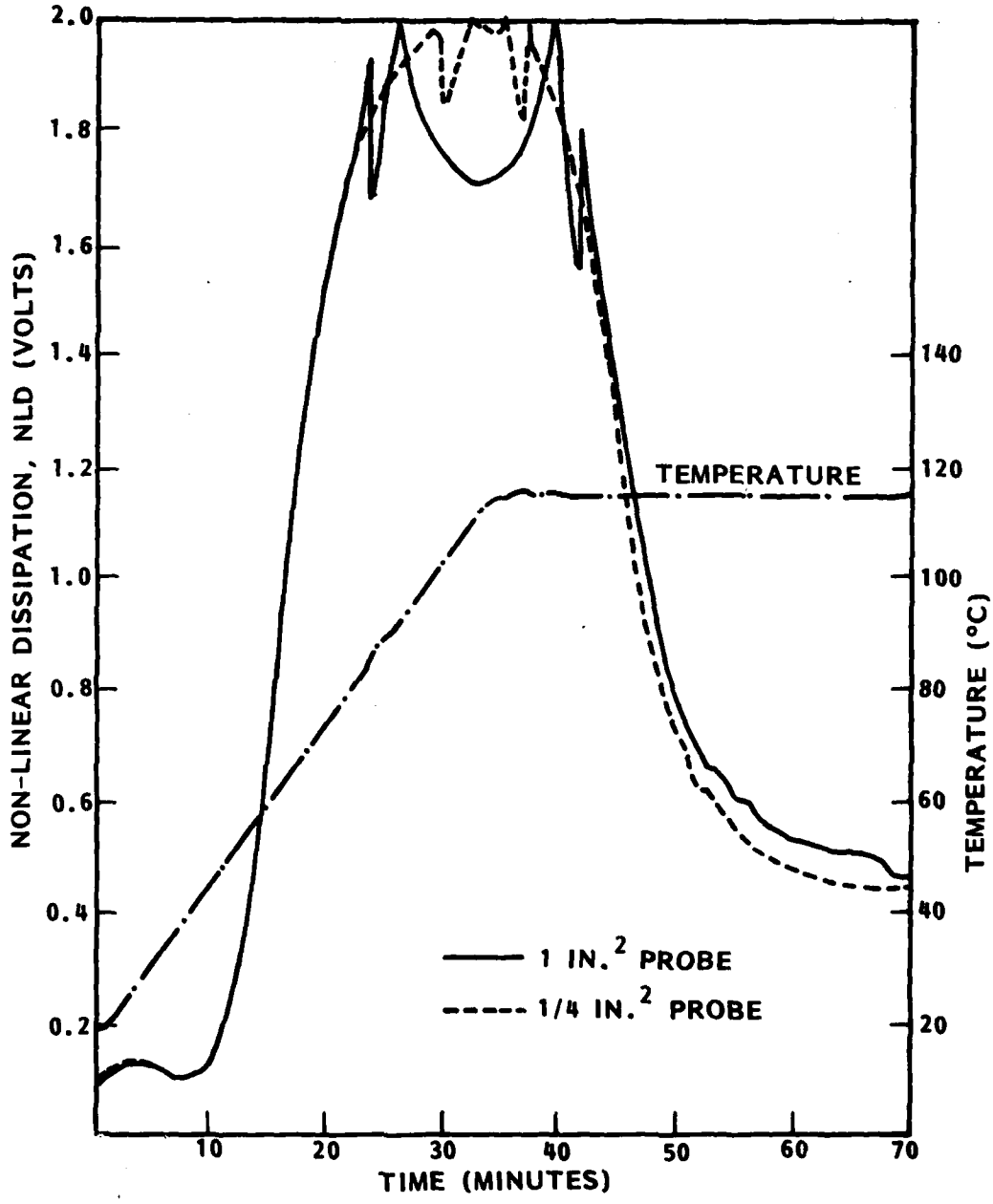

Fig. 12 Effect of Probe Area on Audrey Monitoring Signal For FM-73 Adhesive.

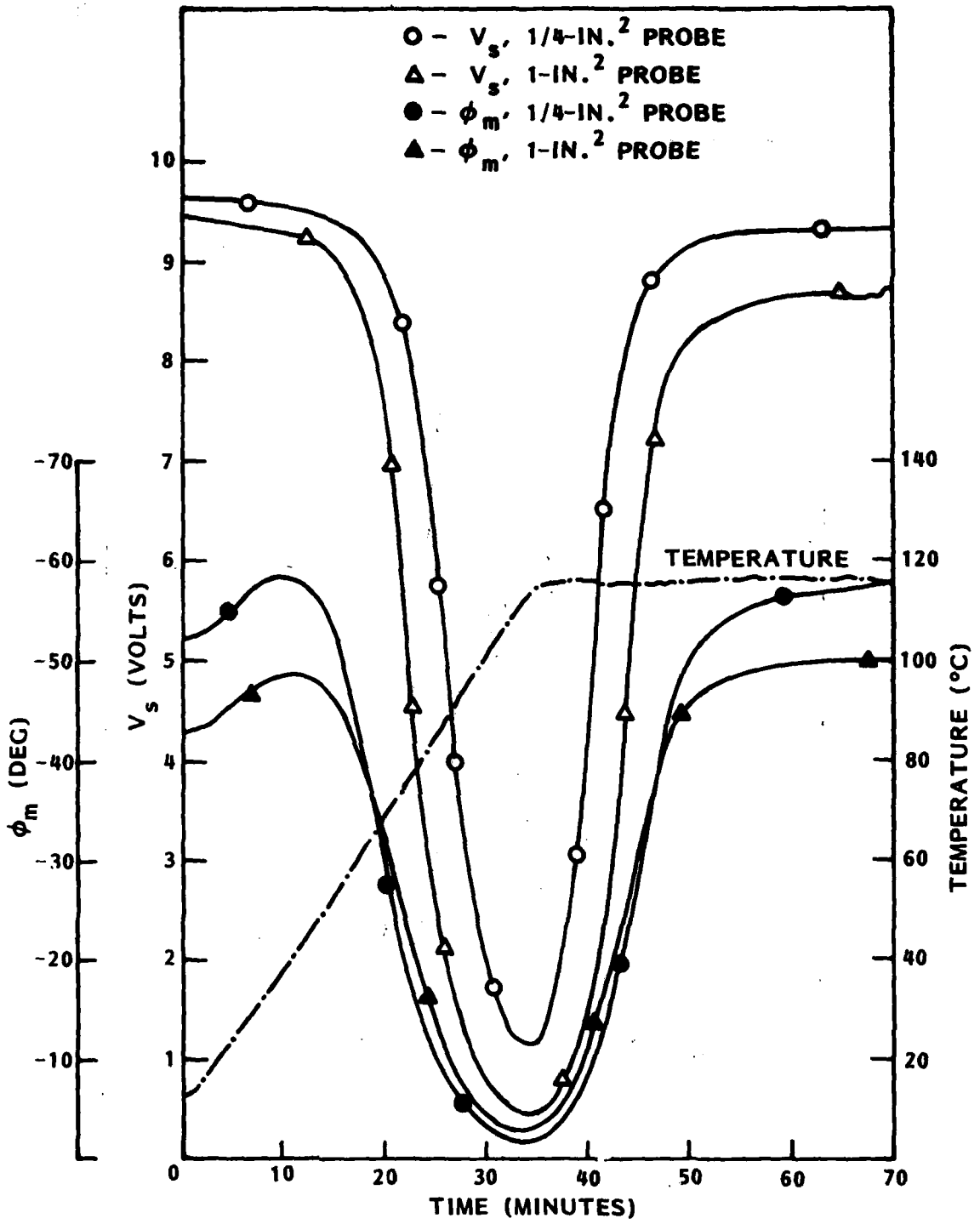

Fig. 13 Effect of Probe Area on Phasemeter Monitoring Signal for FM-73 Adhesive.

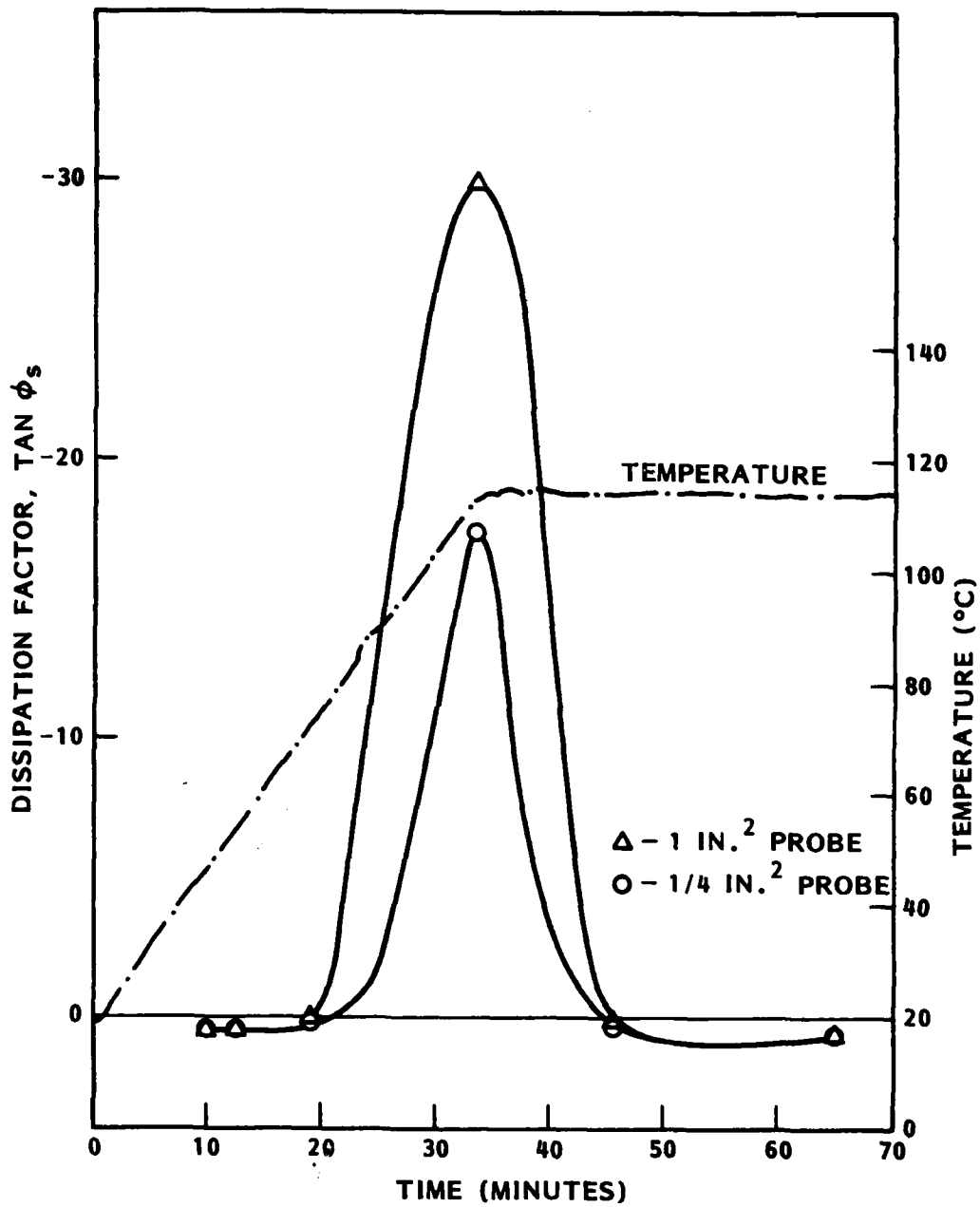

Fig. 14 Effect of Probe Area on Dissipation Factor Derived From Phasemeter Measurements For FM-73 Adhesive.

5. Variation of Bondline Thickness

Three adhesive thicknesses were monitored by the embedded probe technique in order to determine the effect of thickness on dielectric monitoring signals. Both the Audrey and phasemeter were used for bondline monitoring.

Two bondlines, each controlled to 0.0055 and 0.0072 in., contained one full layer of supported adhesive. A small adhesive patch in the immediate vicinity of the probe prevented the probe from shorting to the opposite adherend. The third bondline, controlled to 0.020 in., contained three full layers of supported adhesive. The probe was located asymmetrically between a single and a double layer of adhesive.

The results for the phasemeter appear in Fig. 15. The greater the thickness, the greater the voltage drop across the sample.

When Eq. (8) was used to calculate corresponding values for dissipation factors, the results shown in Fig. 16 were found. The peak dissipation factor increases as bondline thickness decreases. According to Eqs. (8) and (17), the dissipation factor should not depend on thickness, at least for a homogeneous bondline. In a supported bondline the impedance may change with thickness, depending on the distribution of the scrim within the adhesive.

It is interesting to note that large differences between maximum tan ϕ_s values observed with thickness in Fig. 16 are the result of much smaller differences in ϕ_s values as shown in Fig. 17. Note that ϕ_s values bordering the base of the dissipation peak are positive. This is clearly shown when ϕ_s is plotted as the ordinate but minimized when tan ϕ_s is used instead. As mentioned earlier each choice for the ordinate tends to emphasize different features of the data.

The Audrey data for these same three thicknesses show much more subtle differences. In Fig. 18 the curves for NLD voltage show very little differences except in the peak region and the approach to the final plateaus. The

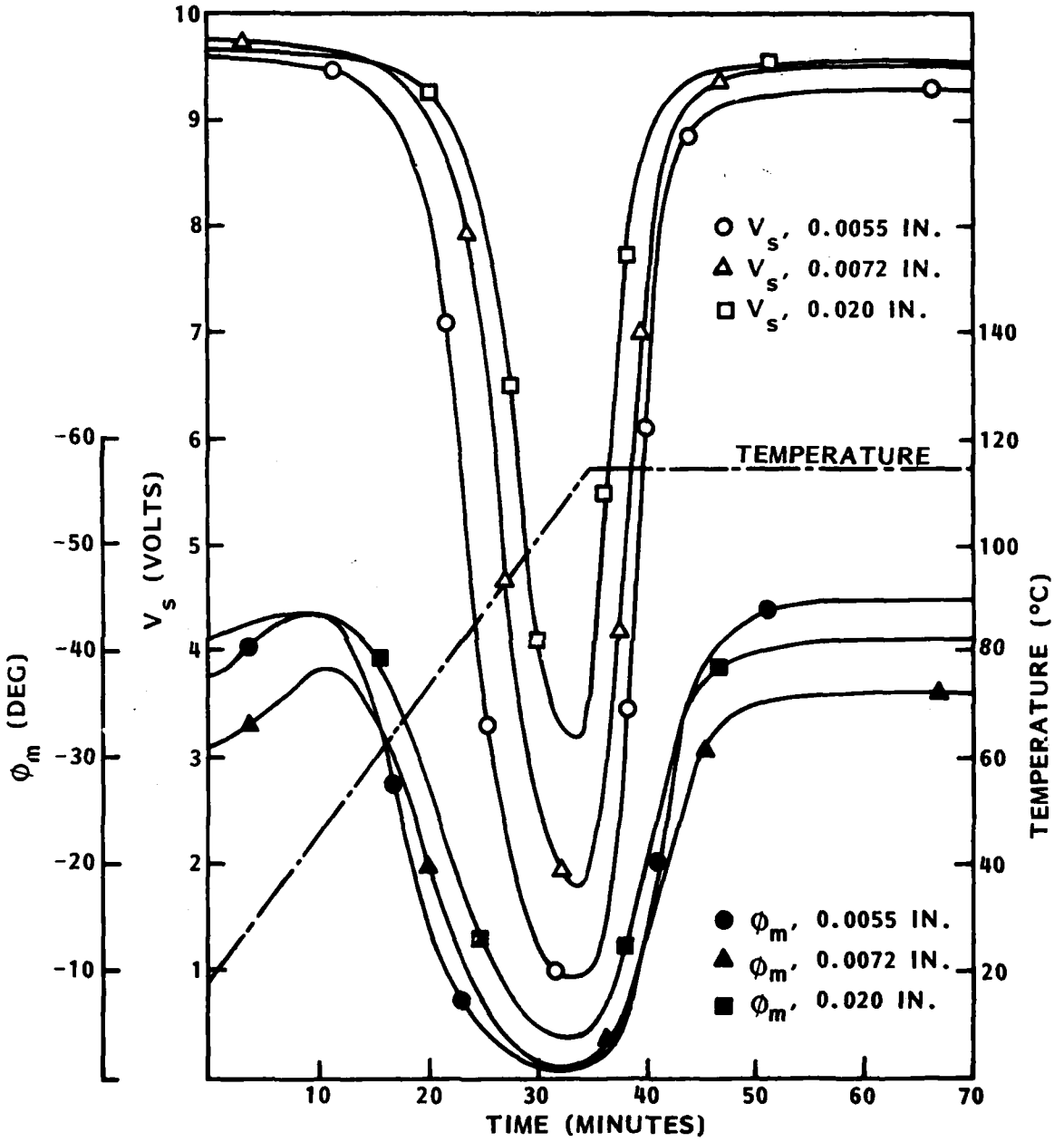

Fig. 15 Effect of Bondline Thickness of Phasemeter Monitoring Signals for FM-73 Adhesive.

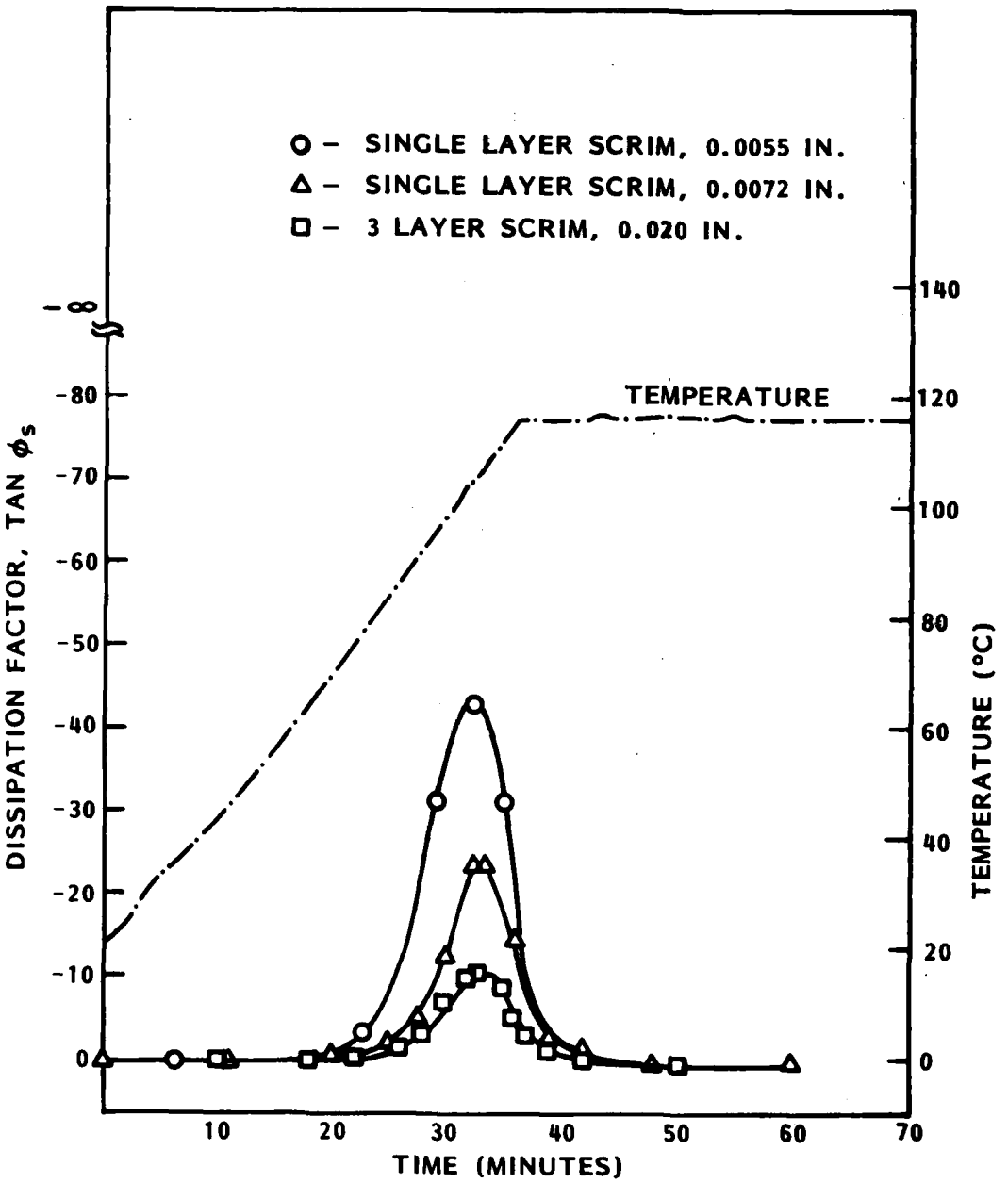

Fig. 16 Effect of Bondline Thickness on Dissipation Factor Derived From Phasemeter Data For FM-73 Adhesive.

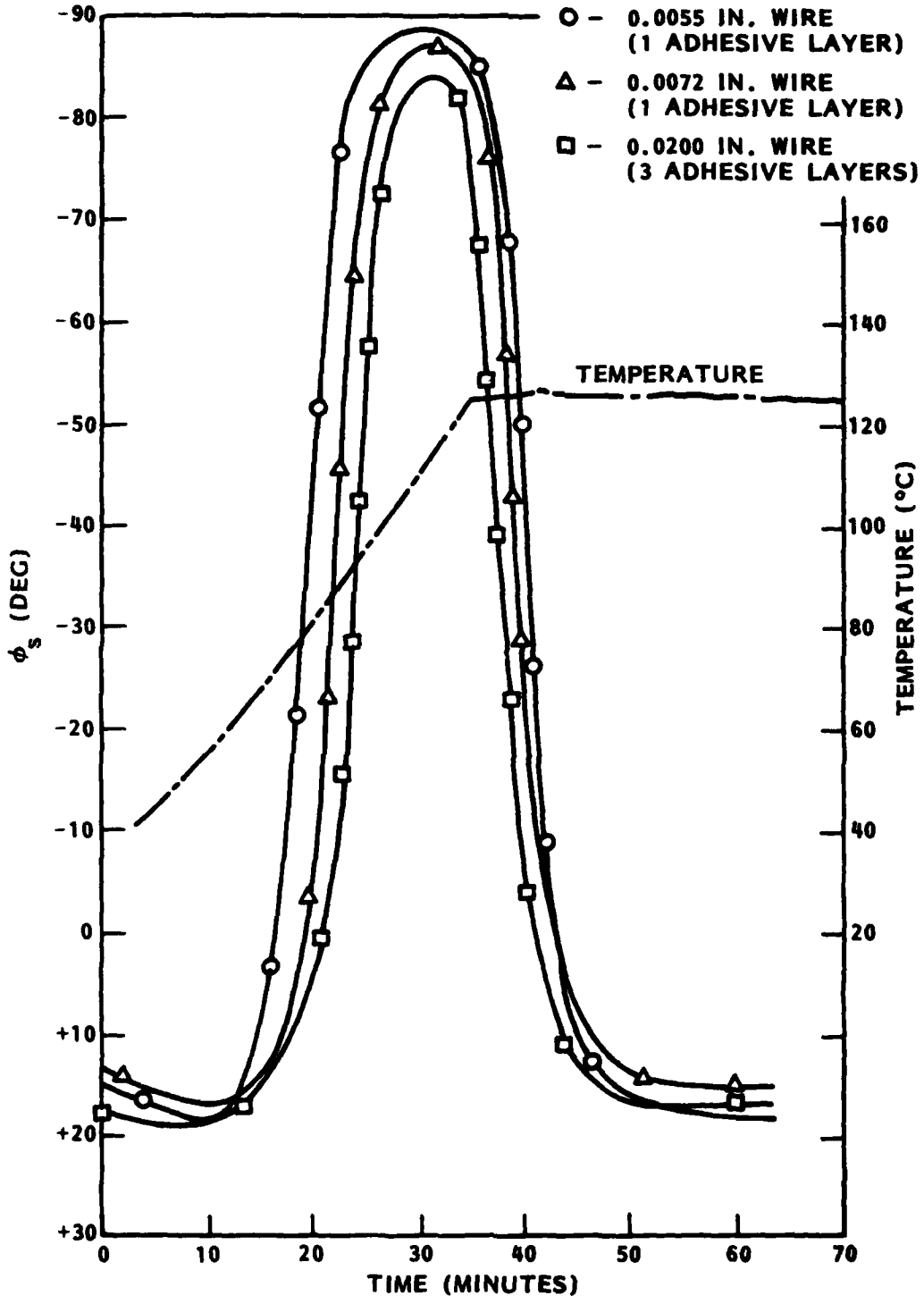

Fig. 17 Effect of Bondline Thickness on Sample Phase Angles Derived From Phasemeter Data For FM-73 Adhesive.

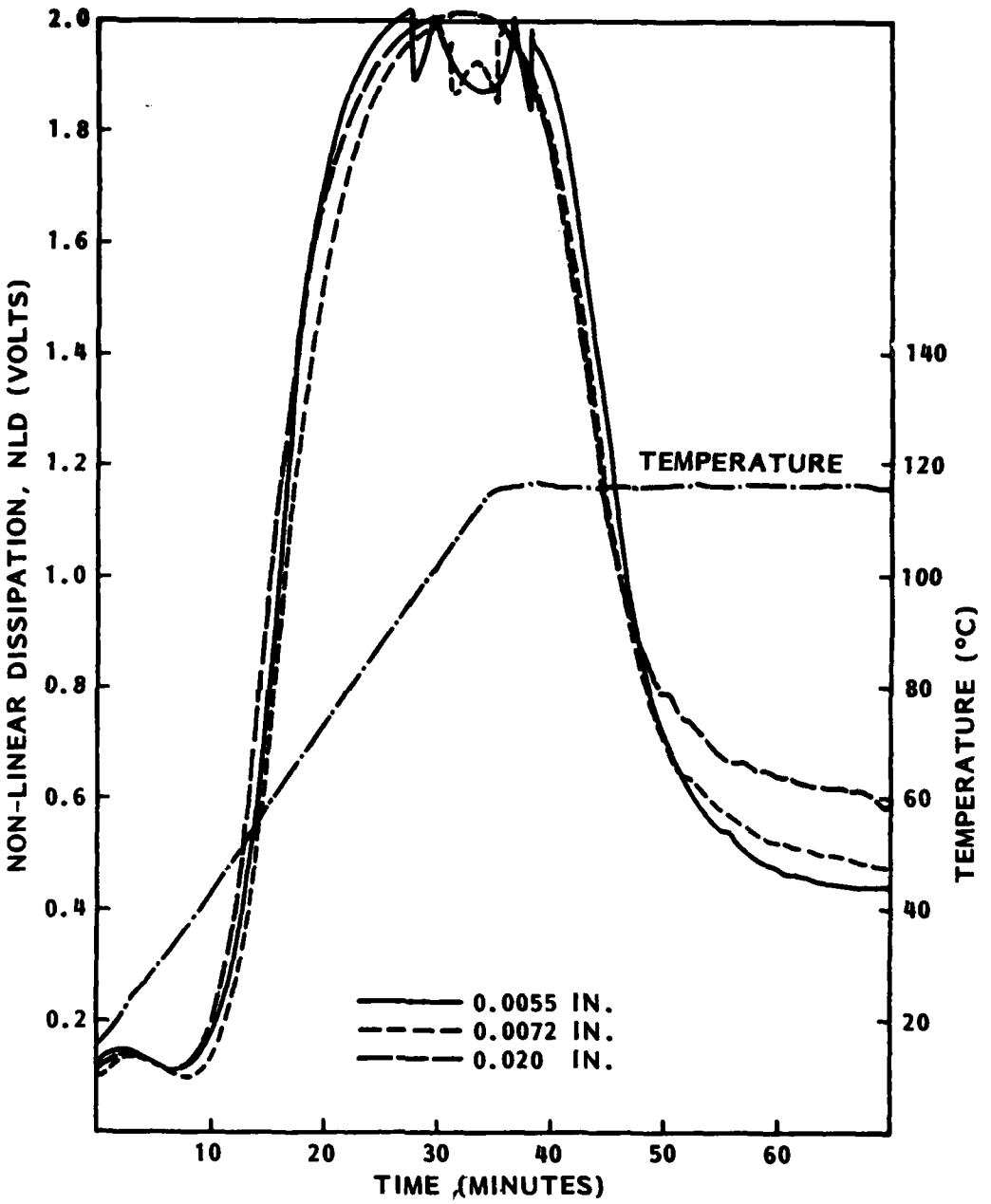

Fig. 18 Effect of Bondline Thickness on Audrey Monitoring Signal for FM-73 Adhesive.

dip associated with the 0.0055 in. bondline suggests a phase angle in excess of 90 deg, whereas the 0.020 in. bondline indicates a phase angle less than 90 deg in the same region. Thus a higher peak dissipation factor can be associated with thinner bondlines.

In the plateau region the NLD voltage is highest for the thickest bondline. The phaseometer data show no such trend in the same time frame, even when plotted as ϕ_s in Fig. 17.

Therefore, dielectric monitoring signals may be quantitatively used to predict bondline thickness if a correlation between bondline thickness and peak dissipation factor can be verified.

6. Effect of Frequency on Signal Response

Frequency variation for the Audrey ranged between 100 and 1,000 Hz, whereas variation for the phasemeter ranged between 50 and 1,000 Hz. Earlier experimentation with the phasemeter was conducted at a frequency of 5,000 Hz. Working with 1,000 Hz showed no appreciable difference and allowed a direct comparison with the Audrey results. Bondline thicknesses were held constant with wire spacers.

Audrey results obtained with the self-contained frequency sweep generator are shown in Fig. 19. Discrete frequency runs at 100, 250, and 1,000 Hz show comparable results as shown in Fig. 20. There appears to be a shift to higher temperatures with higher frequency for the small peak appearing at about 3 minutes. The shift may be used to calculate an activation energy characteristic of the molecular motion involved in the transition. The large peak shows significant broadening with a decrease in frequency but no observable shift in peak temperature. The shift may not be apparent because of the simultaneous end of temperature rise. Both peaks are quite erratic at very high dissipation levels; possibly as a result of a dielectric breakdown. For future quantification of signal features, a frequency of 1,000 Hz appears preferable by virtue of better curve definition.

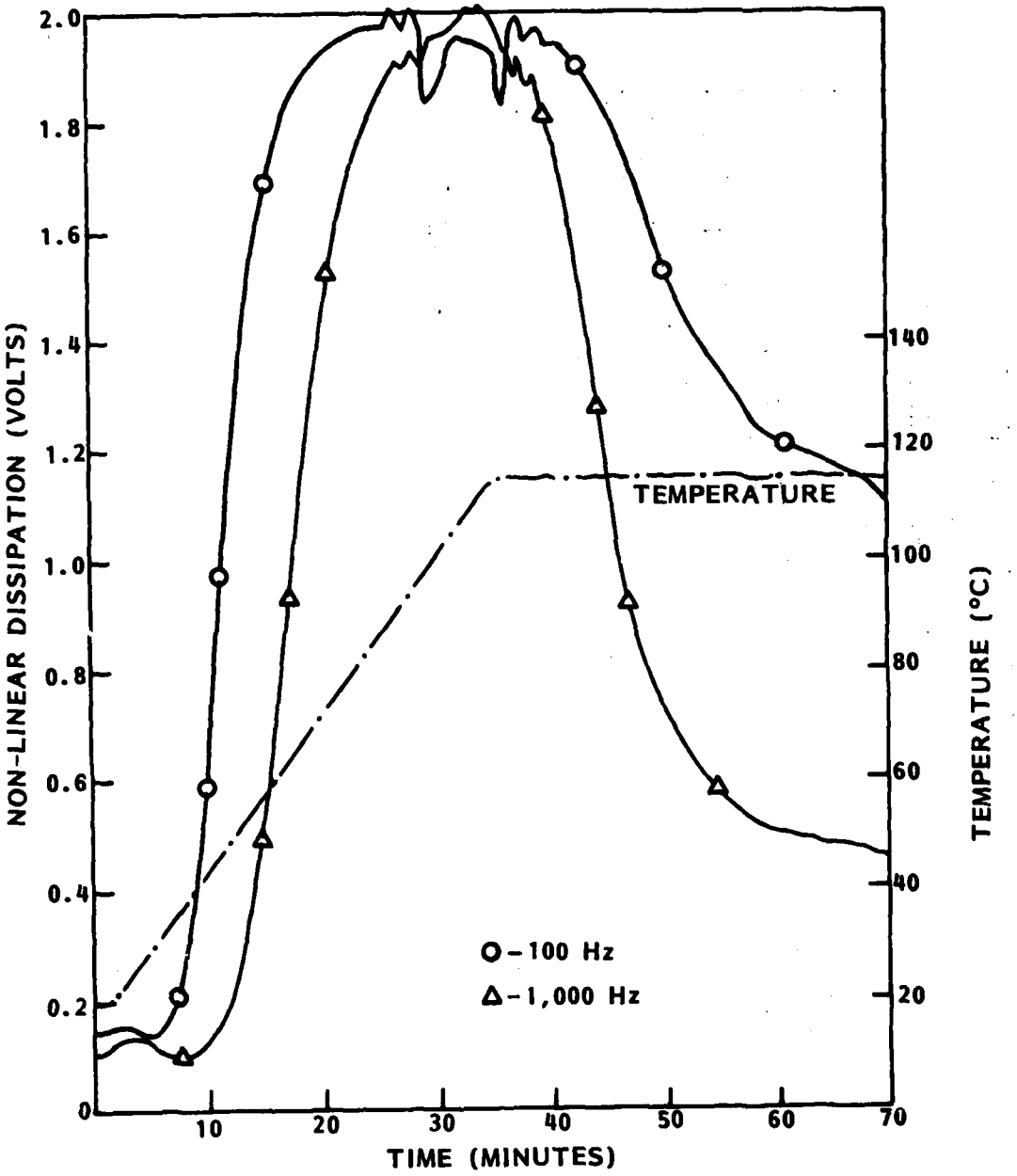

Fig. 19 Effect of Sweeping Frequency on Audrey Monitoring Signal for FM-73 Adhesive.

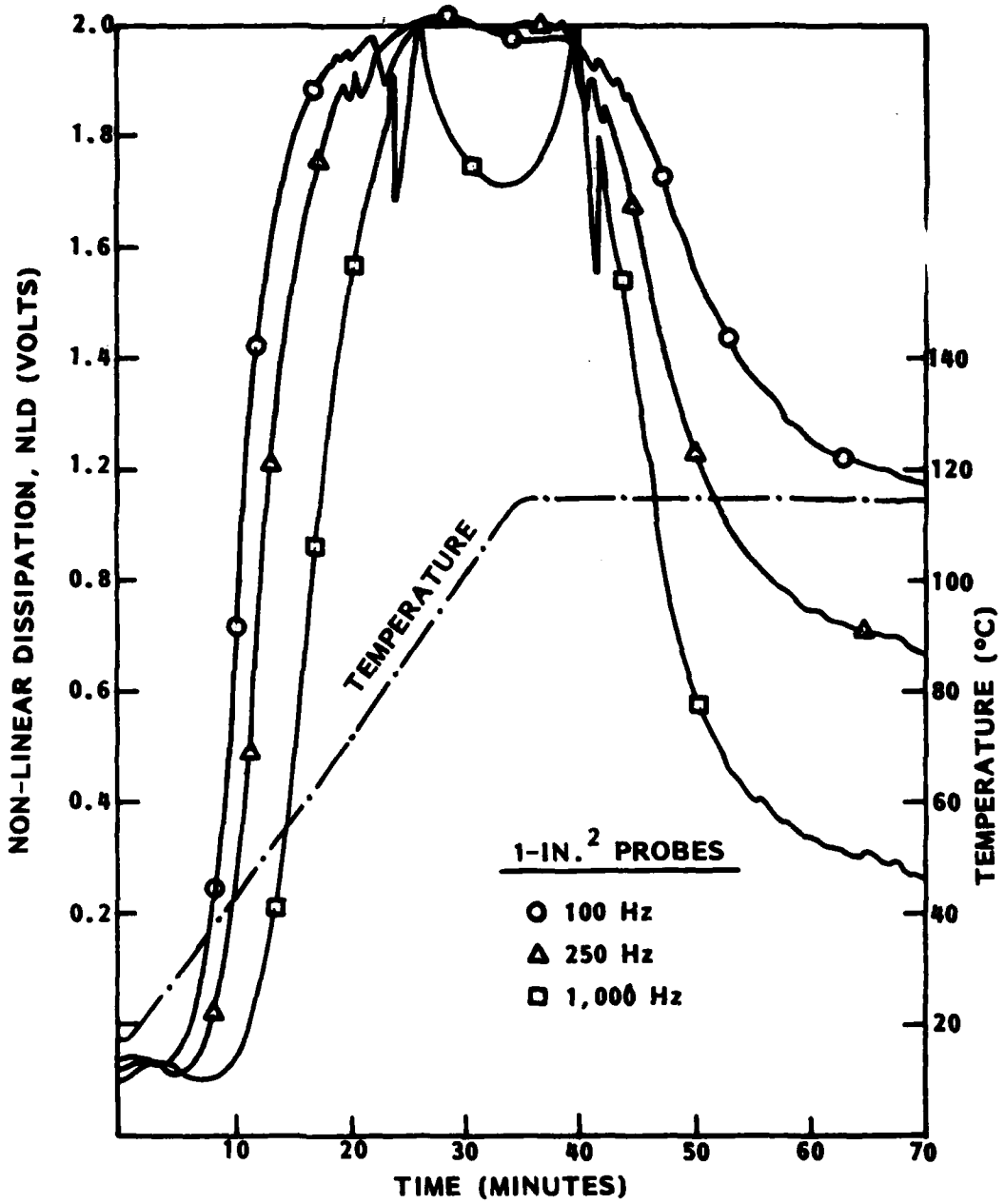

Fig. 20 Effect of Frequency on Audrey Monitoring Signal For FM-73 Adhesive.

Phasemeter results are shown in Figs. 21 and 22 for frequencies of 50, 250, and 1,000 Hz. Sample voltages are quite similar for frequencies of 50 and 250 Hz. The magnitude of the 1,000 Hz response is slightly diminished and the whole curve is shifted to a higher temperature. Since each sample was individually cured, some variation of heating rate occurs from run to run despite the temperature controller. The heating rate was found to be slightly slower for the 1,000 Hz run so that a slower cure could be expected. This is precisely what the monitoring curves show. Thus any affect of frequency on sample voltage is minimal. However, this is not true for phase angle. The shape of the curve changes dramatically as the frequency is progressively lowered to 50 Hz. A valley at 1,000 Hz gives rise to a peak at 50 Hz. The rheological implications of this apparent inversion are being investigated by calculating the corresponding dissipation factors.

7. Limitations of the Multiplexer

Phase angle curves for four samples, each connected to a single multiplexer channel, gave a maximum range of about 1.5 deg during a run. This is considered good sample reproducibility. The multiplexer can be used to advantage when single channels are used for samples with similar impedance. Difficulties arise when switching between circuits with large differences in impedance values. Consider the case where three reference resistors were multiplexed through a single adhesive bondline as discussed below.

a. Channel Effect on Phase Angle

Sample responses and frequencies have been multiplexed with various numbers of channels for ease in recording responses for the phasemeter. The effect of doing this on the phase angle has been explored. Four different probes in the

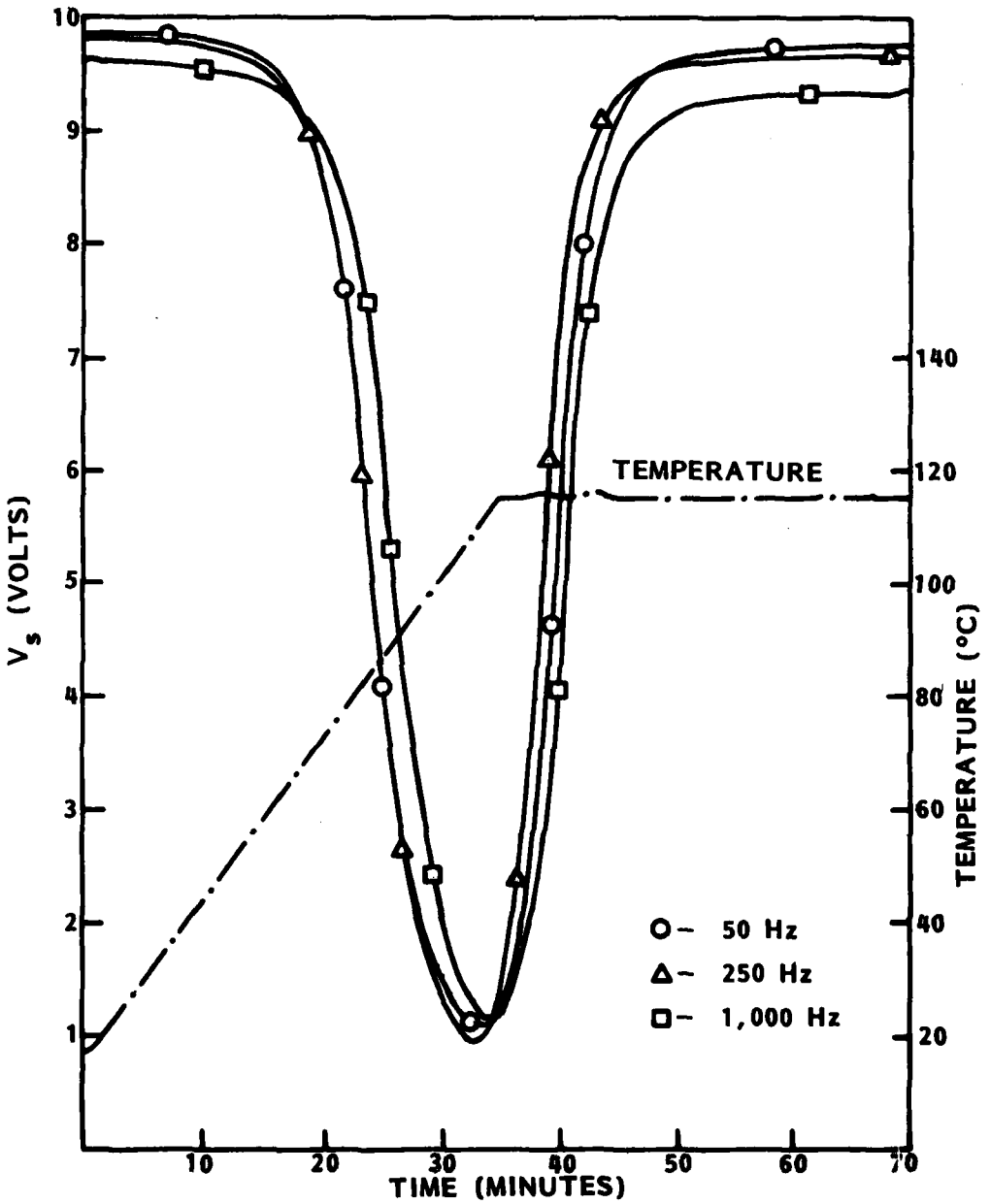

Fig. 21 Effect of Frequency on Sample Voltage for FM-73 Adhesive.

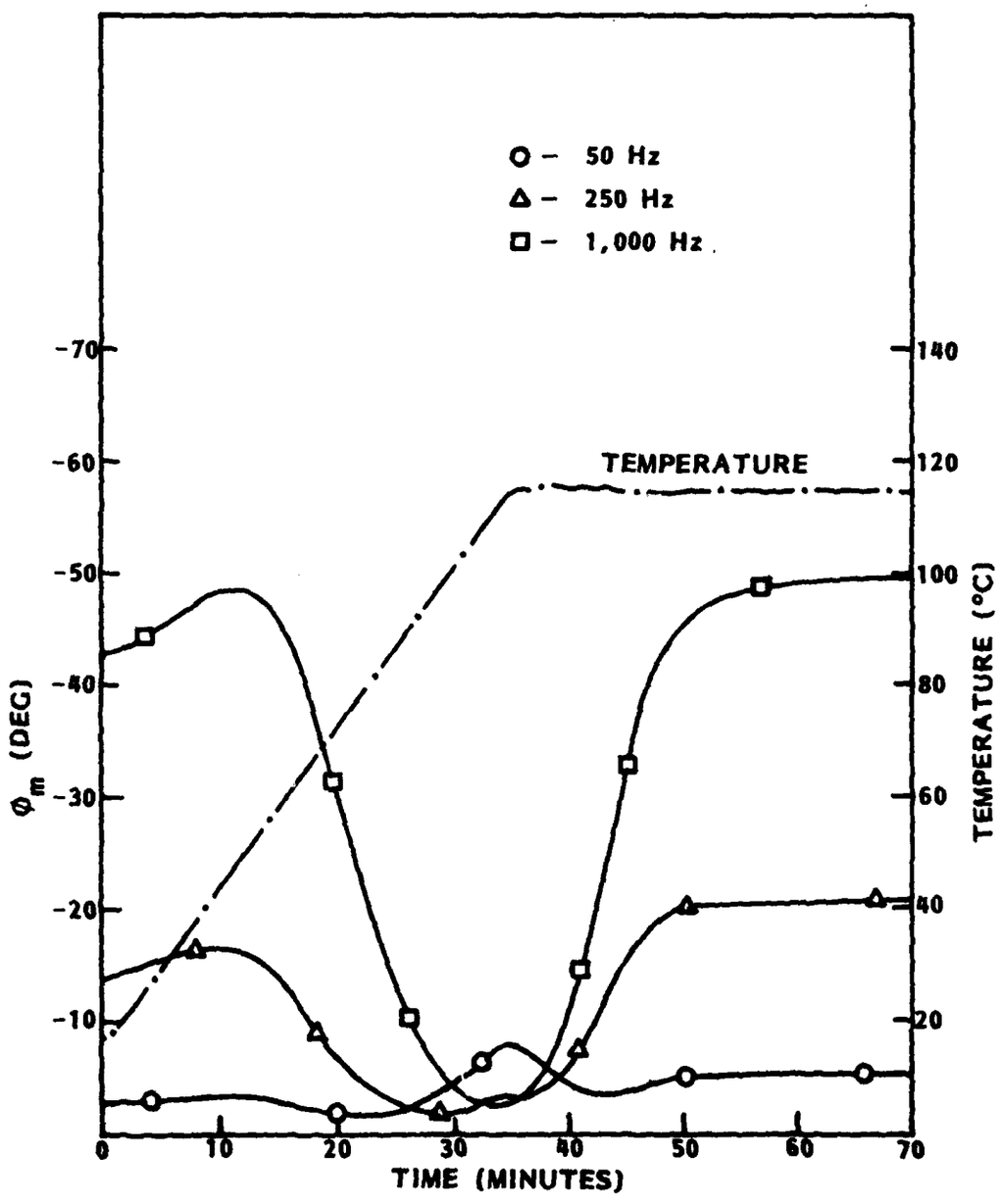

Fig. 22 *Effect of Frequency on Measured Phase Angle for FM-73 Adhesive.*

same bondline, each with the same shape and area, were monitored in various multiplexer channel combinations with the following results:

Sample No.	Channel Combination	Initial Phase Angle (deg)
A	0	-41.98
B	1,2	-44.25
C	3,4,5	-47.26
D	6,7,8,9	-48.23

There is more than a 6-deg difference between the lowest and highest values. To check whether this difference was due to sample variation, channel variation, or the number of channels used per sample, two other experiments were run. In the first, each sample was checked using the same channel with the following results.

Sample No.	Channel	Phase Angle (deg)
A	0	-41.84
B	0	-41.90
C	0	-42.22
D	0	-41.91

The sample range is small, only 0.38 deg.

In the second experiment, sample A was checked in each of the first four channels, showing a maximum difference between these four channels of 0.1 deg. Therefore the phase angle increases as the number of channels used per sample increases.

In another experiment, the following combination was tried with these results:

Sample No.	Channel	Phase Angle (deg)
A	0	-42.06
B	1	-42.12
C	2	-42.98
D	3	-42.38

Switching samples B and C reversed the readout, so this difference can be attributed to the samples. A check of the voltage drop relative to ground gave 3.496 volts for sample C, with the other three being 3.586, 3.582, and 3.565 volts, respectively, for A, B, and D. Reversing input and output to the multiplexer changed the phase angle by 0.5 deg.

b. Multiplexing Reference Resistors

Three reference resistors were multiplexed, each with a different number of channels. A 100-kΩ reference resistor used two channels, a 1-MΩ resistor three channels, and a 9-MΩ resistor, four channels. Frequency used was 1,000 Hz with 0.0055-in. spacing and one-quarter square inch probes in the bondline. This run is comparable to the runs reported in Section II.5 without the multiplexer, with the exception of a 9-MΩ value rather than a 10-MΩ resistor. The circuit with multiplexer is shown in Fig. 23.

The sample voltages with the multiplexer are shown in Fig. 24. Comparing these to runs without the multiplexer in Fig. 4, the shape and position of the 100-kΩ and 1-MΩ curves are very similar. The voltage drop with the 10-MΩ reference resistor is much smaller (except near the minimum) than with the 9-MΩ reference resistor, which is reflected in the shallower curve starting and ending at a lower voltage. The large difference between the 9-MΩ and 10-MΩ sample voltage response is surprising.

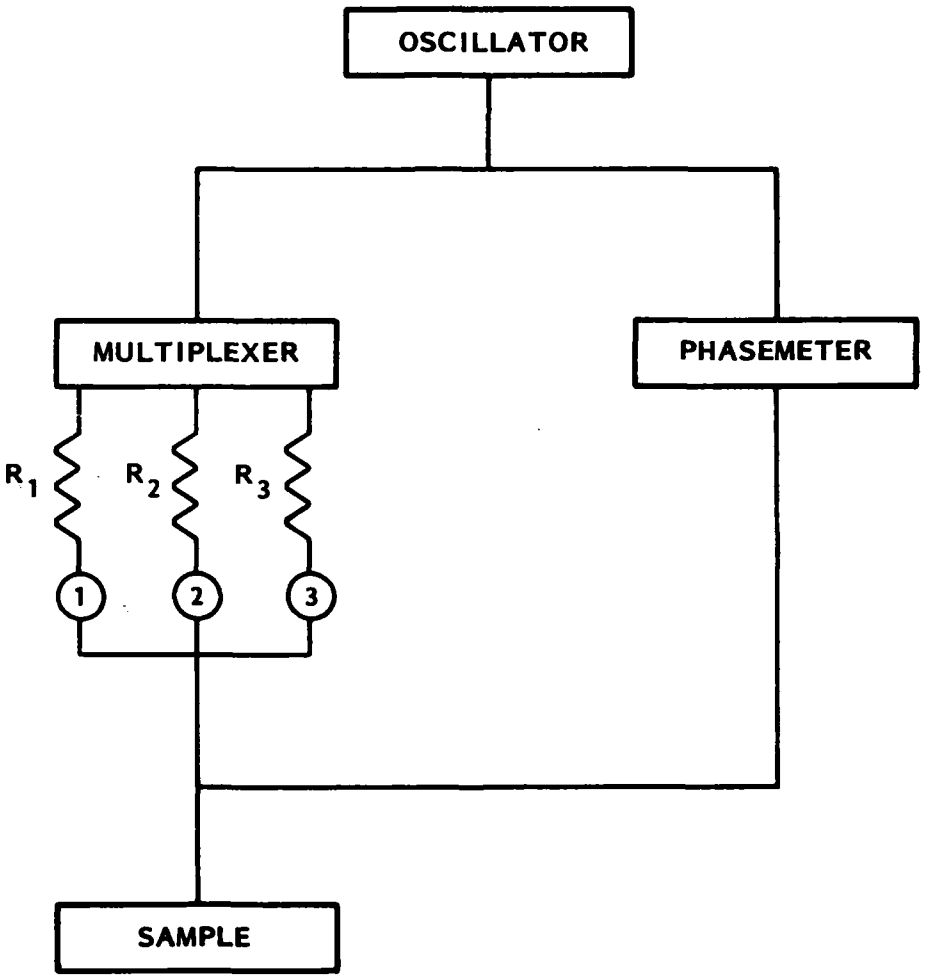

Fig. 23 Reference Resistor Multiplexing Circuit

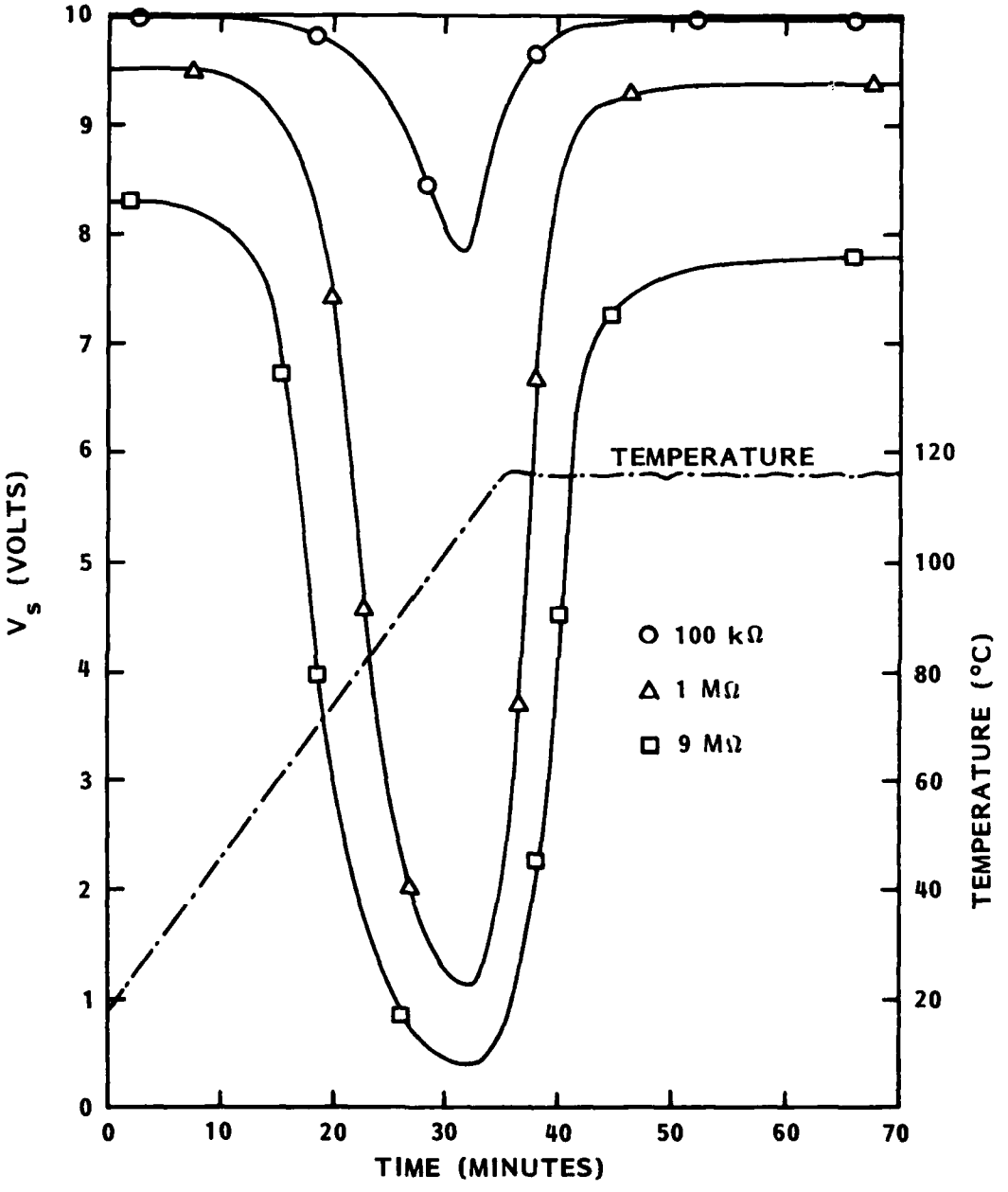

Fig. 24 Effect of Reference Resistor on Measured Sample Voltage For FM-73 Adhesive With Multiplexer.

In Fig. 25 the phase angles become much more positive with use of the multiplexer, up to plus 55 deg at the minimum in the case of a 9 MΩ reference resistor. Even though the shapes and ranges of the phase angle curves for multiplexed and nonmultiplexed reference resistors (Fig. 3) are similar for corresponding resistor magnitudes, the relative positions of the curves are quite different as are the actual phase angle values. These results cannot be explained with the current circuit model in which internal instrument impedances have been neglected. In order to account for positive phase angles in a mathematical model, an inductive term is suggested. However, we lack the physical evidence to support its existence.

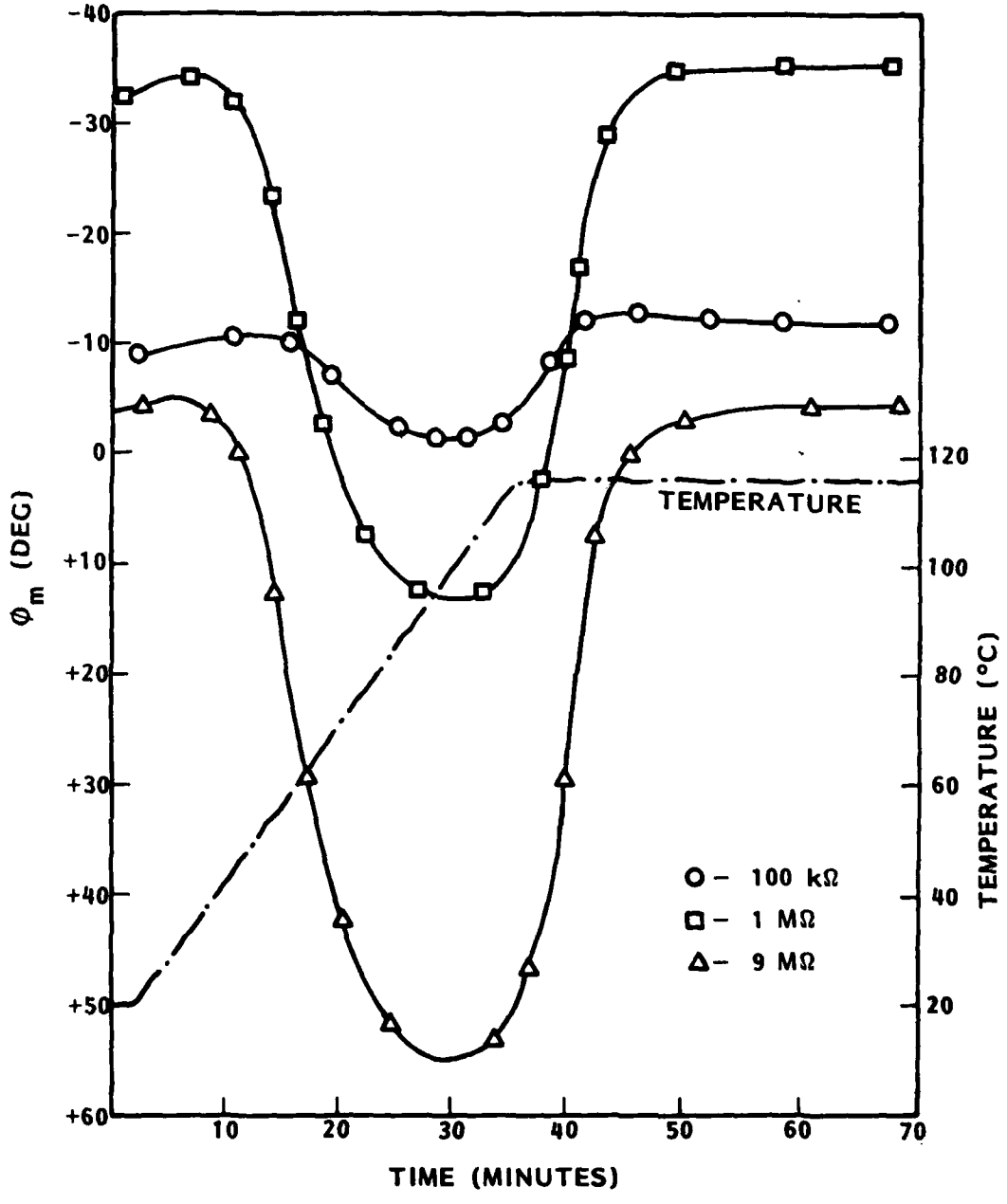
-40
-30
-20
-10
0
+10
+20
+30
+40
+50
+60
ϕ_m (DEG)
10
20
30
40
50
60
70
TIME (MINUTES)
120
100
80
60
40
20
TEMPERATURE (°C)
TEMPERATURE
O – 100 kΩ
□ – 1 MΩ
△ – 9 MΩ

Fig. 25

SECTION III

CHEMORHEOLOGICAL INTERPRETATION OF DIELECTRIC MONITORING SIGNALS

The dielectric signals obtained during the cure of a thermoset resin appear useful for process documentation and promising for process control. The question is their true meaning in terms of adhesive rheology. The purpose of this section is to shed some light on this elusive subject.

A good place to start is with the Audrey curves obtained during the previous contract (F33615-76-C-5170). Both FM-73 and PL-729 adhesives gave two major dissipation peaks, one of which appeared in the softening region and another in the gel region. In sharp contrast the Audrey curves appearing in this work display a single dissipation in the region of minimum viscosity. The obvious questions are what (1) causes this difference and (2) which curve is rheologically significant? The answer to the first question is that different dielectric monitoring configurations were used in each case. The dissipation curve displaying two peaks was obtained by using the adherends as capacitor plates. The curve displaying a single peak was obtained with a foil probe embedded directly in the bondline. Equivalent circuit diagrams are shown below in Figure 26a. In the first case (a) the Kapton in-

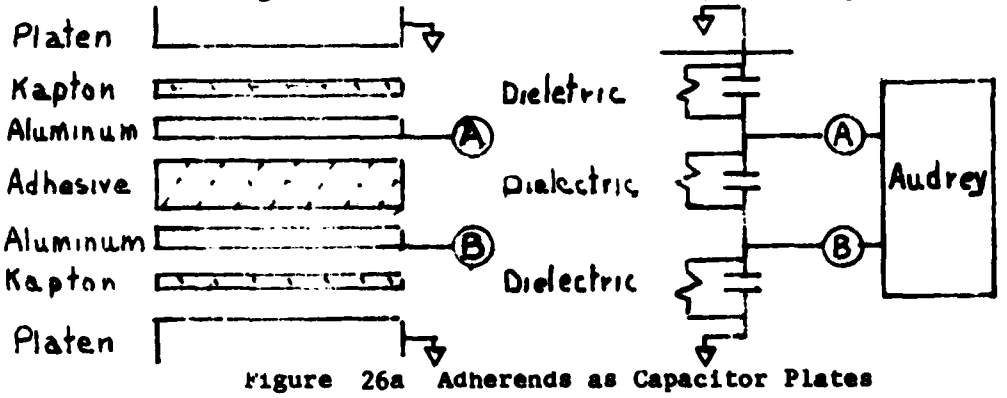

Figure 26a Adherends as Capacitor Plates

sulator can influence dissipation factor because the current reaching junction A sees both the Kapton and the adhesive and divides according

to their relative capacitance values encountered during cure. However, in the second case (b) all of the current passes through the adhesive

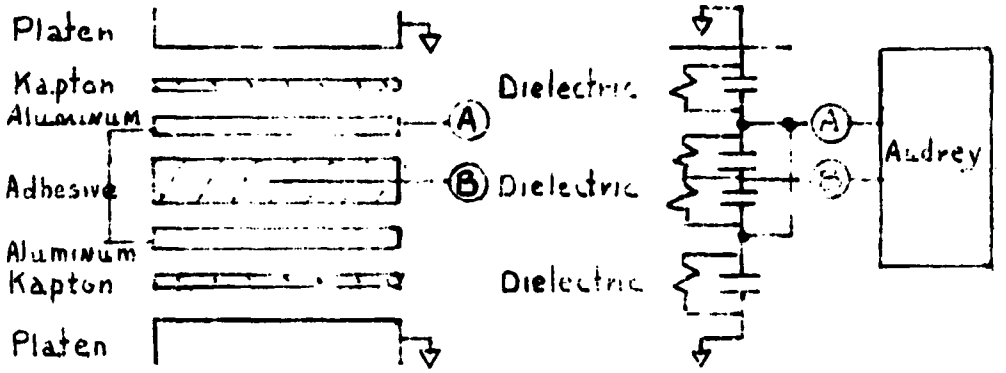

Figure 26b Foil Probe Capacitor Plate

before it sees the Kapton and here the alternative path is directly back to the signal generation. This effectively removes the Kapton from the monitoring circuitry. It would therefore appear that the single peak is rheologically significant as far as the curing adhesive is concerned. This interpretation is supported by the dynamic mechanical spectroscopy data discussed next.

A Rheometrics mechanical spectrometer was run in the oscillating parallel plate mode with the following parameters: 25 mm plate diameter, 0.7 mm gap, shear strain of 25 and a frequency of 10 rad/sec. A plot of tan δ, G' and η as a function of time are shown in Figure 3.2 for FM-73 as it was heated at 3°C/minute.

Tan δ is given by the ratio of G" (loss modulus) to G' (storage modulus) and is the mechanical analog of the electrical dissipation factor. η is the complex viscosity which can be expressed as $\eta = \eta' - \eta''$ where η' and η'' are the in phase and out of phase components of the viscosity. The quantities are interrelated by $G^* = i\omega\eta^*$.

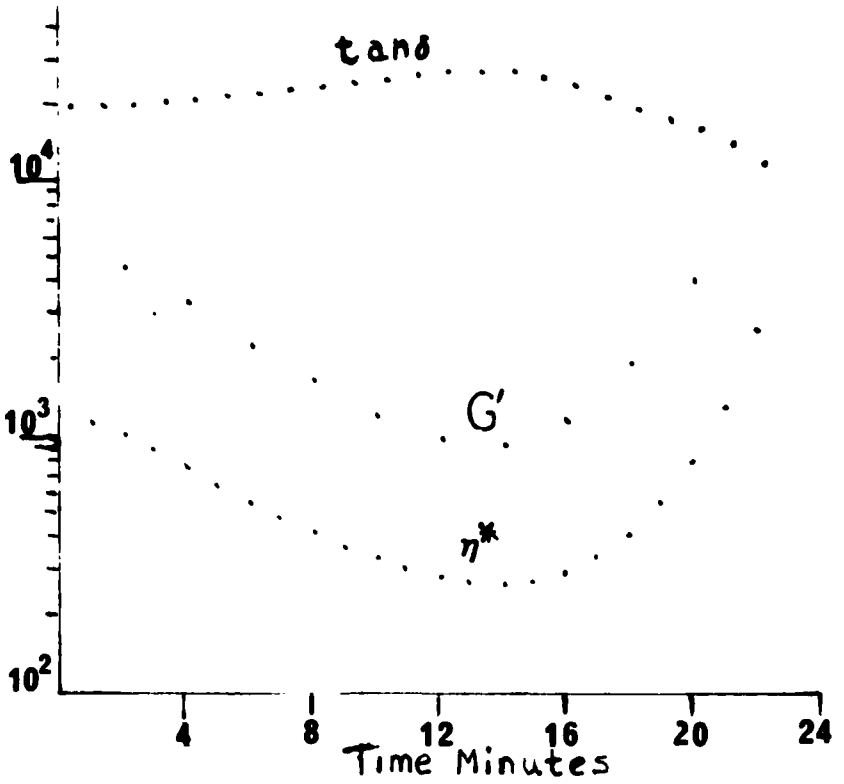

Figure 27 Viscosity-Temperature Data on FM-73

Note that a maximum in a broad tan δ curve corresponds to a minimum viscosity of 265 poise which occurs at 110°C. When compared to the dielectric monitoring curves at the same heating rate in Figure 28 using the probe/plate capacitor, one finds the maximum dissipation factor, tan ϕ_s, can vary from 88 - 112°C depending on frequency. The correlation is quite close in the case of 1000 Hz measurement. Keep in mind that the dynamic viscosity is also a function of frequency which, in the data shown, was 1.6 Hz (ω=10 rad/sec). The data suggest an interesting possibility for process control, i.e., the peak dissipation factor can be made to coincide with the minimum viscosity for FM-73 or in fact made to precede it and used to signal the entry into a critical phase of cure. The implications are far greater for composite cure where timely application of pressure is of the utmost importance.

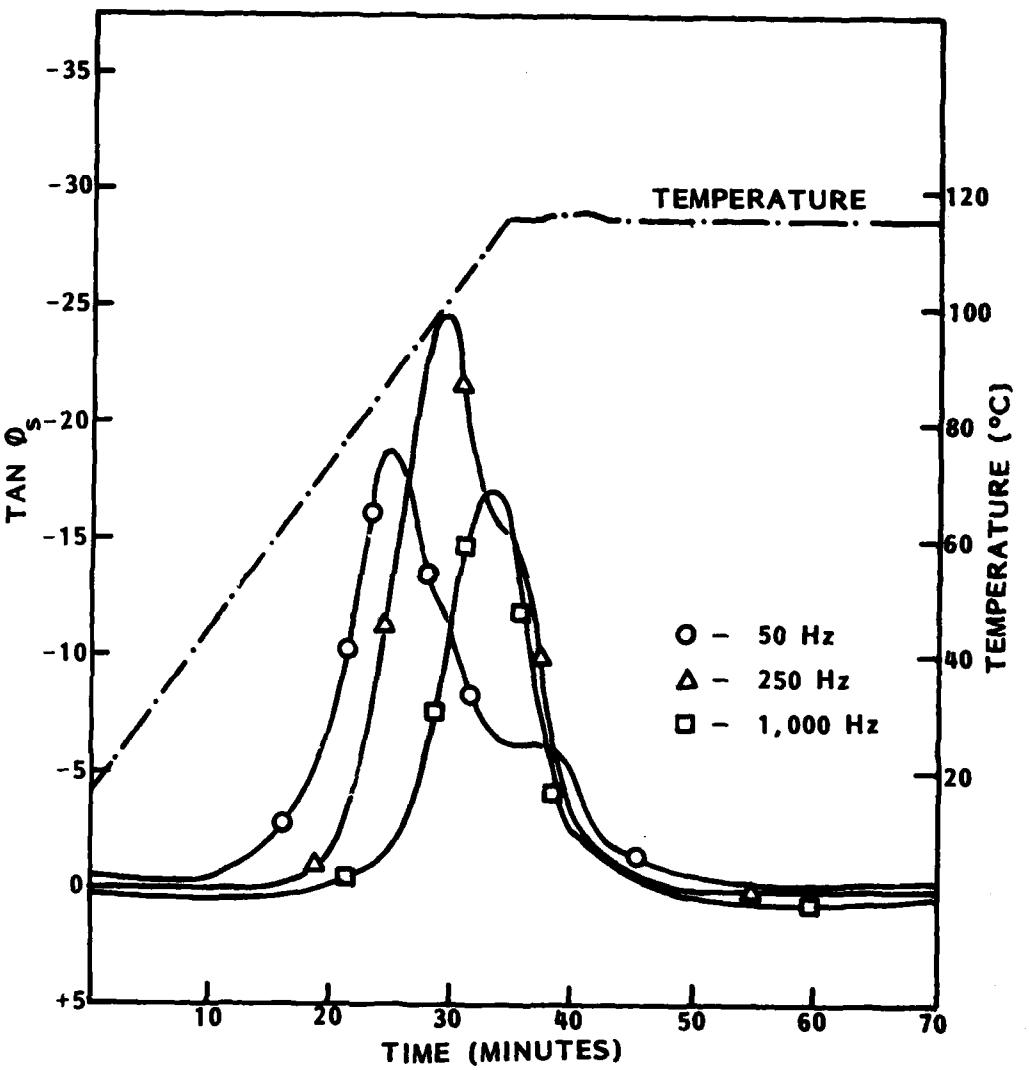

Figure 28 Dielectric Monitoring Curves of FM-73

The activation for the process responsible for the dielectric dissipation peaks was calculated to be 34.9 kcal/mole which appears reasonable for a flow process. Furthermore, high-temperature shoulders appear on the lower temperature peaks which occur near the start of the isothermal hold. They may be associated with gelation. The following evidence supports this supposition.

A measure of gelation can be obtained from the viscosity vs temperature data for FM-73 as shown in Figure 29. Gelation is indicated by a nearly vertical rise in viscosity due to crosslinking. The measurements stopped short of this point for ease of sample removal from the rheometer. However, good estimates of gel temperatures can be made in this manner. At 3°C/minute the gel temperature is in the neighborhood of 135-140°C. If an isothermal hold is introduced at 116°C, as for the previous dielectric data, (Figure 28) gel should occur in somewhat less than 7 minutes which is close to where the peaks bottom out. At 1°C/min the gel temperature is closer to 115°C. Finally it should be pointed out that the observation of a single peak in the dielectric tan ϕ curve is not a universal material characteristic. In this case the maximum molecular mobility corresponds with the minimum viscosity. In other systems more than one peak has been observed. An example is the conventional MY-720/DDS 350°F composite matrix system, where the minimum viscosity is considerably lower (1-10 poise). Thus the molecular mobility is high since dissipation losses are low resulting in two peaks separated by a valley in the tan ϕ curve. In fact, looking at Figure 53 in Section VI, dissipation factors calculated from these data would give a plot with two peaks. This is the result of a higher cure temperature wherein the FM-73 gel hardens and returns to the rubbery state as the temperature rises.

In order to show that the dielectric measurements do reflect the irreversable rheological changes of the cure the data shown in Figure 30 were generated. A sample of FM-73 was cured, cooled to room

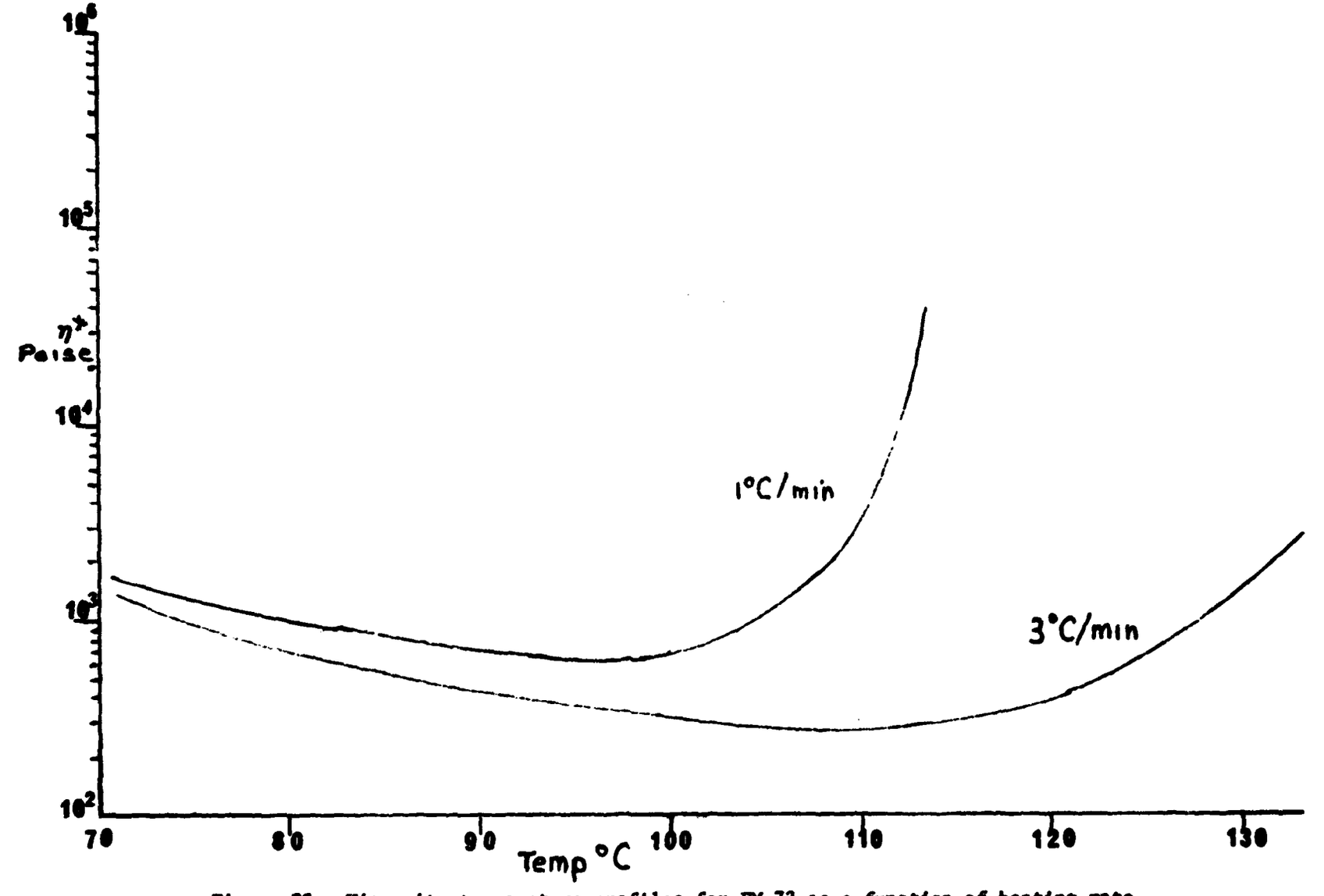

Figure 29 Viscosity-temperature profiles for FM-73 as a function of heating rate

temperature and then reheated to the cure temperature. Both the vector voltage and the measured phase angle show slight temperature dependence and return to the original values obtained at the end of the first heating cycle.

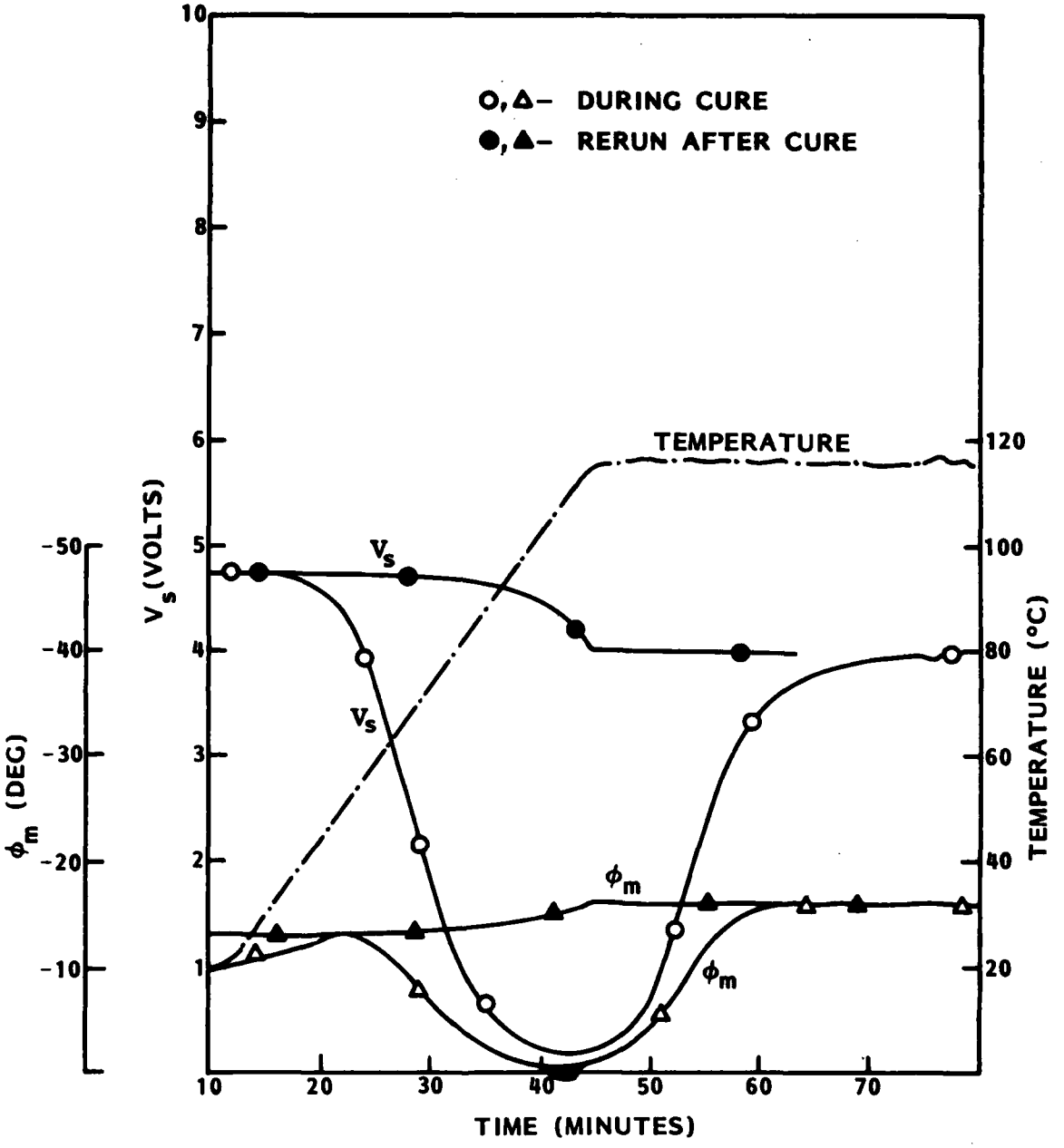

Figure 30 Phasemeter Monitoring Signal During Cure (Hollow Symbol) Followed by Cooling and Reheating (Solid Symbols) With the Same Temperature Profile

SECTION IV
PROBE RELIABILITY

1. Mechanical and Electrical Problems

The heart of the cure monitoring system is the probe. Reliability and ease of handling are of paramount importance. Shorting was found to be a major problem during the previous contract, No. F33615-76-C-5170. This was primarily due to inadequate probe stiffness and improper support, particularly at the edge of the bondline. Another problem was maintaining consistent electrical contact between the probe attachment clips and the probe. Accordingly, a considerable effort was devoted to improving the mechanical and electrical reliability of the bondline probes.

The material selected for the probes was a hardrolled aluminum foil 2 mils thick. Thinner foils were more readily susceptible to damage and could be torn during the bonding operation. Other metals were considered but since this investigation entailed aluminum to aluminum bonding the same metal was the obvious choice for the probe. Undoubtedly, many other conductive materials would work, but the use of a dissimilar metal would invite corrosion problems.

a. Probe Attachment

The first and most obvious problem was to eliminate the clips and fasteners used in previous work. Spot welding and tack welding were investigated but found to be rather cumbersome and required special equipment and techniques. Clamping or crimping of the foil to a connecting wire presented similar problems. Soldering offered a feasible solution for probe connection. Even though aluminum is considered a difficult material to solder, with the proper flux and alloy (Alcoa Flux 69 and Alcoa Solder 807) a satisfactory joint was consistently obtained. This soldered connection, which involved a solder that melts at 260°C (500°F) was found to be highly reliable for all of the adhesives used during the investigation.

Probe shape insulation and connector support were also modified. Whereas, the soldered probe provided a strong bond between the lead wire and the probe it also resulted in a highly stressed area which could cause problems in a production shop bonding process. To overcome these difficulties a Kapton film coated with an acrylic adhesive was bonded to both sides of the probe in the solder joint area as shown in Figure 31. The Kapton provided good support during the handling of a bond layup and during the subsequent cure. It also served as an electrical insulator.

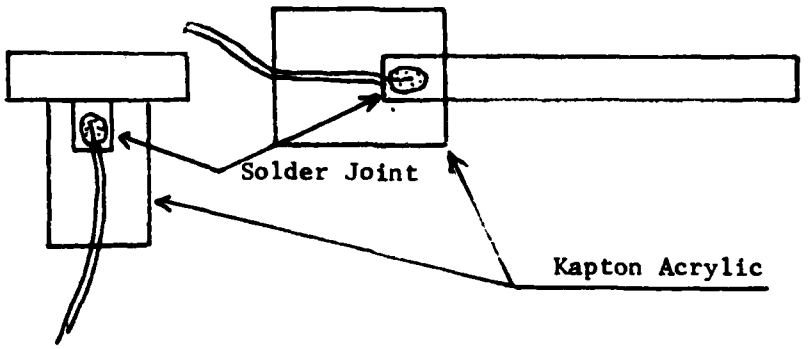

Figure 31 Kapton Film Probe Support

The possibility of developing a short during the cure was further reduced by permitting the Kapton film to intrude into the bondline approximately 1 mm. This prevented any burrs, which are always present on sheared metal edges from shorting to the probe. In subsequent tests the insertion of the Kapton film did not appear to affect the bond strength.

b. Probe Geometry

During the course of the investigation two probe geometries were used. Wherever possible, a 1/4 inch strip of aluminum foil without any Kapton film was used since this was the simplest, most reliable procedure. However, in the case of the lap shear specimens, in order to obtain an adequate dielectric signal, the area of a 1/4 inch strip was too small. The area was increased by using a T-shaped probe which required the Kapton film for support and insulation. It was also necessary to tape the Kapton support to the adherend to prevent slippage during the cure.

c. Feed Throughs and Connectors

Secondary connections were also investigated. It was found that conventional barrier terminal strips provided satisfactory interconnects to the probe leads. Feed throughs of the type supplied by Conax were found to be satisfactory for autoclave processes. There is one precaution that should be observed for the wires, connectors and feed throughs for use in presses or pressure vessels. The wires normally are insulated with thermoplastic coatings. This type of wire may be easily shorted if it passes over a sharp edge, angle or under a plate where the insulation may become locally deformed resulting in shorting. These potential problem areas may be easily protected by a piece of fiberglass cloth. Braided glass coated wires are less susceptible to damage of this type but cause leakage problems in vacuum and under pressure.

2. Non-flat Surfaces

There was also a question on how the probes would work in areas where the bondline was curved rather than flat. To answer this question a joggled specimen was used where three probes were placed in the sample as shown in Figure 32. Each probe represents a different type of curvature.

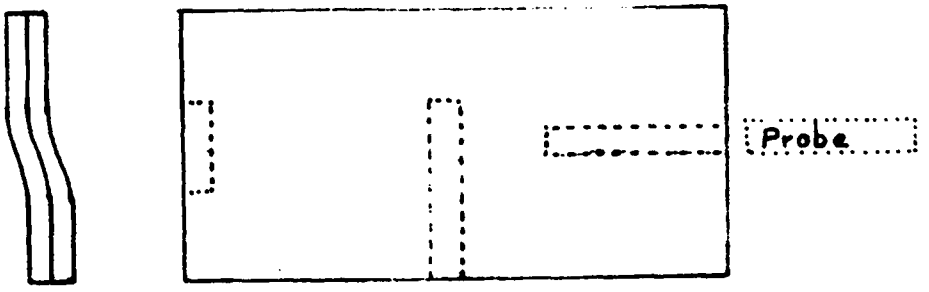

Figure 32 Probe Placement in Nonflat Bondline

Figure 33 shows the data obtained from a multiplexed monitored run involving the three probes. There were no shorts or other abnormalities in the traces obtained. The slight variations noted in the phase angle measurements are believed due to slight variations in lead capacitance. Based on this experiment there is no reason to expect difficulty in the monitoring of non-flat or curved specimens.

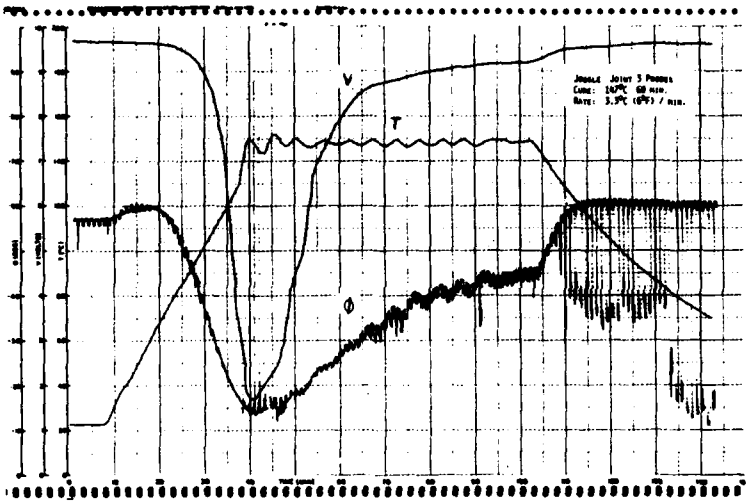

Figure 33 Monitoring Traces from Curved Bondline

3. Probe Surface Treatment

All of the probes used through this investigation were cleaned with an MEK wipe prior to bonding. This was done to preserve the consistency of the data throughout the investigation. Some of the other treatments described below could have been used in the latter stages of the investigation, but as the environmental testing described later shows, the value of these approaches is still unproven. All of the ambient temperature tests after environmental exposure were the same as the initial values.

One alternative treatment that could be used on the probes is anodizing. A comparison of anodized and unanodized probes using both the Audrey Dielectrometer and the phasemeter approach are shown in Figures 34 and 35 respectively. Clearly, anodizing has no effect on the shape or quality of the dielectric signal. One disadvantage is that the probes should be anodized within 2 hours of the bonding process which could add an undue expense to the process.

The answer to the latter problem would be to prime the anodized probe surface. To evaluate this approach electrodeposited primer coated probes supplied by Northrup Corporation were investigated. A series of runs made with these probes is summarized in Figures 36 and 37 for both Audrey and phasemeter. These curves show that the effect of the primer on the monitoring response is significant. The coated probe gave an entirely different response than an uncoated probe and it depended on the heat history of the coated probe. The shape of the dielectric curves changed when the probe was post cured. Whether this is due to coreaction or under cure of the coating is not known. These results indicate that the probe coating had a major effect on the monitor response and would therefore require further investigation and possibly extensive manufacturing control to obtain reproducible signals. Regardless of the post cure, the coated probes give a different dielectric signal. This indicates that the true dielectric response of the adhesive is masked by the coating.

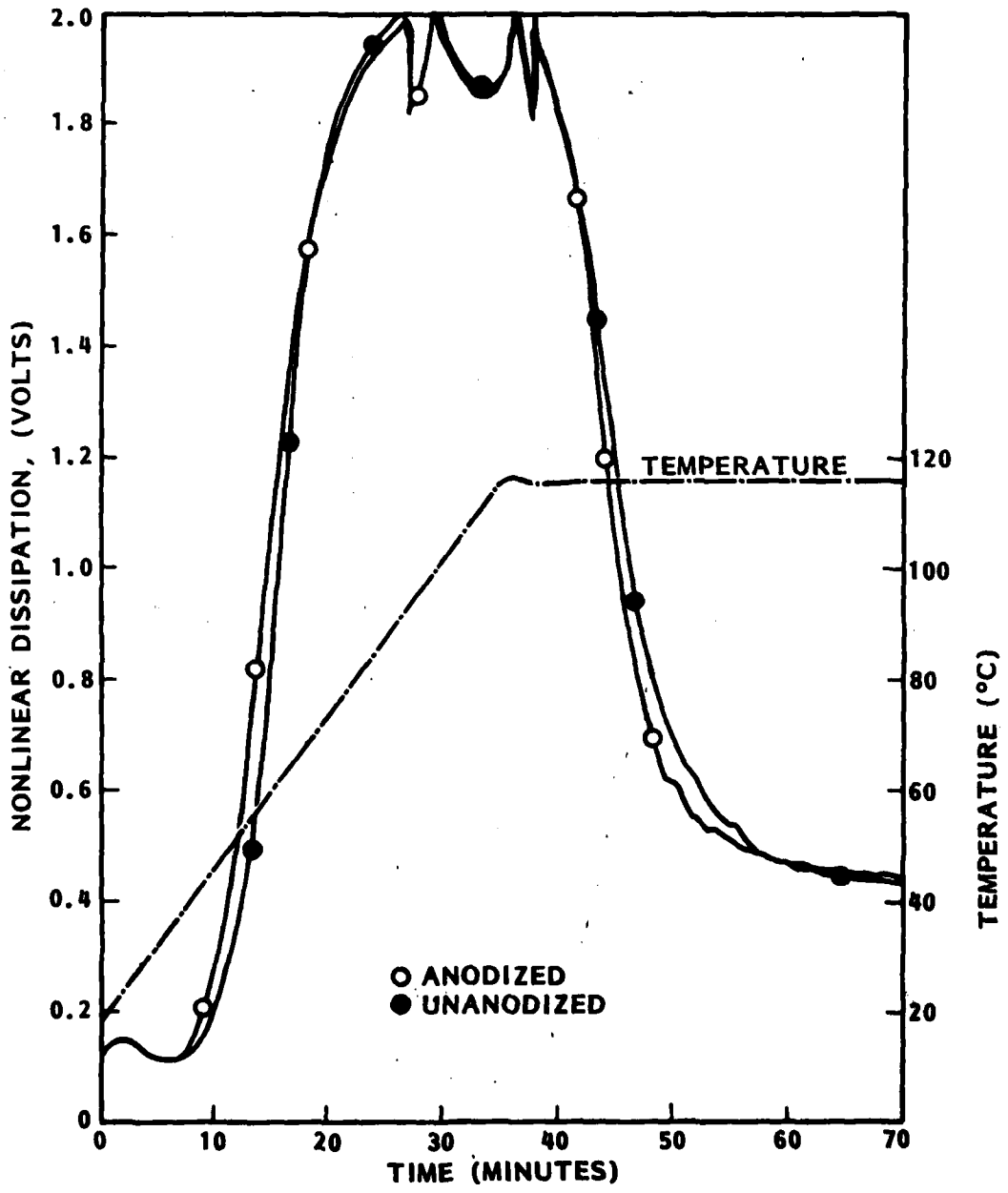

Figure 34 Comparison of Phosphoric Anodized and Bare Aluminum Probes on Audrey Monitoring Signal for FM-73 Adhesive.

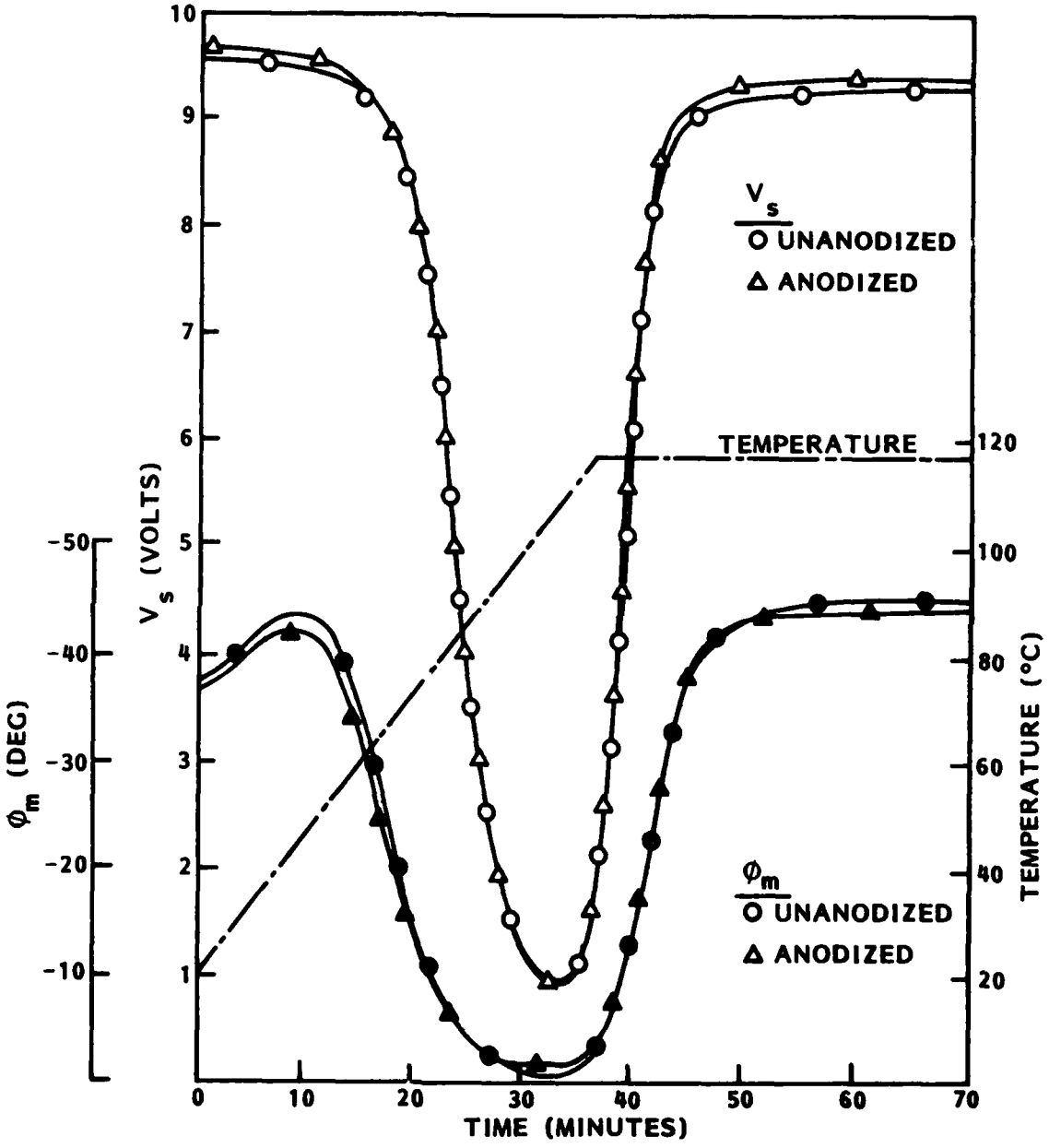

Figure 35 Comparison of Phosphoric Anodized and Bare Aluminum Probes on Phasemeter Monitoring Signals for FM-73 Adhesive.

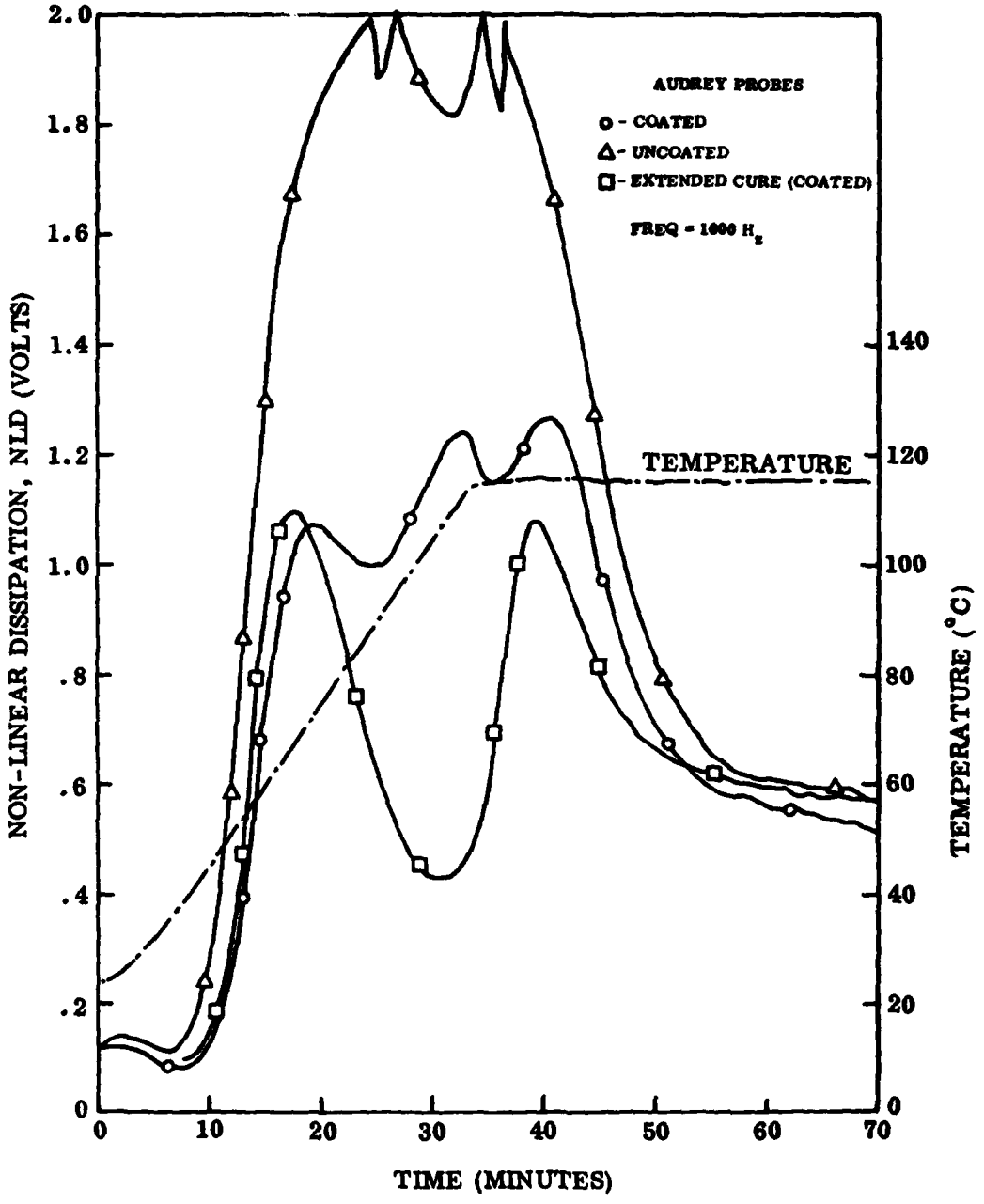

Figure 36 Audrey Responses to Coated and Uncoated Probes

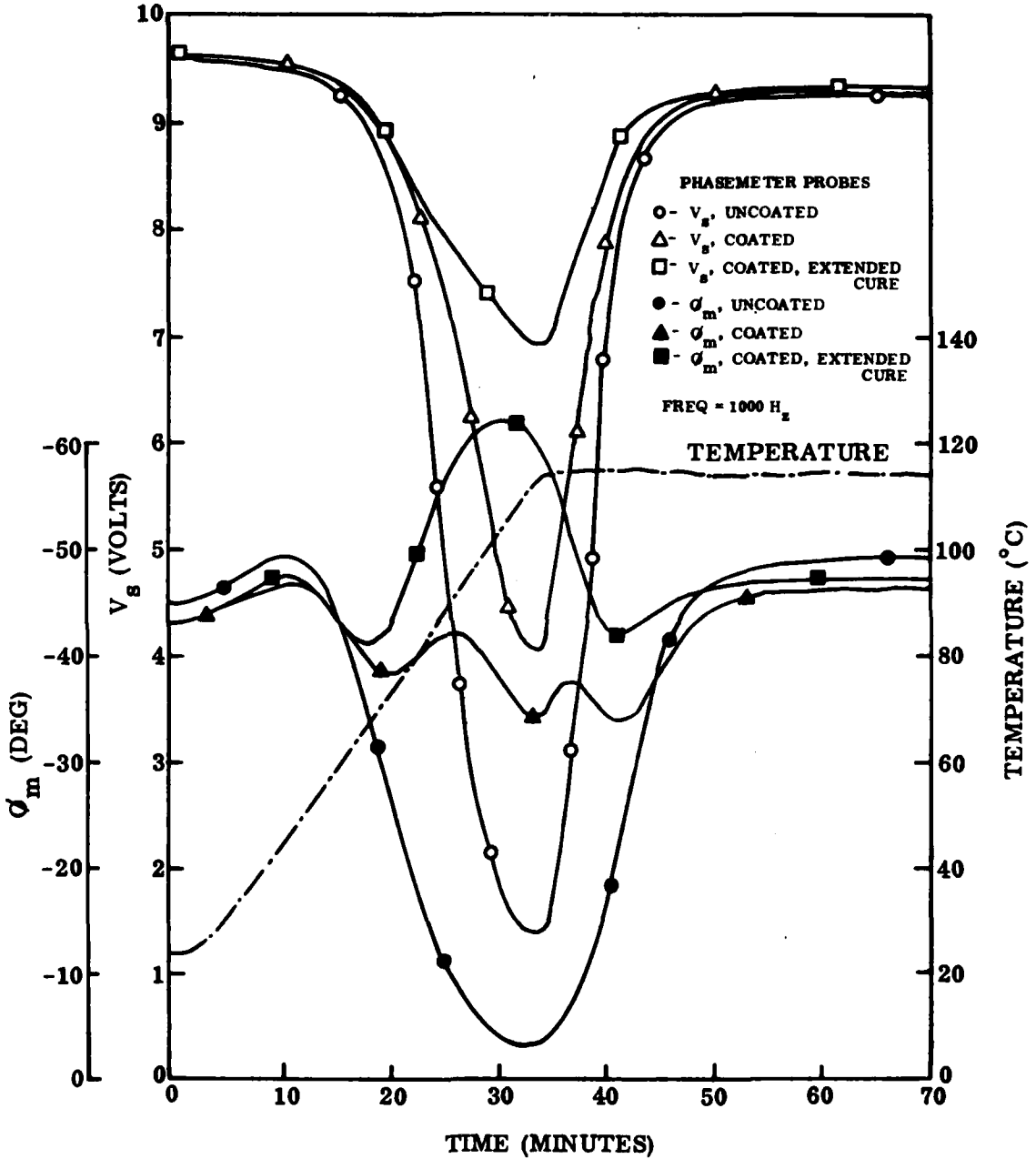

Figure 37 Phasemeter Responses to Coated Probe.

SECTION V
VARIATIONS IN DIELECTRIC FINGERPRINTS

1. Influence of Chemical Composition on Monitoring Curves

It is recognized that FM-73, while highly valuable to the aerospace industry, is not the only structural adhesive available. A wide variety of useful products exist and these vary widely in chemical composition. It was of interest therefore to briefly examine materials representative of other chemical types.

During this phase of the investigation monitoring traces were developed using a fixed set of phasemeter instrumental conditions. All bonding operations were conducted in a small laboratory press using a Tetrahedron ATC 200 equipped with a Data-Trak Card Reader to control the cure cycle. However, variations in the cure conditions were made since this added additional information on the influence of chemical structure. The five adhesives, HT-424 (an aluminum filled high temperature epoxy-phenolic), FM-1000 (an epoxy/nylon cured with dicyanidiamide), FM-300 (an elastomer modified epoxy cured with dicyandiamide), PL-729 (a nitrile modified epoxy based on diglycidyl p-aminophenylglycidyl ether cured with diaminodiphenyl sulfone), and FM-73 (the program baseline material, an elastomer modified epoxy probably cured with a "kicked" dicyandiamide system) were cured according to a number of different cure cycles to demonstrate how chemical structure changes the shape of the dielectric curve.

2. Discussions and Results

The results clearly show that changes in the chemical composition change the shape and significance of the monitoring traces. All traces have the same general shape: a pronounced decline in the

phase angle and vector voltage as the material softens followed by a marked increase as it solidifies. It was noted that as the vector voltage of some of the adhesives approached zero, the phase angle became positive. As stated earlier, we have no logical explanation for this observation. A possible cause may be the result of a mismatch between the phasemeter internal resistance, the reference resistor and sample resistance. A 1 megohm reference resistor was used for this study based on the earlier findings for FM-73. It is speculated that this may be caused by stray inductances in the instrumentation which were not accounted for in the mathematical model. Each adhesive is discussed individually in the sections which follow.

a. HT-424, Aluminum Filled Epoxy Phenolic

This was the only conductively filled adhesive studied and some difficulties were encountered in obtaining useful monitoring traces at higher temperatures. However, a curve, Figure 38 could be reproducibly obtained at 127°C (260°F) which leads itself to some interesting interpretations.

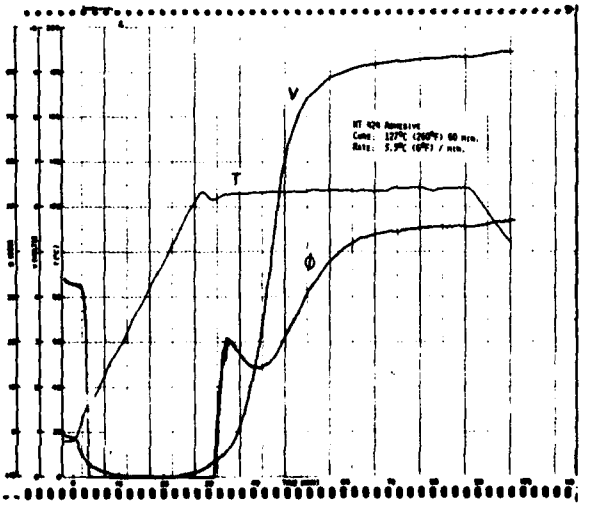

Figure 38 HT-424 Cured at 127°C (260°F) & 3.3°C (6°F)/min.

With the instrumental conditions used, the in_ ial phase angle and vector voltage were lower than that observed for the other adhesives. When heated approximately 10°C above room temperature the vector voltage fell to zero and the phase angle became positive as shown. These phenomena are undoubtedly due to the presence of the aluminum powder making the adhesive more conductive. At around 100°C the vector voltage starts to increase. This would appear to indicate that the viscosity of the adhesive has increased to the point that physical separation of the filler particles is beginning and the conductivity is decreasing. It is akin to saying that the filler particles are a series of wires running between the faying surfaces and in an AC field some of the wires can not respond to the current reversals rapidly enough due to the viscosity of the resin matrix. The sharp peak in the phase angle, approximately 5 minutes after reaching the cure temperature can thus be associated with the gelation of the resin. As a resin system approaches gelation, viscosity increases very rapidly. In the case of a filled adhesive the resistivity rapidly increases as the gel point is approached.

Beyond this sharp peak the effect of the conductive filler is minimized and the dielectric curve takes on the shape expected of the epoxy phenolic matrix. However, a word of caution should be injected at this point on the interpretation of phase angle data. The dip in the curve following the sharp peak <u>is not a lowering in viscosity</u>, it is a phenomenon associated with the instrumentation and the mathematics of phase angle measurement. If tan δ, which is a true material parameter, were calculated from the phase angle and vector voltage measurements, the data could be more easily interpreted in terms of the physical events which occur during the cure.

This adhesive system is interesting and lends itself to further study which is beond the scope and funding of this program. Undoubtedly, dielectric monitoring could be used to control cures of adhesives containing conductive fillers. However, this would entail changes in some of the instrumental circuitry. With further experimentation better results should be attainable at higher cure temperatures.

b. FM-100 Dicyandiamide Cured Epoxy-Nylon

In the case of FM-1000, the epoxy-nylon system, Figures 39 and 40, the cures at 187°C (368°F) indicate that the cure temperature is above the glass transition temperature (Tg) of the system. This is evidenced by the fact that the vector voltage (V) is essentially zero and the phase angle ϕ is positive until the bondline is cooled down following cure.

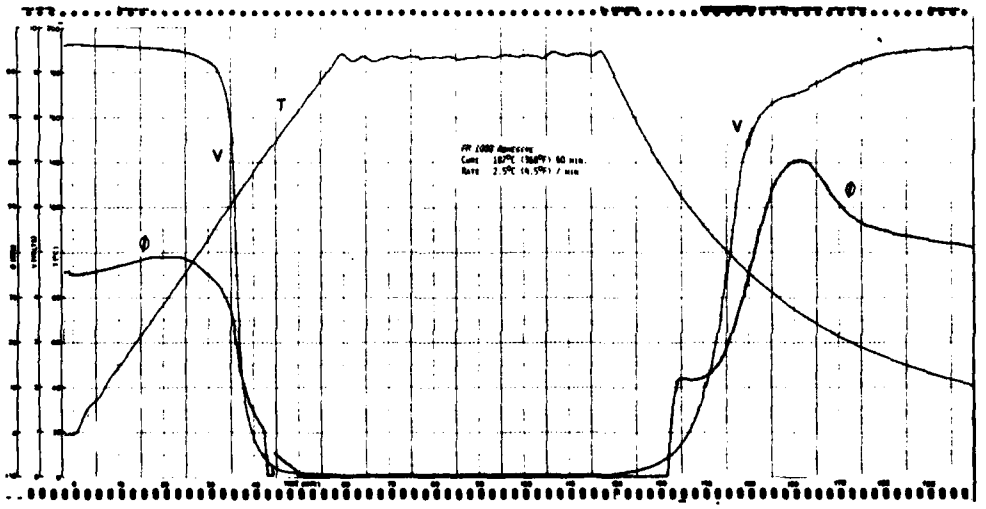

Figure 39 FM-1000 Cured at 187°C (368°F) & 2.5°C (4.5°F)/min

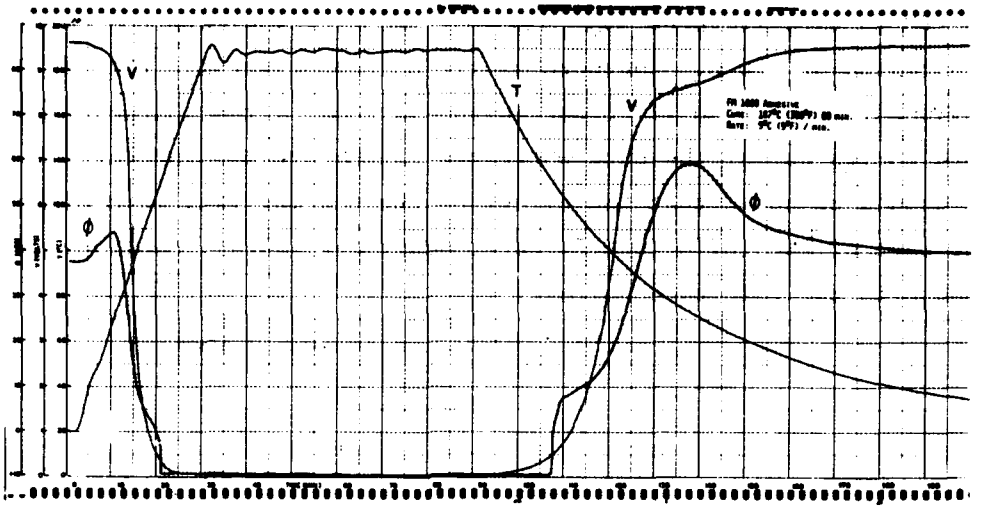

Figure 40 FM-1000 Cured at 187°C (368°F) & 5°C (9°F)/min.

Heating rate seems to have little effect other than causing a steeper drop in the phase angle and vector voltage during the early stages of the cure. In fact, the inflection in the phase angle between 120°C and 130°C indicates this is the T_g region. This observation agrees well with the data obtained on curing at 127°C (260°F), Figure 41.

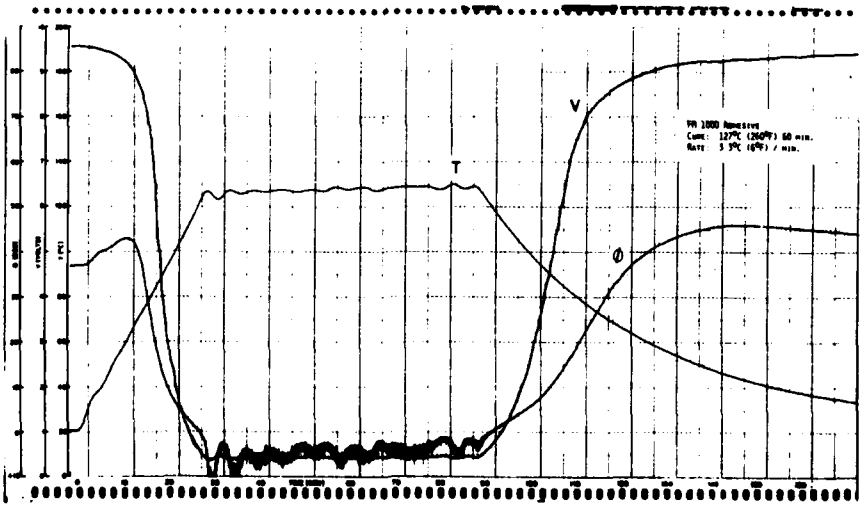

Figure 41 FM-1000 Cured at 127°C (260°F) & 3.3°C (6°F)/min.

c. FM-73, Elastomer Modified Epoxy

The FM-73 data (Figures 42, 43, 44 and 45) indicate the T_g is in the region of 120°C. The cure at 122°C is near the T_g, the 187°C obviously above, the 177°C cure displays some of the characteristics of both curves during the cure where the minima are present but not pronounced. It should be noted that the effect of the heating rate is minimal. In the case of the 187°C (368°F) cure, additional detail could be gained by a change in the reference voltage.

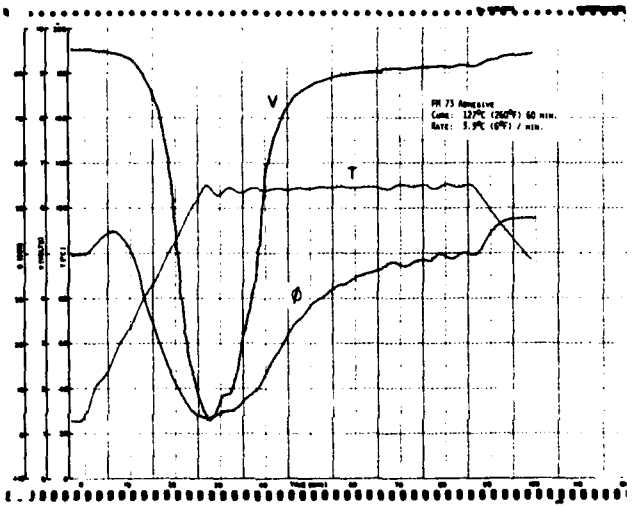

Figure 42 FM-73 Cured at 127°C (260°F) & 3.3°C (6°F)/min.

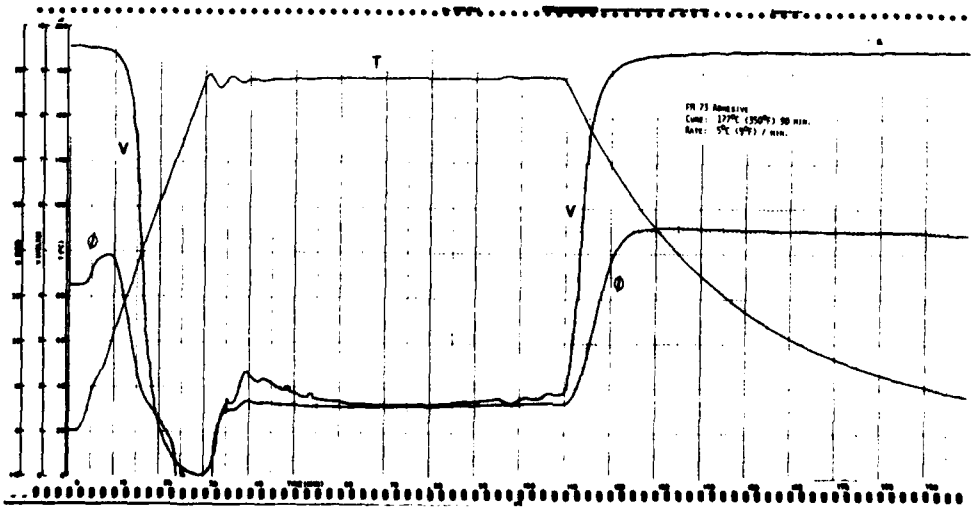

Figure 43 FM-73 Cured at 177°C (350°F) & 5°C(9°F)/min.

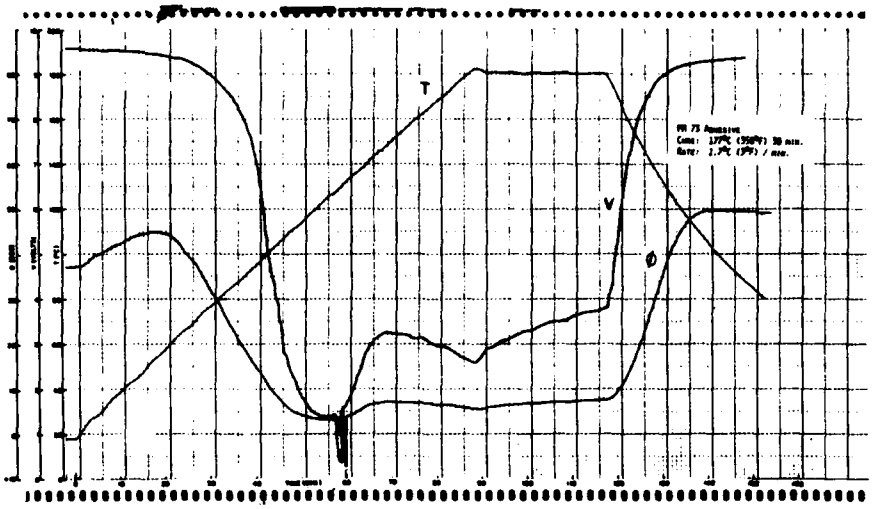

Figure 44 FM-73 Cured at 177°C (350°F) & 1.7°C (3°F)/min.

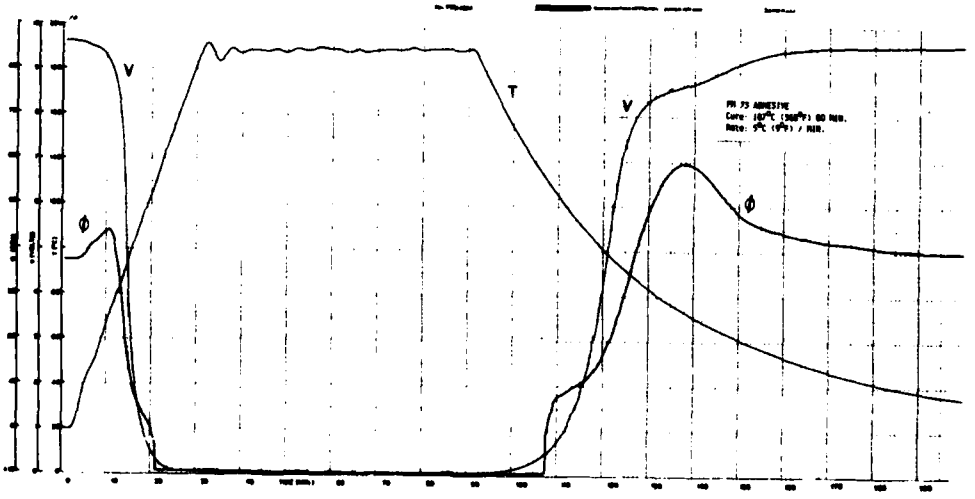

Figure 45 FM-73 Cured at 187°C (368°F) & 5°C (9°F)/min.

d. FM-300, Elastomer Modified Epoxy

The data obtained on FM-300, Figures 46 and 47, indicate that the performance of this product at elevated temperatures should be slightly better than that of FM-73. Again the effect of heating rate is minimal.

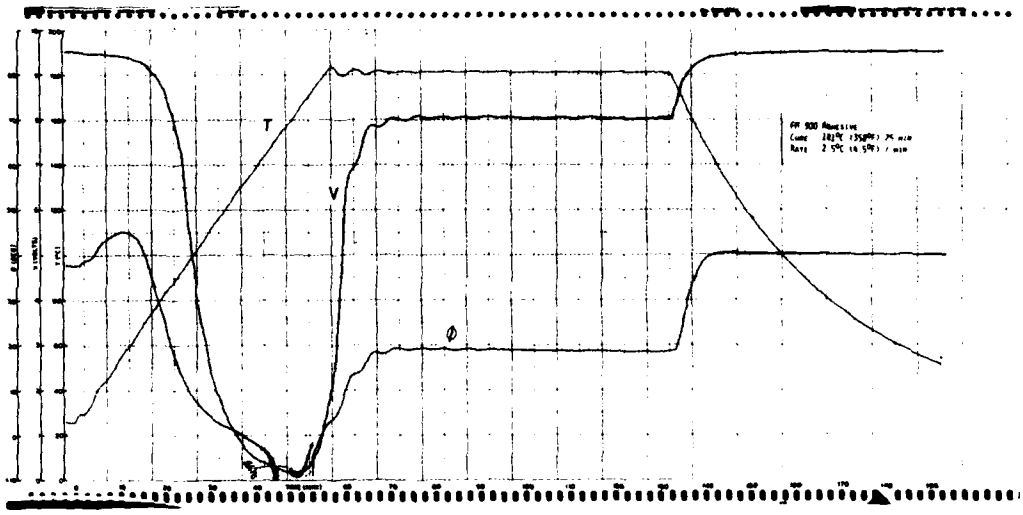

Figure 46 FM-300 Cured at 181°C (358°F) & 2.5°C (4.5°F)/min.

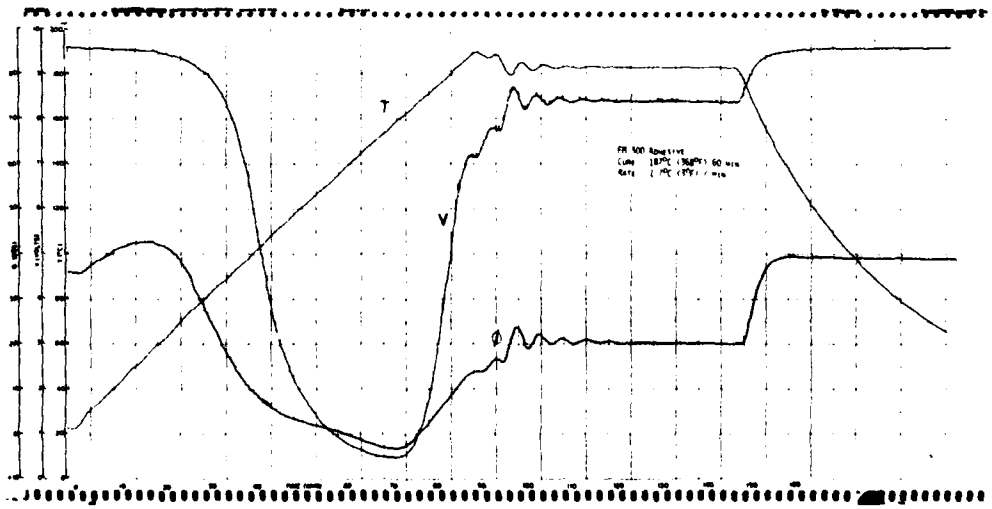

Figure 47 FM-300 Cured at 187°C (368°F) & 1.7°C (3°F)/min.

e. PL-729, Nitrile Modified Epoxy

Figures 48, 49 and 50 indicate that PL-729 adhesive would have better elevated temperature performance than either FM-73 or FM-300. This is not unexpected from this type of glycidylamine resin system. Note also that the adhesive cures quite rapidly as compared to the others even at 127°C (260°F).

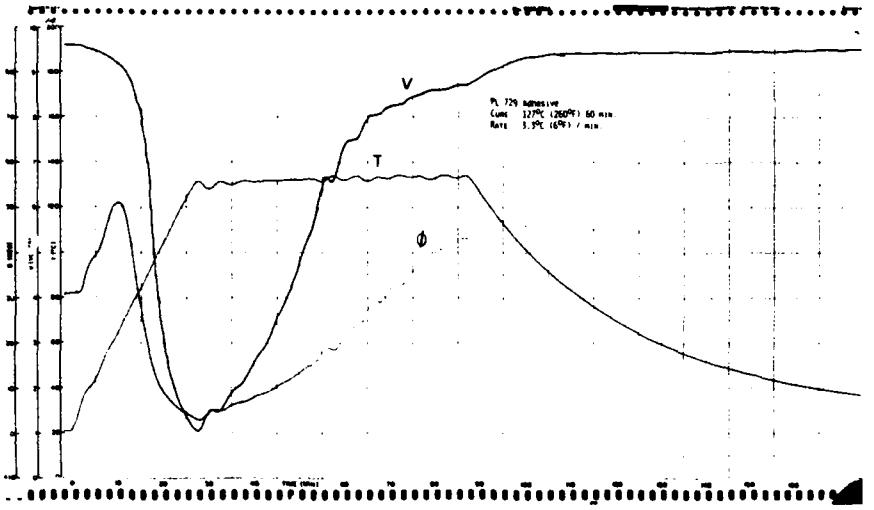

Figure 48 PL-729 Cured at 127°C (260°F) & 3.3°C (6°F)/min.

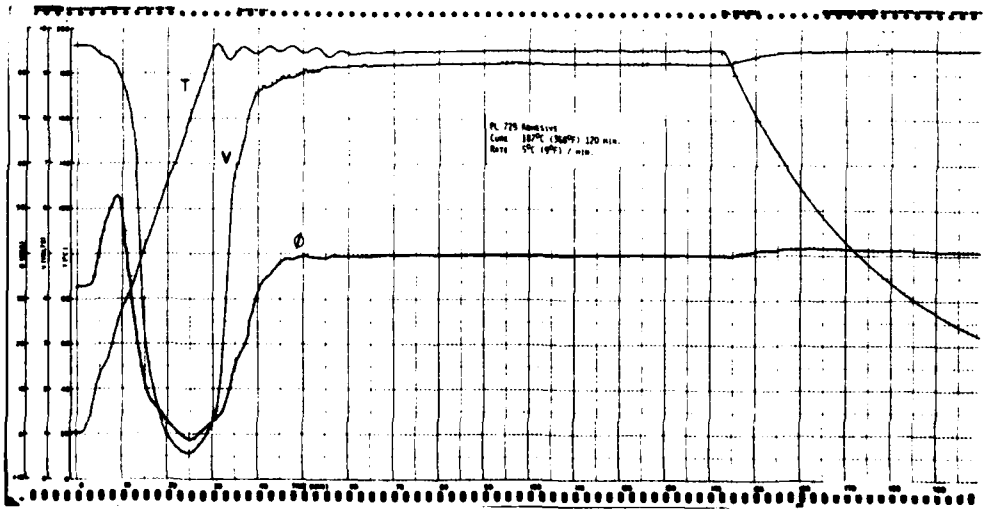

Figure 49 PL-729 Cured at 187°C (368°F) & 5°C (9°F)/min.

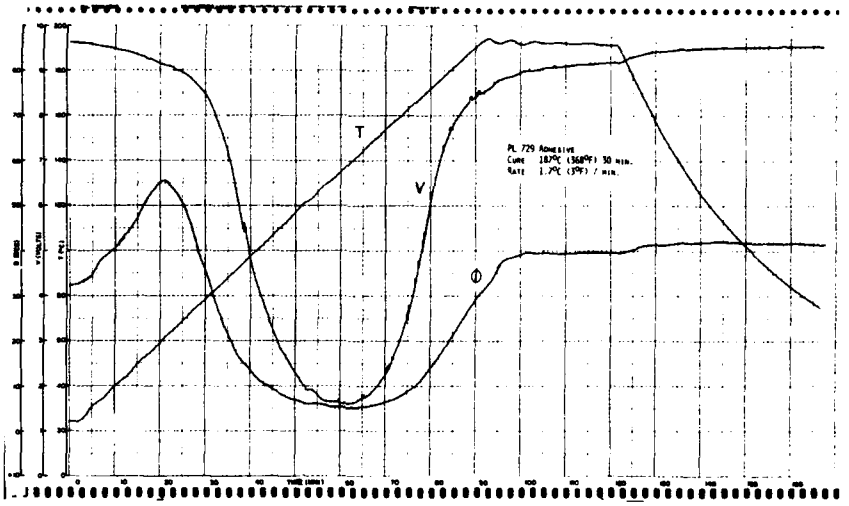

Figure 50 PL-729 Cured at 187°C (368°F) & 1.7°C (3°F)/min.

SECTION VI

CURE OPTIMIZATION

1. General Observations

In addition to the finge-print data discussed in Section V, a comprehensive study of the cure conditions for FM-73 adhesive was undertaken. The test matrix is summarized in Table 1. Lap shear panels were fabricated under a series of varying heat rates, cure temperatures, cure times and cooling rates. The resulting panels were tested for tensile lap shear strength at room temperature and 82°C (180°F). The panels were fabricated in a Wabash press using a pressclave attachment. The base plate was penetrated for probe and thermocouple leads. The panels, 10 cm x 25 cm (4" x 10"), were pinned with rivets to prevent movement during bonding. All panels were phosphoric acid anodized per the Boeing process and primed with BR-127. As stated in Section IV the only treatment given the probes was an MEK (methyl ethyl ketone) wipe.

The cure conditions, heating rate and lap shear data for probed and unprobed specimens at room temperature (RT) and 82°C (180°F) are shown in an inset on each curve. A number of general conclusions should be pointed out before continuing with a detailed discussion of the data.

1. The amplitude and rate of inflection of the dielectric curves varies with the heating rate.
2. Changes in bonding pressure are readily noted.
3. When appreciable noise is present there is no difficulty in visually distinguishing the dielectric curve.
4. The probed tensile values are around 15-20% lower than the unprobed specimens.

2. Control Runs

Control experiments were run at random times during the course of the study to assure reproducibility. The control cure conditions were 2.8°C (5°F)/min. to 127°C (260°F) followed by a hold for one hour at temperature. The environmental test panels were also made under these conditions since the data shown herein indicate that this cure cycle was adequate.

The three control curves are shown in Figures 51, 52 and 53, representing runs 5, 11 and 15.

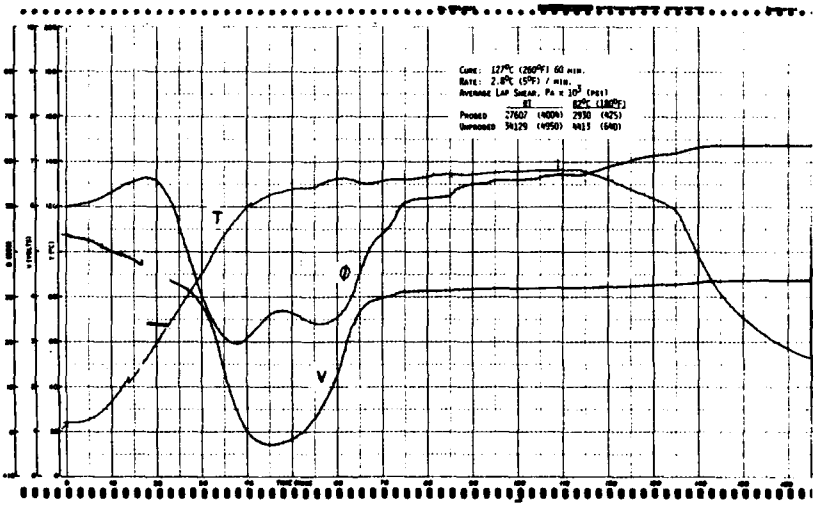

Figure 51 Control Sample, Reference Voltage 1

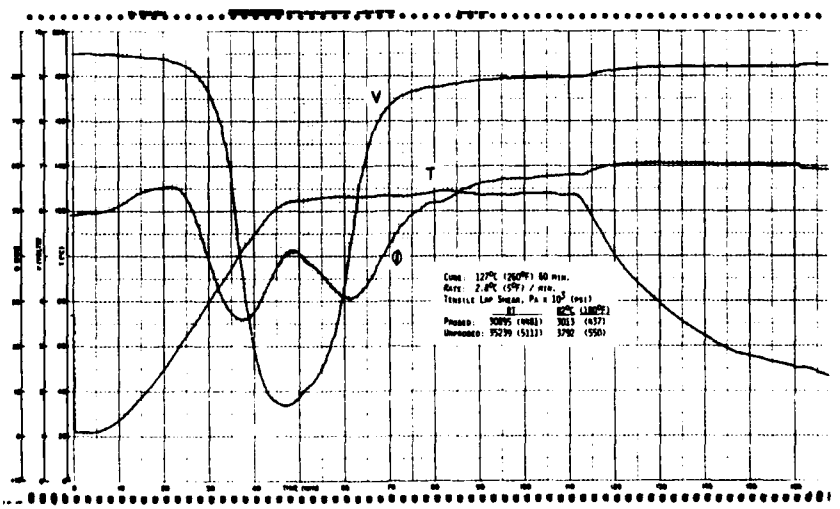

Figure 52 Control Sample, Reference Voltage 10

TABLE 1 BOND STRENGTH OPTIMIZATION MATRIX FOR FM-73

Experimental Run	1	2	3	4	5*	6	7	8	9	10
Process Variable										
Heating Rate °F	1	5	10	1	5	10	1	5	10	5
°C/min.	.55	2.8	5.5	.55	2.8	5.5	.55	2.8	5.5	2.8
Hold Temp °F	220	220	220	260	260	260	300	300	300	260
°C	104	104	104	127	127	127	149	149	149	127
Hold Time (min.)	60	60	60	60	60	60	60	60	60	30
Pressure (PSI)	40	40	40	40	40	40	40	40	40	40
Pa x 10^3	27.58	27.58	27.58	27.58	27.58	27.58	27.58	27.58	27.58	27.58
Cooling Rate	Cooled at natural rate of pressclave									

Experimental Run	11*	12	13	14	15*	16	17*	18	19
Process Variable									
Heating Rate °F	5	5	5	5	5	1	5	1	5
°C/min.	2.8	2.8	2.8	2.8	2.8	.55	2.8	.55	2.8
Hold Temp °F	260	260	260	260	260	260	260	260	260
°C	127	127	127	127	127	127	127	127	127
Hold Time (min.)	60	90	60	60	60	60	60	60	60
Pressure (PSI)	40	40	40	40	40	40 PSI @ 100°C		40 PSI @ 120°C	
Pa x 10^3	27.58	27.58	27.58	27.58	27.58	27.58	27.58	27.58	27.58
Cooling Rate	Natural	Natural	F*	I*	S*	← Natural →			

* - denotes "Control"
*F - fast cool - rapid water cooling
*S - slow cool - natural rate of pressclave
*I - intermediate cool - intermediate between other two

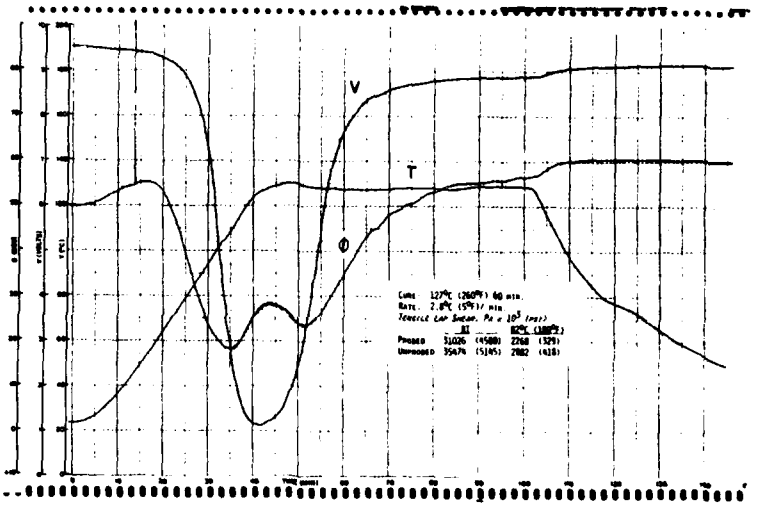

Figure 53 Control Sample, Reference Voltage 10

In Figure 51. the reference voltage used was incorrectly set at 1 volt, not 10 volts. However, while this change reduces the amplitude of the vector voltage, the effect on the phase angle curve is minimal. It should be noted in every case that the first phase angle inflection occurred between 55° and 58°C, the second between 102° and 108°C, the third between 124° and 126°C, and a fourth inflection occurred after the cure temperature was reached. The total phase angle excursion (Figures 52 and 53) is 29° to 37° with the difference between the second and third inflection being 10° to 15° and between the third and fourth inflection differences are 4° and 10°. A vector voltage change is 8.3-7.9 volts in the two curves with a minimum appearing around 125°C. The data show good reproducibility between runs. However, absolute values for phase angle and vector voltage should not be used for process change decision points because the magnitude varies somewhat. This suggests that first derivative or inflection point data be used for process automation studies.

3. Effect of Cure Temperature

The effect of the cure temperature was studied at the same heating rate. Using a heating rate of 2.8°C (5°F)/minute, cures were carried out at 104°C, 127°C and 149°C. These are represented by runs 2, 10 and 8 of Table 1, respectively. The data are shown in Figures 54, 55, and 56.

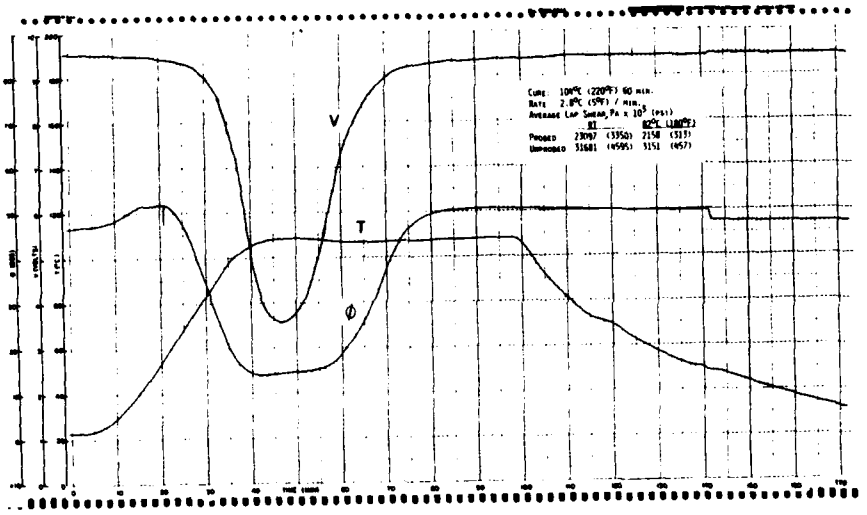

Figure 54 Cure at 104°C (220°F)

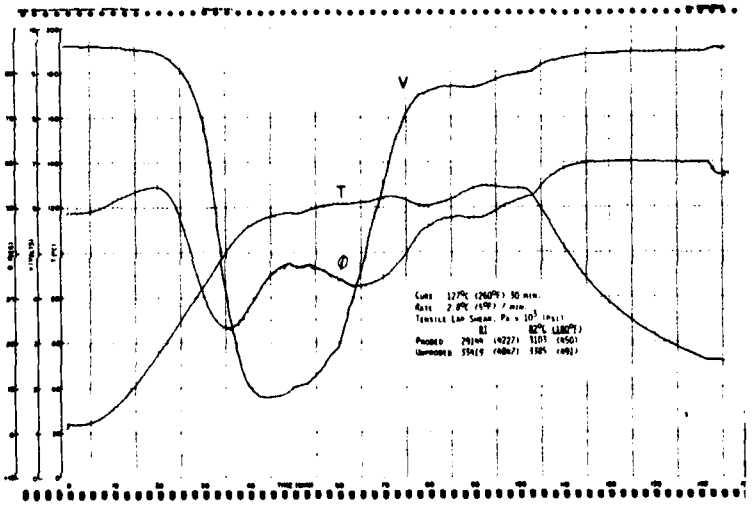

Figure 55 Cure at 127°C (260°F)

The double valley characteristic of the FM-73 control cure essentially disappears at the lower cure temperature as evidenced by a noticeable increase in either phase angle or vector voltage during the cool down period (Figure 53). The lower temperature cure is below the glass transition temperature. It should be noted that the average room temperature bond

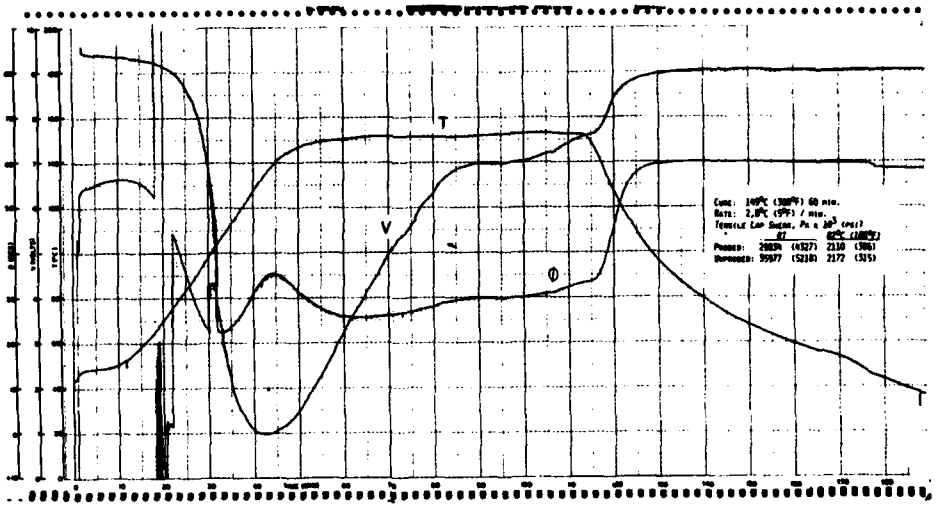

Figure 56 Cure at 149°C (300°F)

strength of the probed coupons cured at 104°C (220°F) is approximately 20% below that produced by the other cures. This indicates that the minimum cure temperature is around 127°C.

4. Effect of Heating Rate

The effect of heat rate was studied at the three cure temperatures discussed above. The results obtained at the lower cure temperature, Figures 56, 57, and 58 were the most interesting in that the phase angle characteristics of the dielectric response curves were quite different than those obtained at higher temperatures. These results correspond to runs 1, 2 and 3 in Table 1. The double valley that had been observed with the normal or control cure is only slightly apparent in these data. As discussed previously, the reasons for this are not readily apparent, but the effect is reproducible.

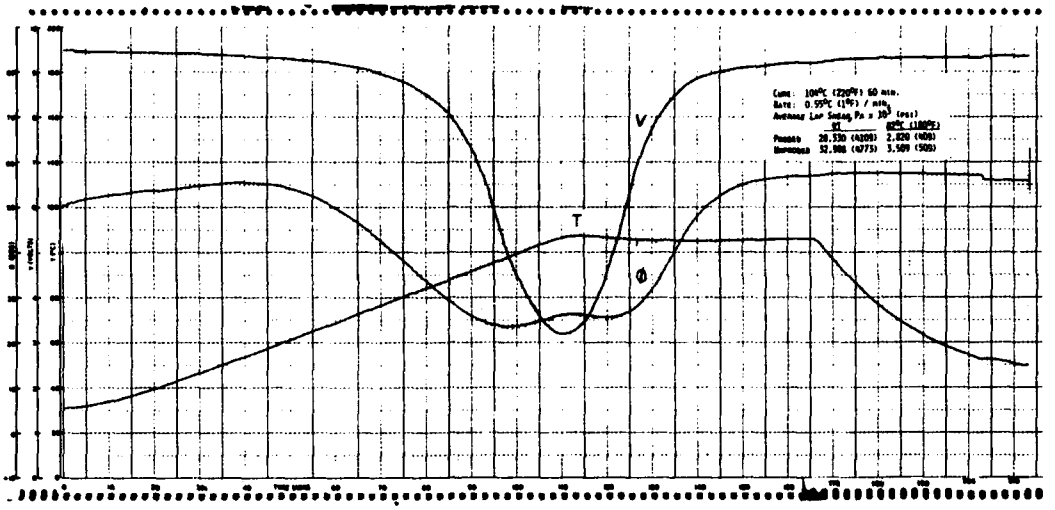

Figure 57 Cure at 104°C (220°F) Heated at 0.55°C (1°F)/min.

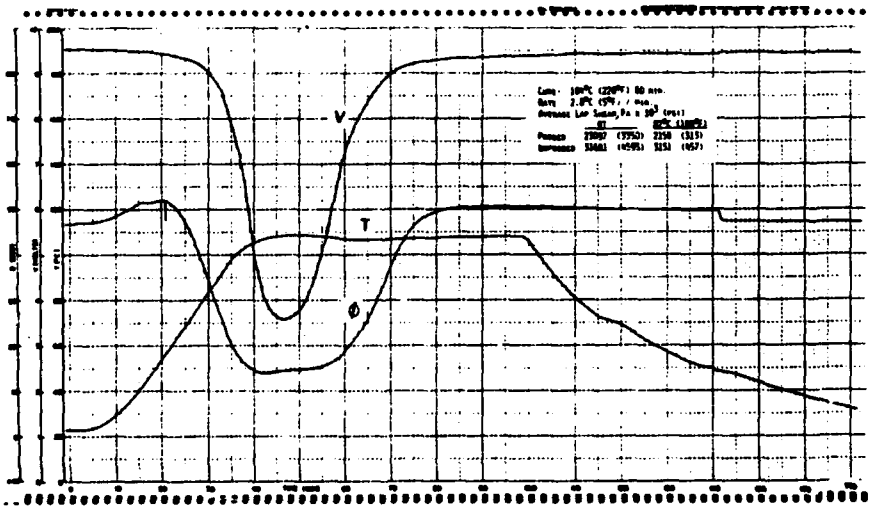

Figure 58 Cure at 104°C (220°F) Heated at 2.8°C (5°F)/min.

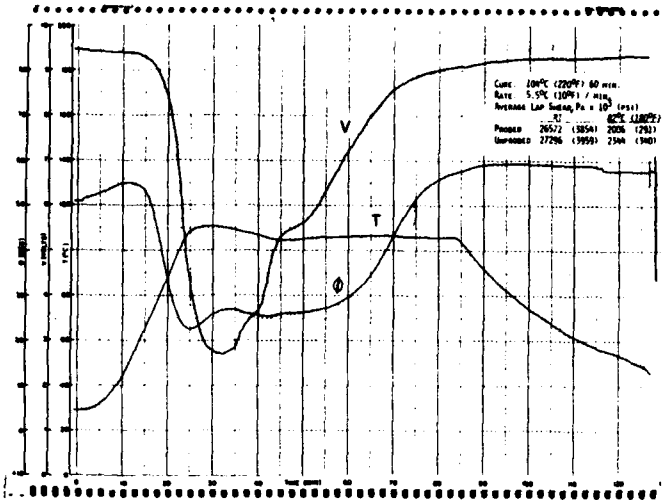

Figure 59 Cure at 104°C (220°F) Heated at 5.5°C (10°F)/min.

It can be concluded, however, that the phenomenon occurs at the lower heating rates and/or lower cure temperatures. Again, it should be pointed out that this cure is below the T_g of the adhesive for reasons cited above.

The next three curves, Figures 60, 61, and 62, are the cures at 127°C designated as runs 4, 12 and 6 respectively in Table 1.

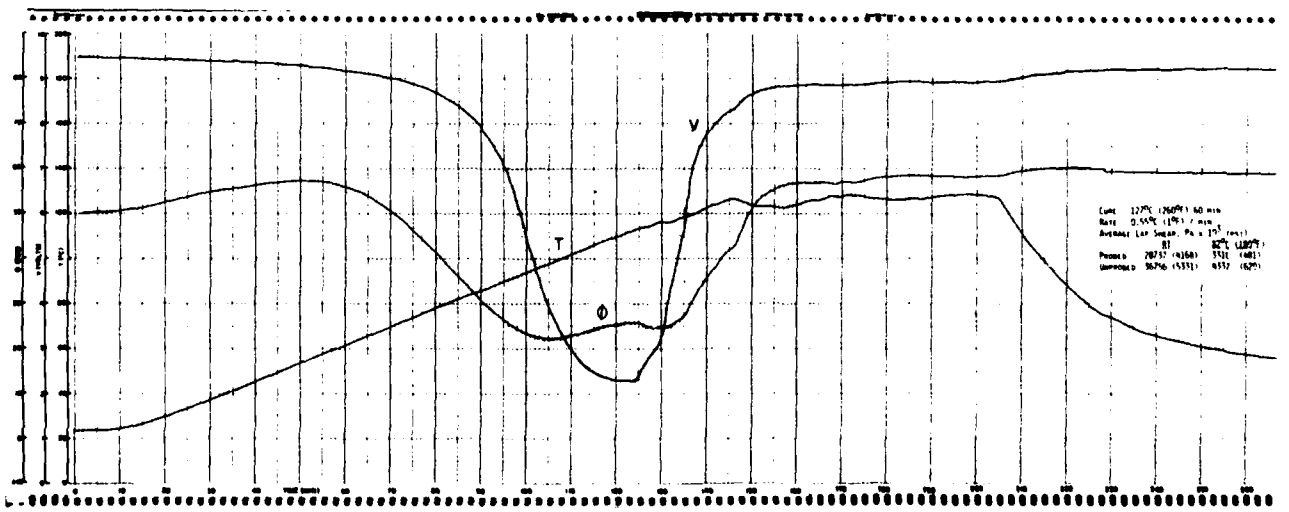

Figure 60 Cure at 127°C (260°F) Heated at 0.55°C (1°F)/min.

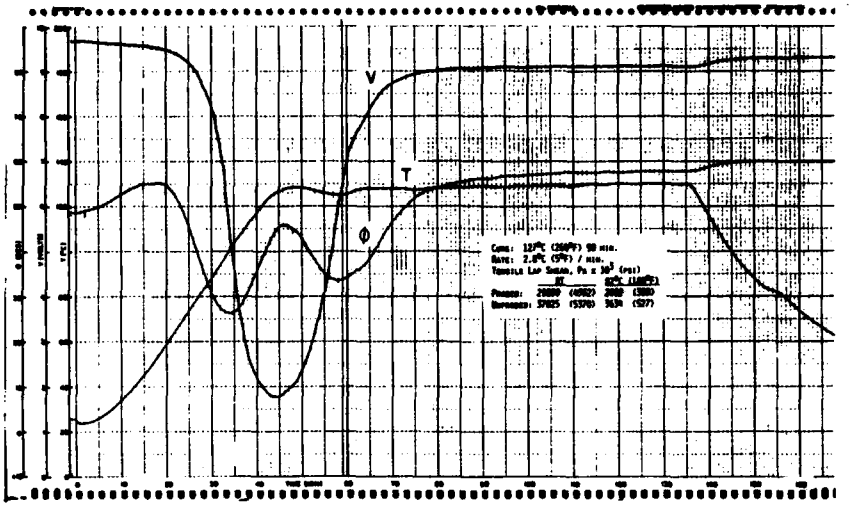

Figure 61 Cure at 127°C (260°F) Heated at 2.8°C (5°F)/min.

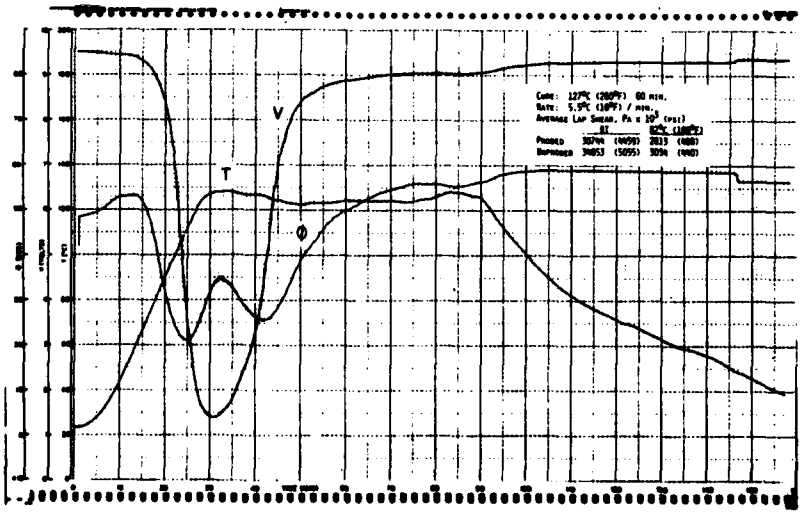

Figure 62 Cure at 127°C (260°F) Heated at 5.5°C (10°F)/min.

As observed at 104°C, the phase angle response for the slowest heating rate was again atypical. The cure following the 2.8°C upheat rate was held for 90 minutes rather than the normal 60 minutes to see if the longer cure caused any significant differences. Neither bond strength nor dielectric response indicate any abnormalities as compared to the control data.

The influence of rate at the highest cure temperature, 149°C is shown in Figures 63 through 66. This corresponds to runs 7, 8 and 9 in Table 1.

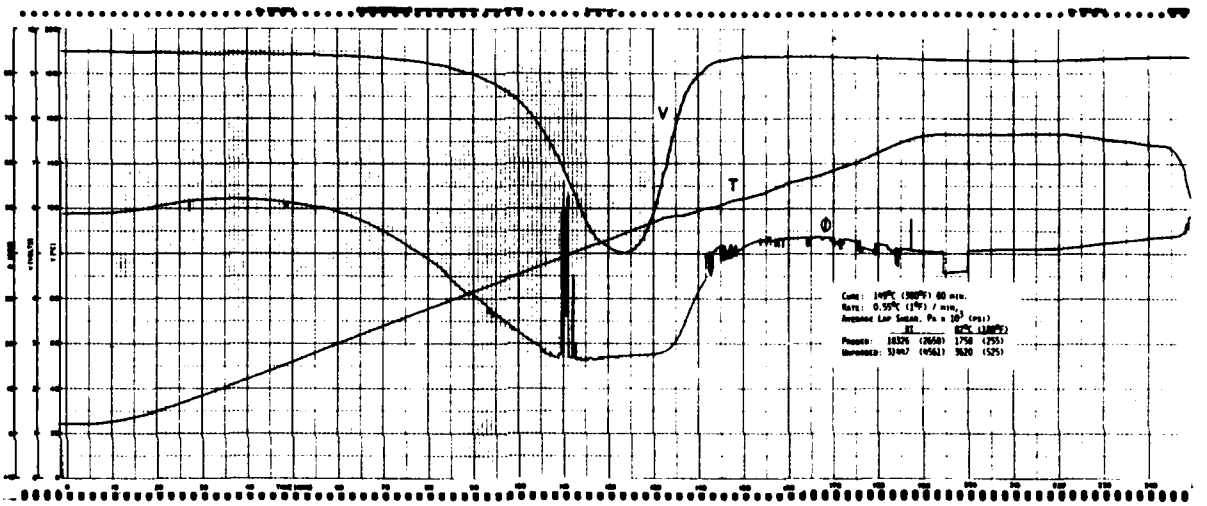

Figure 63 Cure at 149°C (300°F) Heated at 0.55°C (1°F)/min.

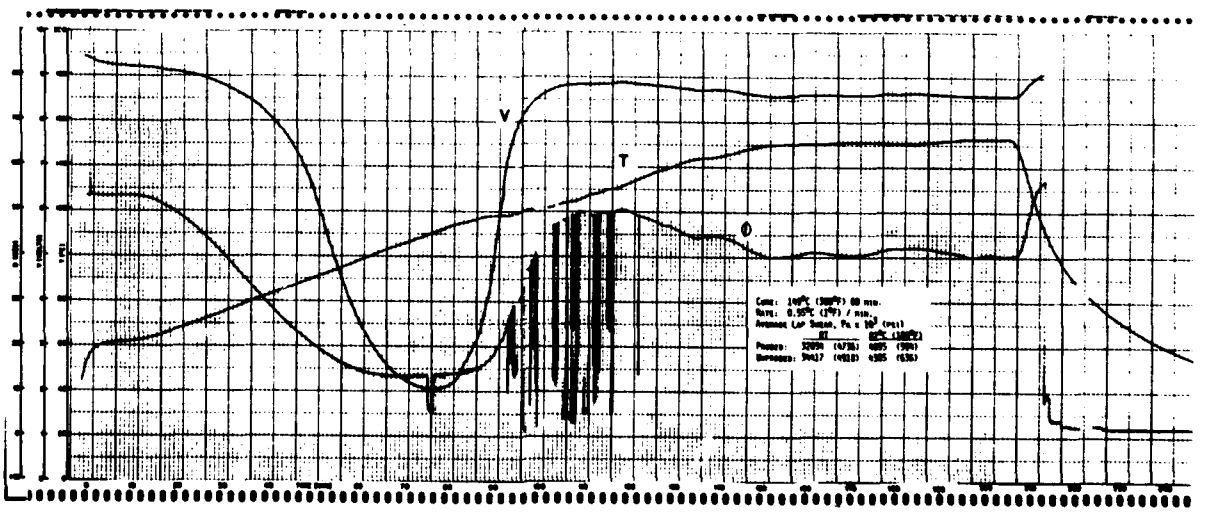

Figure 64 Repeat of Figure 63

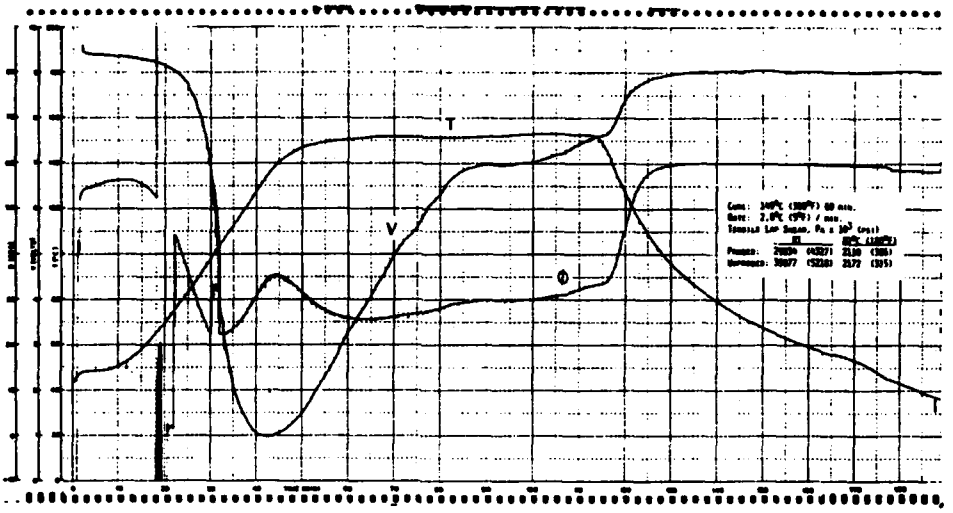

Figure 65 Cure at 149°C (300°F) Heated at 2.8°C (5°F)/min.

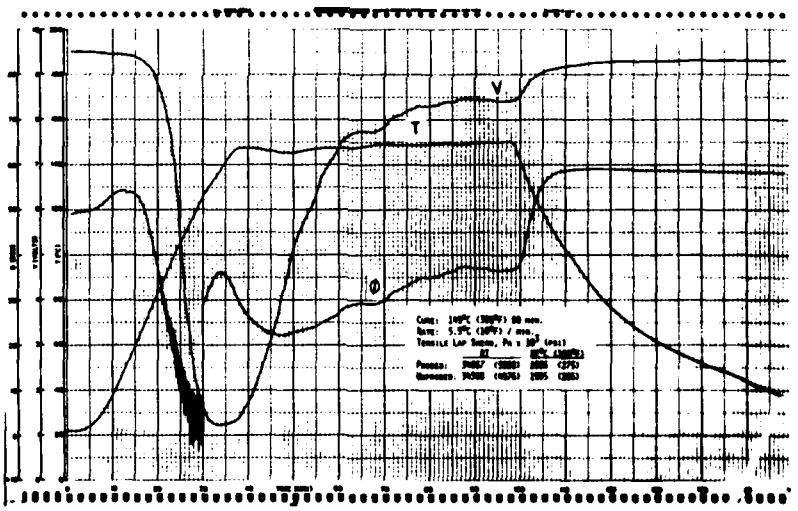

Figure 66 Cure at 149°C (300°F) Heated at 5.5°C (10°F)/min.

Run 7 (Figures 63 and 64) was repeated because a pressure leak occurred during the first run. The lower pressure obtained (Figure 63) caused a definite reduction in the magnitude of the dielectric response. This suggests that an operator during a production run may have reason to suspect a leak if the dielectric response data is below normal. The leak definitely reduced the bond strength of the probed sample at room temperature.

Note also the pronounced use in the vector voltage and phase angle during the cool down period after bonding. This is indicative of a cure well above the T_g. In each case the uppermost inflection point is in the neighborhood of 115°C. This represents another way of measuring the T_g of the adhesive and could be useful as a quality control procedure. The observed T_g's are consistent with the results discussed in Section III.

5. Effect of Cooling Rate

The effects of cooling rate are shown in Figures 67 through 71, and correspond to runs 13, 14 and 15 of Table 1.

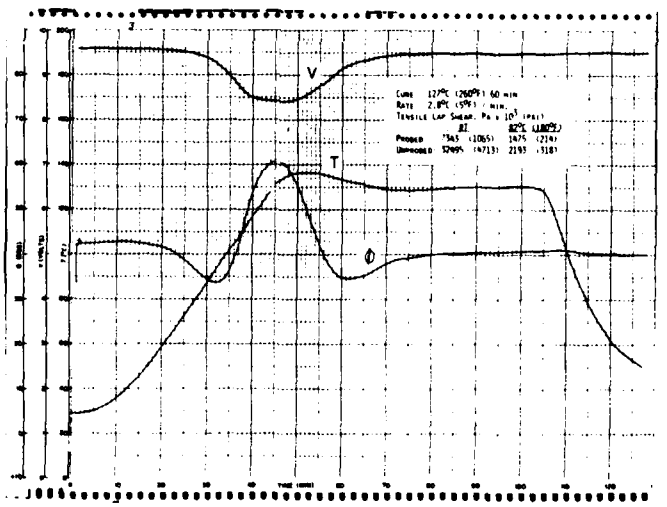

Figure 67 Dielectric Response and Bond Strength After a Fast Cool Down Rate

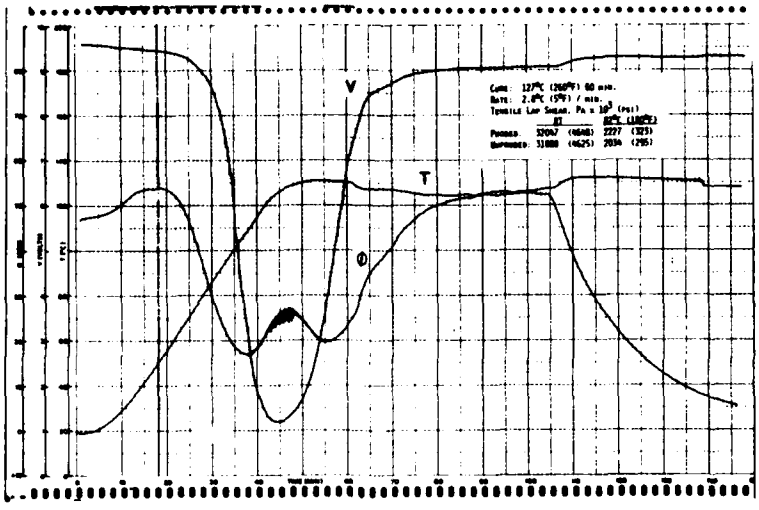

Figure 68 Repeat of Figure 67

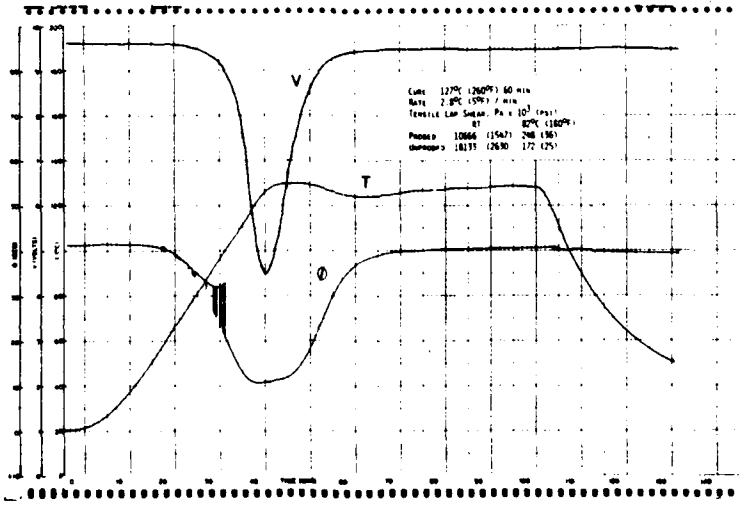

Figure 69 Dielectric Response and Bond Strength for an Intermediate Cooling Rate

AD-A099 418 LOCKHEED MISSILES AND SPACE CO INC SUNNYVALE CA MISSI--ETC F/6 11/1
CURE MONITORING TECHNIQUES FOR ADHESIVE BONDING TECHNIQUES.(U)
NOV 80 C A MAY, A WERETA, J S FRITZEN F33615-79-C-5046
UNCLASSIFIED LMSC-D058816 AFWAL-TR-80-4171 NL

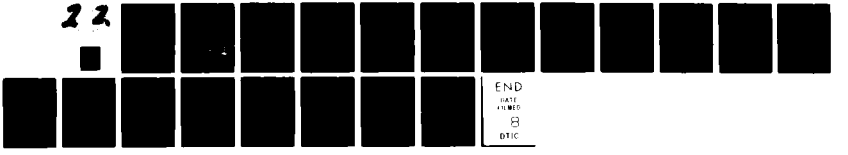

END
DATE FILMED
8
DTIC

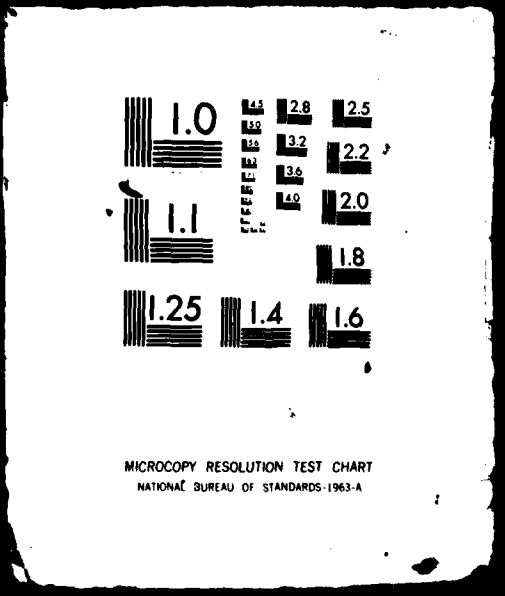

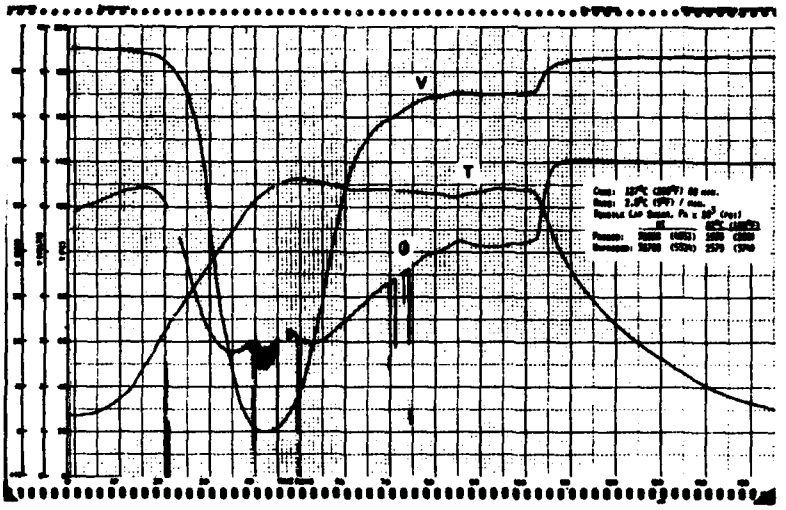

Figure 70 Repeat of Figure 69

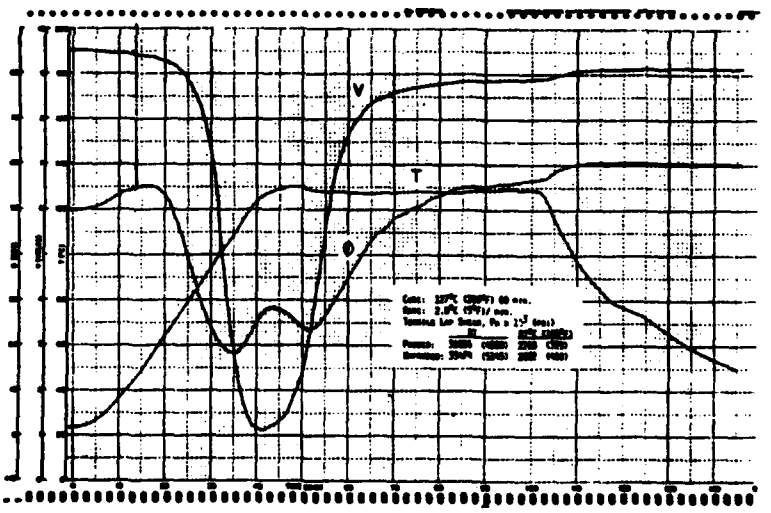

Figure 71 Dielectric Response and Bond Strength For a Slow Cooling Rate - Natural Rate of Pressclave

Runs 13 and 14 were repeated after a leak was discovered in each case. The proper dielectric response data are shown in Figures 68 and 70. The effect of cooling rate on bond strength and the dielectric analysis is of little consequence. However, the effect of lower than normal pressure when leakages occurred is important. The data presented here and also in Figures 63 and 64 above all lead to the same general conclusion. The effect of subnormal pressures causes a reduction in the magnitude of the dielectric response and this is also reflected in the ambient temperature bond strength.

6. Effect of Pressure Application Point

Another part of this study involved the point during the cure cycle when pressure was applied to the bondline. These data are summarized in Figures 72 through 75 and correspond to runs 16 - 19 in Table 1.

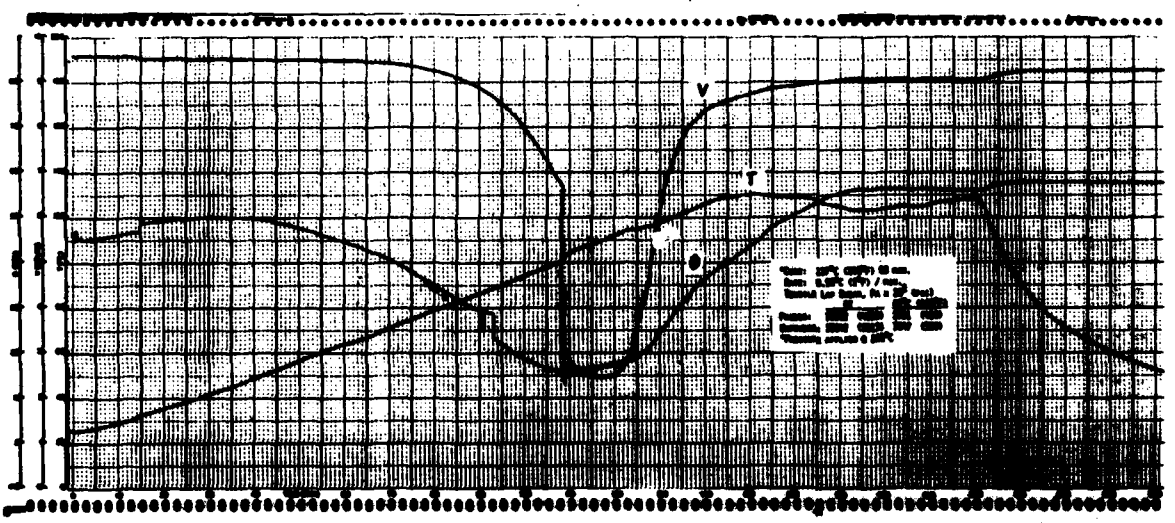

Figure 72 Pressure Applied at 100°C

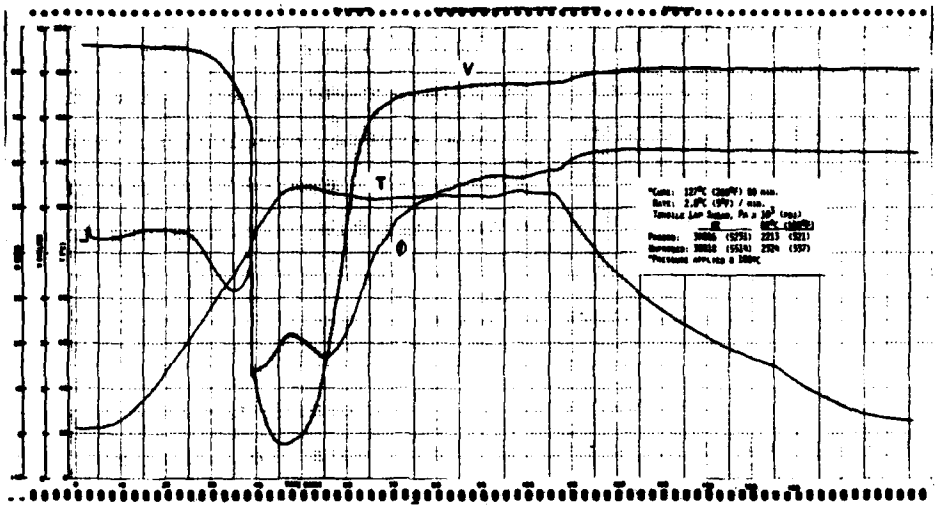

Figure 73 Pressure Applied at 100°C

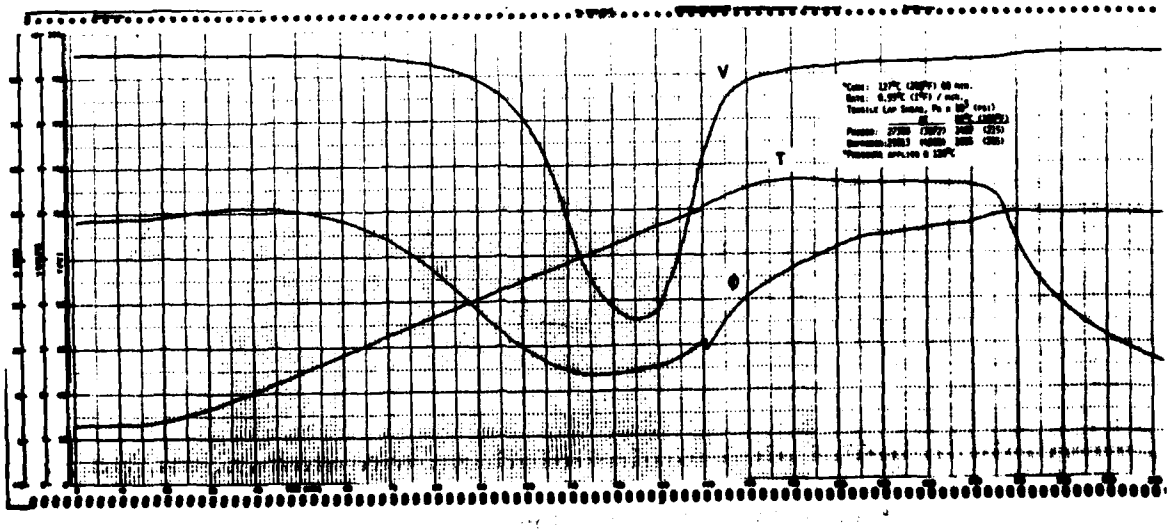

Figure 74 Pressure Applied at 120°C

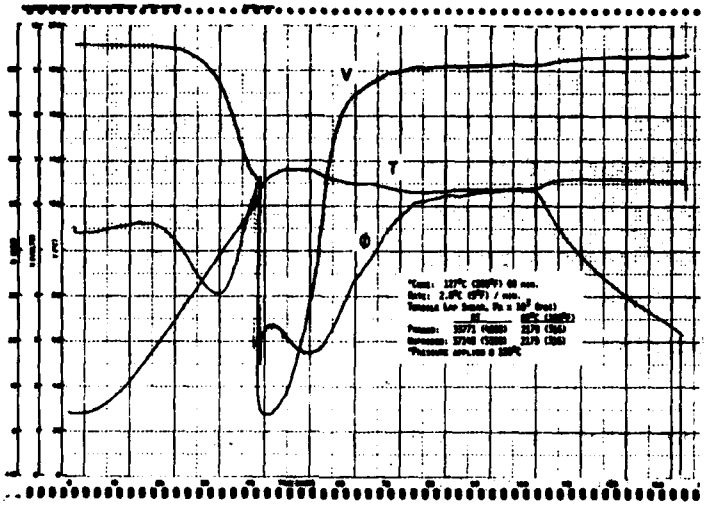

Figure 75 Pressure Applied at 120°C

In every case the application of pressure resulted in a visible shift in the vector voltage and phase angle. However, the very slight changes in the dielectric response when the pressure was applied at 120°C after a slow (0.55°C/minute) upheat cycle leads to an interesting speculation. This slight change could indicate that the adhesive is either past or very close to the gel point. A change in bondline thickness is normally the cause of shifts in the magnitude of the dielectric signal. It should also be noted that there is a reduction in the bond strength as compared to the other three conditions. Information of this type could prove very useful in production. The operator on seeing this type of data could abort the run and possibly save some valuable parts which could be salvaged and rebonded. Most thermoset bonds, even the poor ones, are very difficult to pull apart once the adhesive has been fully cured.

7. Summary

Because of the inordinate amount of data presented in this section, a brief summary of the salient prints would appear in order. There is little question that the dielectric analysis can be used to study cure cycles. The vendor recommended cycle, run 5 Table 1, was well chosen and leads to acceptable bonds. The nature (shape) of the phase angle curves changes with both cure rate and cure temperature. However, none of the data obtained would preclude the use of the procedure as a process control tool. The technique is also sensitive to process pressure and may be useful in a production environment to detect faulty bagging procedures in autoclave bonding.

Probe geometry is important and can influence bond strength. There was a notable reduction of strength in this part of the investigation. In earlier work (Contract F33615-76-C-5170), which involved the use of 1 inch overlap tensile shear specimens as compared to the 1/2 inch used herein, a different shaped probe was used and effect on strength was minimal. This points out the necessity for designing the probe to be compatible with the joint geometry. The effect of cooling rate or heating rate had a minimal effect on bond strength but lower temperature cure cycles tended to give weaker bonds.

SECTION VII

ENVIRONMENTAL TESTING OF PROBED SPECIMENS

1. Bonding Conditions

In addition to the room temperature tests discussed in the previous section, environmental exposure tests were conducted on FM-73 at 82°C (180°F) and 49°C (120°F) and 95% relative humidity were conducted on RAAB and wedge crack opening specimens both in the presence and absence of bondline probes. In all cases the bondline probes were 1/4" wide. Their orientation in the bondline is discussed in greater detail in the subsections which follow. All of the bonds were cured for one hour at 127°C (260°F) using a heating rate of 2.8°C (5°F)/minute. The bonding surfaces were Boeing phosphoric anodised and primed with BR-127.

The monitoring data obtained during sample preparation was excellent and highly reproducible. Using the techniques discussed earlier (Section 4), less than 5% of the probes were lost which indicate that a highly reliable probing method resulted from this investigation. Figure 76 shows

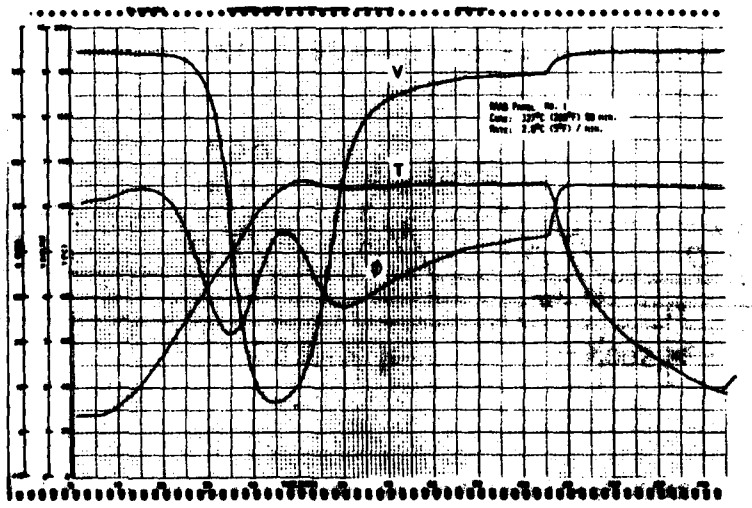

Figure 76 Phasemeter Monitoring Trace of RAAB Specimen Bonding

a typical phasemeter trace obtained monitoring the cure of a RAAB specimen preparation and similar data for the wedge crack specimen preparation are shown in Figure 77. Because of the high degree of reproducibility obtained, it would be redundant to include the data for all of the bonding operations.

2. RAAB Tests

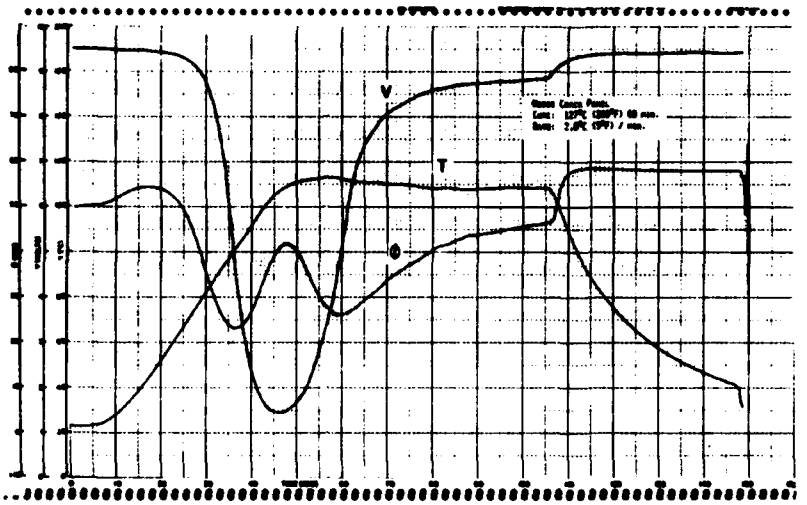

Figure 77 Phasemeter Monitoring Trace of Wedge Crack Specimen Bonding

a. Specimen Preparation

A typical RAAB specimen is shown in Figure 78. Each specimen had four

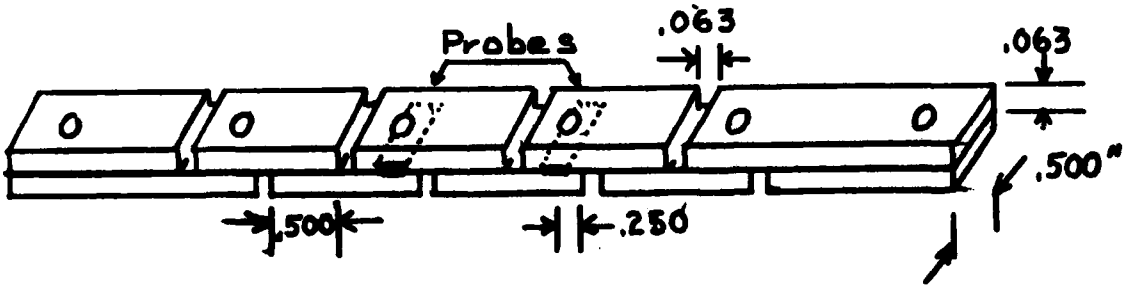

Figure 78 RAAB Specimen Showing Probe Location in Test Area

1/2" x 1/2" tensile shear bond areas with a 1/4" diameter hole through the center. The bonded area was thus 0.25 inches square less the area of the hole. The two center bonds contained a 1/4" strip of aluminum foil as shown in the above sketch to simulate a cure monitoring probe. The actual monitoring probe for sample fabrication was a 1/4" x 2" strip of aluminum foil placed parallel to the length of the specimen in the trim area.

Specimens were tested in both the stressed and unstressed condition in the aforementioned environments. The stressed specimens were loaded at 13,800, 13,100, 12,400, 11,700 and 11,000 Pa x 10^3 (2000, 1900, 1800, 1700 and 1600 psi). Creep was noted especially in the 82°C (180°F) specimens early in the exposure. This required checking and reloading the specimens every 24 hours, however, the creep did appear to stabilize after 72 hours and the load drop was minimized. When the specimen failed at a given hole, the time was noted, the specimen bolted back together through the hole, reloaded and the test continued.

b. Unstressed RAAB Specimens

A summary of the data on the unstressed RAAB specimens is given in Table 2 where each data point represents the average of 4 to 8 individual specimens.

Table 2 Summary of the Unstressed RAAB Exposure Tests

Environmental Conditions	Room Temperature		82°C (180°F)	
	Probed	Unprobed	Probed	Unprobed
	Pa x 10^3 (psi)			
Control (R.T.)	26750 (3880)	26610 (4025)	10720 (1555)	16340 (2370)
40 days @ 82°C	27235 (3950)	27750 (4025)	14995 (2175)	18820 (2730)
40 days @ 49°C/ 95% RH	25165 (3650)	26025 (3775)	7790 (1130)	11650 (1690)

Lap shear tests conducted at room temperature showed that there were no significant changes during the 40 day exposure periods. The presence of the monitoring probe also had no effect on the bond strength either before or after exposure. However, some effects were noted in the 82°C tests. The forty day, 82°C exposure increased the lap shear strength approximately 40% and 15% for the probed and unprobed specimens respectively. On the other hand following the high humidity exposure the lap shear strength decreased approximately 38% and 30% for the probed and unprobed specimens, respectively. It would thus appear that the probe does have a degrading effect on the bond strength, but only above 82°C and particularly in moist environments.

c. Stressed RAAB Specimens

Data on the stressed RAAB specimens after both elevated temperature and high humidity exposures are summarized in Tables 3 and 4. Here, the effect of

Table 3 Stressed RAAB Specimens at 49°C and 95% RH

Time Frame for Failure, Days

Specimen	1	2	1	2
Loading, psi	Probed		Unprobed	
1600	0.1-0.6	2.5-3.6	35*	-
1700	2.0-2.6	2.4-3.6	35*	-
1800	1.8-2.0	2.8-3.6	35*	-
1900	0.1-0.6	1.2-2.0	1.9-2.7	35*
2000	0.1-0.6	1.2-2.0	17.2-18.0	35*

* Test Continued

Table 4 Stressed RAAB Specimens at 82°C

Specimen	1	2	1	2
Loading, psi	Probed		Unprobed	
1600	0.1-0.4	0.1-0.4	12.1-12.5	31*
1700	0.2-0.8	0.2-0.8	10.2-10.8	15.4-16.0
1800	0.1	0.1	8.4-9.0	8.8-10.0
1900	0.1	0.1	1.4-2.0	1.6-2.2
2000	0.1	0.1	1.0-1.1	4.0-6.6

* Test Discontinued

the probe is unmistakable. Under either humid conditions or elevated temperature exposure the monitoring probe caused a severe degradation of the bondline performance. It is also interesting to note the failures of the unprobed specimens on elevated temperature exposure. This is indicative of creep and poor performance in general of the adhesive at elevated temperatures. These results are shown in graphic form in Figures 79 and 80.

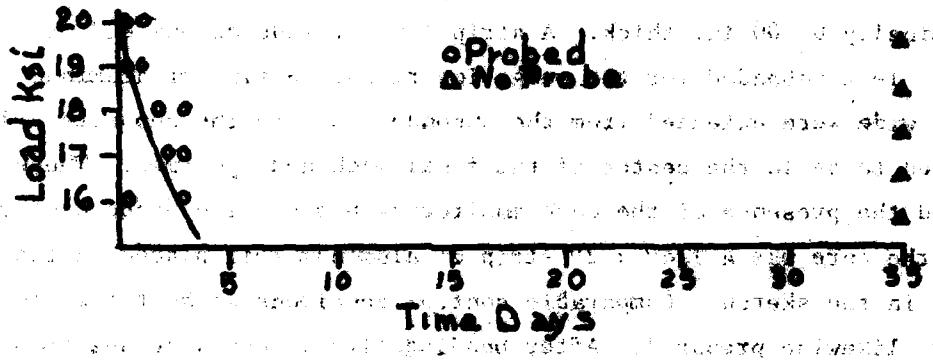

Figure 79 BAAB Exposure Test at 49°C and 95% RH

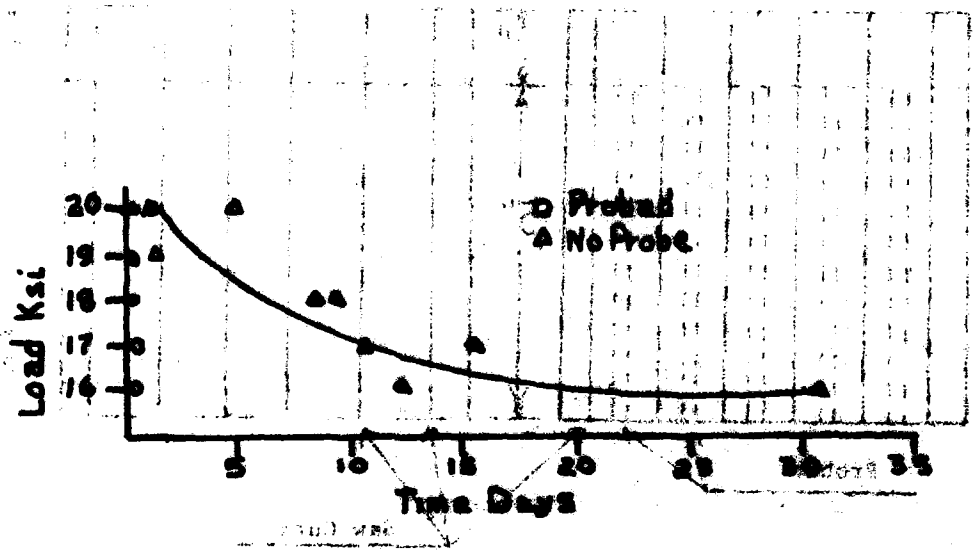

Figure 80 BAAB Exposure Tests at 180°F

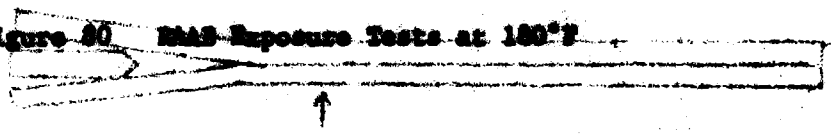

Figure 81 Wedge Opening Crack Specimen Assembly

3. Wedge Opening Crack Tests

a. Specimen Preparation

The configuration of the wedge opening crack specimen assembly and the specimen details are shown in Figure 81. The laminated assembly was 6 x 6 inches. The 2024 T3 aluminum phosphoric acid anodized adherends were nominally 0.100 in. thick. A strip 1.0 in. wide on one end of the panel was left unbonded for the wedge insertion. Strips of aluminum foil 0.25 in. wide were extended from the unbonded edge to the opposite side and so located to be in the center of the final machined specimen. These specimens simulated the presence of the cure monitoring probe. The probe used to monitor the cure was a 1/4" x 2" strip of aluminum foil placed in the assembly as shown in the sketch. Comparable control specimens without the aluminum foil were likewise prepared. After bonding, five 1 inch wide specimens were machined from each panel.

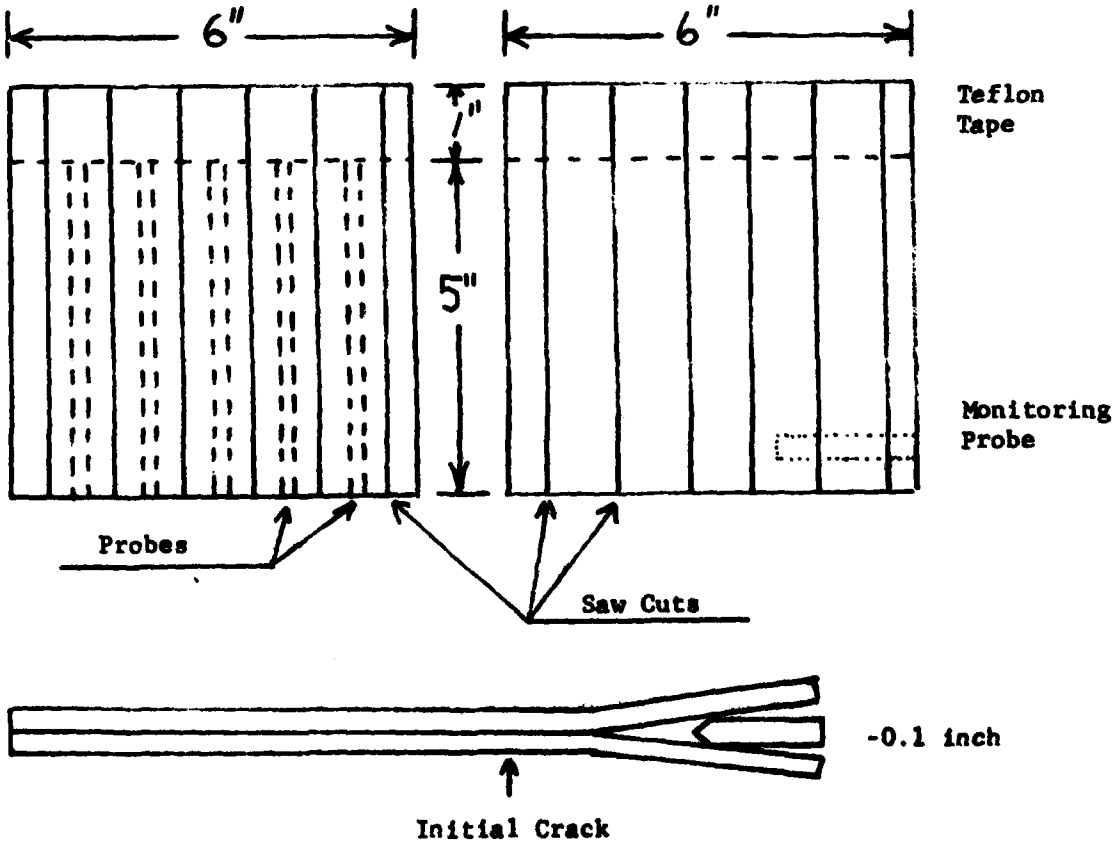

Figure 81 Wedge Opening Crack Specimen Assemblies

b. Test Results

The test results are summarized in Table Each data point represents an average of four test specimens. The results are also summarized in graphic form in Figure 86. In every case, including the unexposed control, the probed specimens gave poor results.

Time, Days	Crack Length, Cm					
	Control		120°F, 95% RH		180°F	
	Probed	Unprobed	Probed	Unprobed	Probed	Unprobed
1	0.0127	0.0000	0.0984	0.0476	0.1810	0.0603
2	0.0254	0.0000	0.1207	0.0699	0.1905	0.0635
5	0.0318	0.0000	0.1492	0.0984	0.2191	0.0826
7	0.0381	0.0064	0.1651	0.1048	0.2286	0.0826
12	0.0889	0.0381	0.1969	0.1111	0.2318	0.0826
16	0.0889	0.0445	0.2064	0.1111	0.2318	0.0826
23	0.0889	0.0445	0.2096	0.1111	0.2318	0.0826
33	0.1016	0.0445	0.2127	0.1175	0.2318	0.0826

Table 5 Wedge Opening Crack Test Summary

4. Discussion

There is little question that the monitoring probes cause a reduction in bond performance at least under the conditions tested herein. The seemingly poor results at 82°C as compared to the high humidity exposure could be an artifact of the material involved. Bond strengths at 82°C are extremely low and in such a condition would be highly susceptible to creep.

Surface treatment of the probe (anodizing) could be beneficial. However, the magnitude of the improvement could not be assessed within the scope of the current funding and available time. In view of the fact that the monitoring technology appears to be a valuable adjunct to the bonding process, an additional expenditure, which could be of a modest nature, would definitely appear worthwhile.

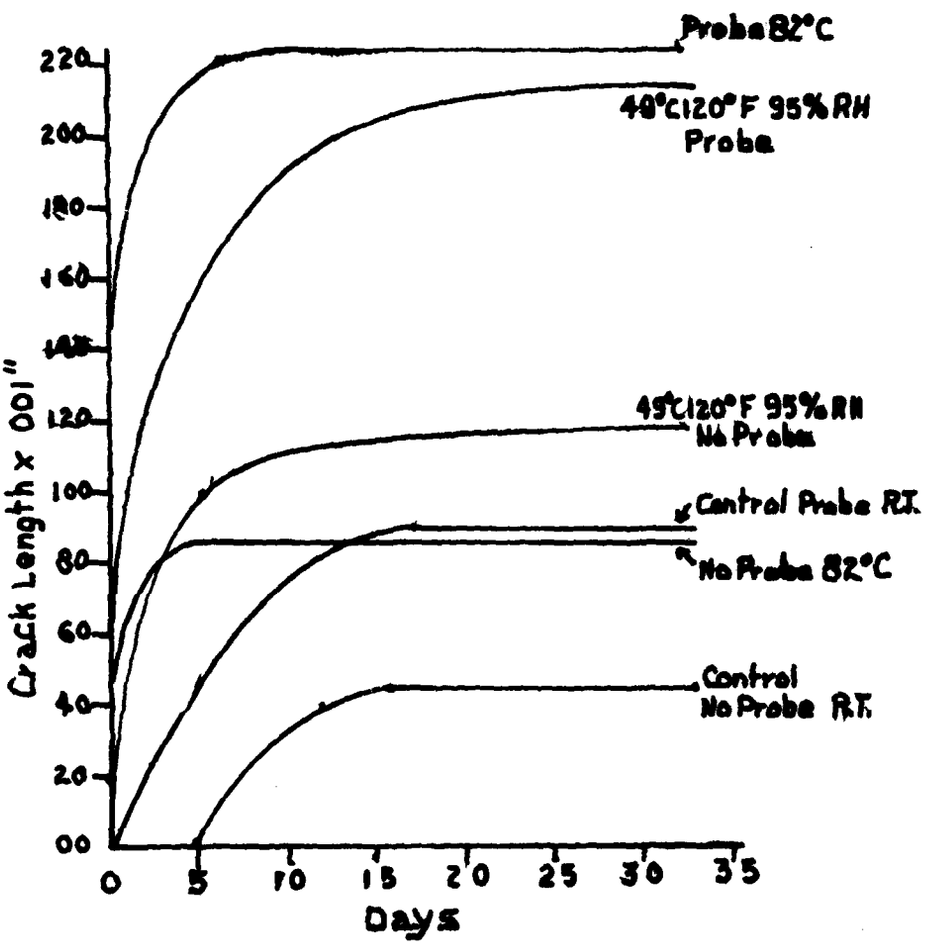

Figure 82 Summary of Wedge Crack Tests

SECTION VIII

MONITORING PROBES AS A MOISTURE DETECTOR

1. Moisture Detector Feasibility

The presence of moisture in a bondline can obviously affect the performance of the bond. It has been demonstrated in AFML-TR-79-3086 that a small capacitor imbedded in a matrix resin will change in capacitance in the presence of moisture. Accordingly, a brief investigation was made to determine the feasibility of using a shop practical probe, such as the ones used in this program, to monitor the moisture pickup in an adhesively bonded joint.

Since the absorption of water is a slow diffusion controlled process, it was decided to test the idea by immersing a simulated bondline in water. A series of probed bonds (probe 1/4" x 2") were fabricated between aluminum adherends with a layer of FEP film adjacent to each adherend. This gave a cast layer of adhesive, 0.007 mils thick, with an imbedded probe which could be soaked in water to speed the water uptake process. A multiplex monitoring trace made during the fabrication of three specimens of this type is shown in Figure 83. Note that the characteristic double valley

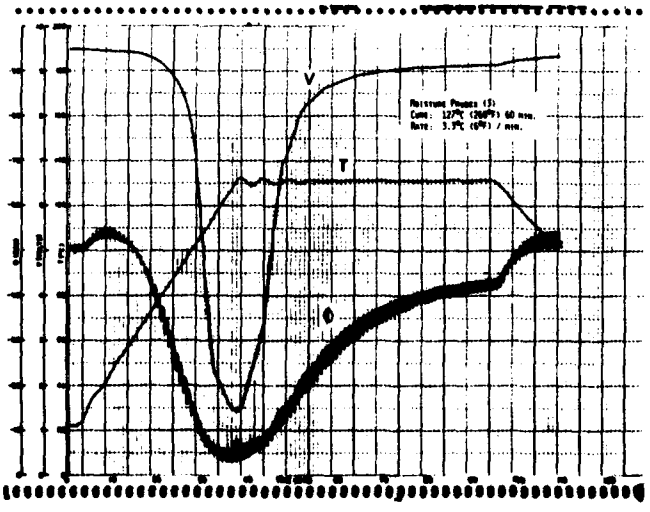

Figure 83 Simultaneous Monitoring Traces Taken During Preparation of Three Probed Test Specimens

in the phase angle curve is not present. This change is probably caused by the presence of the FEP film. The experimental procedure consisted of immersing three probed specimens in distilled water periodically removing the samples after periods of 24, 96 and 120 hours, wiping them with a dry, soft tissue, weighing to determine the moisture gain and measuring the phase angle and vector voltage at frequencies over a range of 1-500 kHz. The dielectric measurements were made by pressing the samples between two aluminum plates in a laboratory press so that pressure and electrical contact were eliminated as experimental variables. Because of the small sample size, however, the results were highly variable. The weight gain was around 2% for all three samples and they attained equilibrium rapidly, 24 hours exposure being adequate. The changes in vector voltage and phase angle offered some hope that the probes could be used for moisture detection but the results were inconsistent. For instance, at 20 kHz the change in phase angle after a 24 hour soak was 2.8°, 3.3° and 6.8°. Similar variability was found for vector voltage change and the variability did not seem to be frequency dependent. Although it appears that the dielectric properties do change as a function of moisture content, a much more carefully designed and controlled experimentation would be required before the method proves viable for real time use.

SECTION IX

RECOMMENDATIONS AND CONCLUSIONS

1. Conclusions

As a result of this investigation, the main objective of providing a foundation for automated bonding cycle control has been realized. The major dielectric monitoring techniques, phasemeter and Audrey, have been developed to the point where a mathematical model of the monitoring systems was derived in which phasemeter signals could be used to calculate tan δ and capacitance, the typical Audrey response. The reverse was also true. Audrey signals could be converted to the phasemeter signals, vector voltage and phase angle. In addition, a chemorheological interpretation of the dielectric signals was possible, prerequisite information needed for automated bonding cycle control.

The minor malfunctions of the monitoring probes have been reduced to the point where probe failures are rarely a problem. This was accomplished by optimizing the probe design depending on the bondline geometry reducing the probe size, increasing the reliability of the probe/instrumentation interface and minimizing the noise level.

Cures were monitored over a wide variety of experimental conditions. The effects of bonding temperatures and chemical structures of adhesives were demonstrated during the investigation. Other parameters included the effects of fillers, heating rates, cooling rates, time at temperature, hold times and changes in the time to pressure application points. Dielectric monitoring was used for a cure optimization study on FM-73. Unfortunately, this product proved extremely forgiving and produced a broad acceptable processing window. Thus, as a demonstration, the full power of this tool was not illustrated. It also made mathematical correlation between the dielectric signals and bond strengths virtually impossible. It was noted, however, that dielectric signals reflected the time/temperature characteristics of a particular cure cycle. Visually all failures were of a similar cohesive nature.

A number of joint types were fabricated to determine the mechanical and environmental effects of the probe on bond performance. These included tensile lap shear, wedge-opening crack extension and blister detection (Raab) types. The peel specimens originally planned were eliminated by mutual agreement with the

AFML Project monitor in favor of more extensive Rasb tests. It was generally agreed that peel testing would tell us little about influence of the probes. As a general conclusion, the probes had little effect under ambient conditions, but definite degradation was noted at elevated temperatures both in the presence and absence of moisture.

2. Recommendations

The major goal of laying a foundation for automated bonding cycle control, has been achieved and an investigation toward this goal could be started. Work along this line in the composites area is in progress at LMSC as an independent development project. However, problems encountered in the electronics/signal/computer interfaces, although solvable, have slowed progress and starting a bondline monitoring program to do a similar job should be postponed until a later date. We feel that the techniques that will evolve from our in-house program will be fully applicable to the adhesive bonding process.

As with any program that has numerous facets, additional findings occur which highlight areas where additional investigation appears warranted. Certainly one important area is the influence of the probe on mechanical performance during and after environmental exposure. Work to date indicates that probe surface treatment, the use of primers and bondline geometry all could be important factors. As progress proceeds toward automated bonding processes, an investigation of this type grows in importance.

Preliminary work indicates the probe could be useful in detecting the ingress of moisture into bonded structures. This also could be an extensive study. However, we would not recommend a study of this type at the present time. Understanding the data would be difficult and there are more pressing needs in the area of bond monitoring.

Quite aside from this investigation, our studies on the monitoring of fiber reinforced composite cures indicate that the presence of moisture in an uncured matrix drastically alters the characteristics of the dielectric signals. Chemorheological studies by Hinrichs and Thuen have shown that moisture affects the processing characteristics of both composites[18] and adhesives[19].

Thus, another recommended and important study is how to handle the presence of moisture in automated bondline processing cycles based on dielectric signals.

SECTION X

REFERENCES

1. May, C. A., Fritzen, J. S., and Brown, G. R., "Analysis of Resin Matrix Changes During Composite Cure", 1975 International Conference on Composite Materials, Geneva and Boston, April 1975, to be published in SAMPE Quarterly.

2. May, C. A., "Dielectric Measurements for Composite Cure Control - Two Case Studies", *National SAMPE Symposium and Exibition*, 20, 108-16, San Diego, April 1975.

3. May, C. A., Whearty, D. K. and Fritzen, J. S., "Composite Cure Studies by Dielectric and Calorimetric Analyses", National SAMPE Symposium and Exhibition, 20, 803-18, Los Angeles, April 1976.

4. Von Hippel, A., "Dielectric Properties of Materials", MIT Press, Cambridge, Massachusetts (1954).

5. Turner, A., Jr., "Mechanical Behavior of High Polymers", Intra-Science Publishers, New York (1948).

6. Smyth, C. P., "Dielectric Behavior and Structures", McGraw-Hill, New York (1955).

7. McCrum, N. G., Reed, B. E., and Williams, G., "Anelastic and Dielectric Effects in Polymeric Solids", John Wilson & Sons, New York (1967).

8. Wrasidlo, W. J., "Motions in Poly-Pyromellitimide", Boeing Scientific Research Laboratories, Rpt. No. D1-82-1061.

9. Yaloff, S. A. and Wrasidlo, W. J., J. Appl. Polymer Sci. 16, 2159 (1972).

10. Walker, J. M., "Dielectric Analysis of an Epoxy Preimpregnated Material", USERDA Report BDX-613-1396, January 1976.

11. Arvay, E. A. and Centers, P. W., Air Force Materials Laboratory Tech. Rpt., AFML-TR-74-12, March 1974.

12. Crabtree, D. J. and Bischoff, G. H., "The Electrical Analysis of Adhesive Cure", National SAMPE Technical Conference Series, 5, 405-12, Kiamesha Lake, N. Y., October 1973.

13. May, C. A., Fritzen, J. S. and Wereta, A. Jr., Air Force Materials Laboratory Tech. Rpt., AFML-TR-77-58, March 1977.

14. Fritzen, J. S., Wereta, A. Jr., and Arvay, E. A., "Cure Monitoring Techniques for Adhesive Bonding Processes", National SAMPE Symposium and Exposition 22, 430-4, San Diego (April 1977).

15. Arvay, E. A., "Aspects of Adhesive Cure Monitoring", National SAMPE Symposium and Exposition 25,115-125, San Diego (May 1980)

16. Fritzen, J. S., Wereta, A. Jr., and May, C. A., "Dielectric Bond Monitoring in the PABST Program" (Sept. 1977) subcontract to Douglas Aircraft Co., McDonnell Douglas Corp., Long Beach under Air Force Contract F33615-75-C-3016.

17. May, C. A., and Wereta, A. Jr., "Dielectric Monitoring of the Bonding Process" to be published, Journal Adhesion. Presented at 3rd Annual Meeting of the Adhesion Society, Savannah (Feb. 1980).

18. Hinrichs, R., and Thuen, J., "Environmental Effects on the Control of Advanced Composite Materials Processing", National SAMPE Symposium and Exposition 24, 557-74, San Francisco (May 1979).

19. Thuen, J., and Hinrichs, R., "Structural Adhesives Rheological Behavior Response to Process-Environmental Variations", National SAMPE Symposium and Exposition 25, 126-53, San Diego (May 1980).

*U.S.Government Printing Office: 1981 — 757-002/433

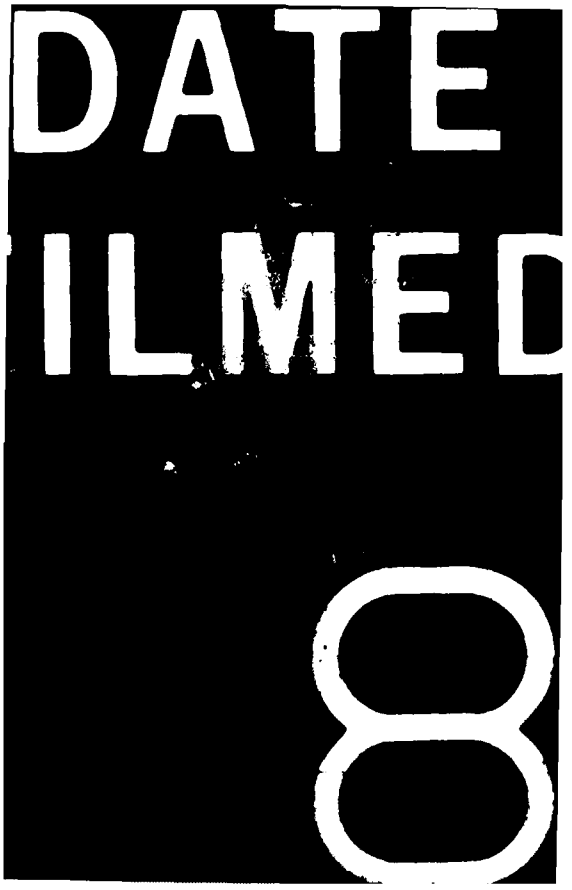
DATE
ILMED
8